

Durham E-Theses

Bulk and boundary scattering in the q-state potts mode

Pocklington, Andrew Jonathan

How to cite:

Pocklington, Andrew Jonathan (1998). *Bulk and boundary scattering in the q-state potts mode*, Durham e-Theses. <http://etheses.dur.ac.uk/4818/>

Use policy

The full-text may be used and/or reproduced, and given to third parties in any format or medium, without prior permission or charge, for personal research or study, educational, or not-for-profit purposes provided that:

- a full bibliographic reference is made to the original source
- a [link](#) is made to the metadata record in Durham E-Theses
- the full-text is not changed in any way

The full-text must not be sold in any format or medium without the formal permission of the copyright holders.

Please consult the [full Durham E-Theses policy](#) for further details.

Bulk and Boundary Scattering in the q -State Potts Model

Andrew Jonathan Pocklington

A thesis presented for the
degree of Doctor of Philosophy
at the University of Durham

The copyright of this thesis rests
with the author. No quotation
from it should be published
without the written consent of the
author and information derived
from it should be acknowledged.

Department of Mathematical Sciences
University of Durham

July 1998

30 SEP 1998

Bulk and Boundary Scattering in the q -State Potts Model

Andrew J. Pocklington

Ph.D. Thesis 1998

Abstract

This thesis is concerned with the properties of $1 + 1$ dimensional massive field theories in both infinite and semi-infinite geometries. Chapters 1, 2 and 3 develop the necessary theoretical framework and review existing work by Chim and Zamolodchikov [1] on integrable perturbations of the (bulk) q -state Potts model, the particular model under consideration in this thesis. Chapter 4 consists of a detailed analysis of the bootstrap for this model, during the course of which unexpected behaviour arises. The treatment of [1] has consequently been revised, but further investigation will be necessary before complete understanding of this behaviour can be reached. In the final chapter, attention turns to the imposition of boundary conditions on two dimensional systems. After looking at this from a statistical mechanical point of view, a brief review of boundary conformal field theory and its integrable perturbations is given. This leads once more to a consideration of the q -state Potts model. After summarising [2], where fixed and free boundary conditions are considered, a third and previously untreated boundary condition is discussed.



Declaration

This thesis is the result of work carried out in the Department of Mathematical Sciences at the University of Durham, between October 1994 and September 1997, under the supervision of Dr. P. E. Dorey and Prof. W. Zakrzewski. No part of it has been previously submitted for any degree, either in this or any other university.

Chapters 1 to 3 are entirely devoted to reviewing the necessary background material, and no claims are made to any originality. Chapter 4 starts with a brief restatement of work done by Chim and Zamolodchikov on integrable perturbations of the bulk q -state Potts model, before giving an extensive treatment of the bootstrap beyond $\lambda = 1$. The initial observation of the generalized bootstrap in $\mathcal{S}_{B_1 K_1}$ and $\mathcal{S}_{B_1 B_1}$ is due to Patrick Dorey, but the remaining work in this chapter is solely the author's. This work will form part of a joint paper, currently in preparation, being written in collaboration with Patrick Dorey and Roberto Tateo. It has also been cited by Cardy and Delfino in [3].

In chapter 5, the work of Cardy and others on boundary conformal field theory is reviewed, before turning attention once more to the q -state Potts model. The work by Chim on fixed and free boundary conditions is summarised, and a detailed analysis of the pole structure in the free case is added. Finally, a solution is given for the boundary scattering amplitudes of a previously untreated boundary condition. This boundary condition was suggested by Patrick Dorey, but its solution is due to the author alone.

Acknowledgements

I would like to thank Patrick Dorey, Roberto Tateo and Wojtek Zakrzewski for their help throughout my time at Durham, and the Engineering and Physical Science Research Council whose funding made it possible. I would also like to thank my family for their support and sufferance. Amongst the legions of people I have met over the last few years, the following must (I suppose) be singled out. Thanks go to David, Rob and Isobel for numerous discussions on a wide range of subjects; Gary, Michael, Taz, Xaréu and the rest for physical and verbal abuse; Richard, Suzanne, Moncef, Amanda, Rick, Teti and Justin for keeping me sane, and to Greg for showing that — for those with a sense of humour — sanity is not the only option.

If you cannot understand this primal script of magic—swallow
the whole damn book: then you will obtain astonishing results.

Austin Osman Spare

Contents

1	Statistical mechanics and field theory	14
1.1	Statistical mechanics	15
1.1.1	The q -state Potts model	17
1.1.2	Ice-type formulation and location of the critical point	19
1.2	Universality and the renormalization group	27
1.2.1	Universality	28
1.2.2	The Renormalization Group	28
1.2.3	Behaviour close to criticality	31
1.3	Quantum field theory	34
1.3.1	Path integrals and quantum mechanics	34
1.3.2	Connection with statistical mechanics	36
2	Conformal field theory	38
2.1	Conformal symmetry	38
2.2	Conformal theories in 2 dimensions	42
2.2.1	Correlation functions	43
2.2.2	The stress-energy tensor	45
2.2.3	Virasoro algebra and the structure of \mathcal{A}	48
2.2.4	Integrals of motion	50

2.2.5	Unitarity and crossing symmetry	50
2.3	Perturbations of Conformal Field Theories	51
3	S-matrices for integrable 2-d theories	54
3.1	Conditions on $\mathcal{S}_{a_1 a_2}^{b_1 b_2}(\theta)$	57
3.2	Bulk S-matrix for q -state Potts model	62
3.2.1	Particle content for $3 < q < 4$ ($1 < \lambda < \frac{3}{2}$)	69
4	Particle spectra and the generalized bootstrap principle	74
4.1	$0 < \lambda < 1$: Pole structure of $\mathcal{S}_0, \dots, \mathcal{S}_3$	75
4.2	Closure of bootstrap for $1 < \lambda < \frac{3}{2}$	80
4.2.1	$\mathcal{S}_{B_1 K_1}$	81
4.2.2	$\mathcal{S}_{B_1 B_1}$	84
4.3	$\frac{3}{2} \leq \lambda < 2$	87
4.3.1	Scattering amplitudes for K_2 and B_3	87
4.3.2	Pole structure of K_2, B_3 amplitudes	90
4.4	$2 < \lambda < \frac{9}{4}$	107
4.4.1	S-matrix elements of B_2	109
4.4.2	S-matrix elements of B_5	112
4.5	$\lambda = 2, \frac{9}{4}$ and $\frac{5}{2}$	117
4.5.1	$\lambda = 2, q = 3$	117
4.5.2	$\lambda = \frac{9}{4}, q = 2$	121
4.5.3	$\lambda = \frac{5}{2}, q = 1$	121
4.6	Summary	122
5	Statistical Mechanics & Field Theory with Boundaries	125
5.1	Boundary conditions and duality relations in statistical me- chanics	125

5.1.1	Fixed & free boundary conditions in the 2-d Ising model	126
5.1.2	Fixed & free boundary conditions in 3-state Potts model	129
5.2	Boundary conformal field theory	132
5.3	Boundary S-matrices	134
5.4	Boundary S-matrix for q -state Potts model	139
5.4.1	Fixed boundary condition	143
5.4.2	Free boundary condition	148
5.4.3	'Excluded' boundary condition	156
A	Calculation of $\mathcal{A}_{K_2K_2}^0$ for $t = \frac{1}{\lambda}$ pole	166
B	Bootstrap and generalised bootstrap scattering processes for $\lambda < \frac{9}{4}$	172
C	Yang-Baxter equations for 'excluded' boundary condition	201
D	Calculation of normalization factor for 'excluded' boundary condition	206

List of Figures

1.1	Medial lattice \mathcal{L}' (empty circles) around \mathcal{L} (solid circles) . . .	20
1.2	Separation of edges for (a) no bond on (i, j) and (b) bond on (i, j)	21
1.3	Arrow configurations on \mathcal{L}' and their respective weights	23
1.4	Distinct arrow configurations on \mathcal{L}'	24
3.1	$\mathcal{S}_{a_1 a_2}^{b_1 b_2}(\theta)$	56
3.2	A_c bound state in $\mathcal{S}_{a_1 a_2}^{b_1 b_2}(\theta)$	60
3.3	Geometrical interpretation of fusing angles	60
3.4	$A_{a_1} A_{a_2} \rightarrow A_c$ vertex	61
3.5	Kink interpolating between vacua a and b	64
3.6	$\mathcal{S}_{ac}^{bd}(\theta)$	65
3.7	Kink amplitudes $\mathcal{S}_0(\theta)$ and $\mathcal{S}_1(\theta)$	65
3.8	Kink amplitudes $\mathcal{S}_2(\theta)$, and $\mathcal{S}_3(\theta)$	66
3.9	$KK \rightarrow K$ bootstrap	67
3.10	Direct channel $KK \rightarrow K$ bound state	68
3.11	Cross channel $KK \rightarrow K$ bound state	68
3.12	Direct channel $KK \rightarrow B$ bound state	70
3.13	Cross channel $KK \rightarrow B$ bound state	70
3.14	$BK \rightarrow KB$ and $BB \rightarrow BB$ scattering	71

4.1	K_1K_1 fusion vertices	78
4.2	$K_1B_1 \rightarrow K_2$ vertex	81
4.3	K_1B_1 scattering: $t = (\frac{1}{6} + \frac{1}{2\lambda})$, $\lambda < \frac{3}{2}$	82
4.4	B_1B_1 scattering: $t = (\frac{1}{\lambda})$, $\lambda < 2$	85
4.5	B_1B_1 scattering: $t = (\frac{1}{\lambda} - \frac{1}{3})$, $\lambda < \frac{3}{2}$	85
4.6	Factorised scattering in Figure (4.5)	86
4.7	$\mathcal{S}_{K_1K_2}$ bootstrap	88
4.8	$\mathcal{S}_{K_2K_2}$ bootstrap	89
4.9	K_2K_2 scattering: $t = (\frac{2}{3})$ second order poles	90
4.10	K_2K_2 scattering: $t = (\frac{2}{3})$ third order poles	92
4.11	K_2K_2 scattering: $t = (\frac{2}{3} - \frac{1}{\lambda})$	92
4.12	K_2K_2 scattering: $t = (\frac{2}{3} - \frac{1}{\lambda})$, $\lambda = 2$	94
4.13	K_2K_2 scattering (direct channel): $t = (\frac{2}{3} - \frac{1}{\lambda})$, $\lambda = 2$	94
4.14	K_2K_2 scattering: $t = (\frac{2}{3} - \frac{1}{\lambda})$, $\lambda = \frac{9}{4}$	95
4.15	K_2K_2 scattering: $t = (\frac{1}{\lambda})$	96
4.16	K_2K_2 scattering: $t = (\frac{1}{\lambda})$, $\lambda = 2$ third order poles	98
4.17	K_2K_2 scattering: $t = (\frac{1}{\lambda})$, $\lambda = 2$ second order poles	99
4.18	K_2K_2 scattering: $t = (\frac{1}{\lambda})$, $\lambda = \frac{9}{4}$	100
4.19	K_2K_1 scattering: $t = (\frac{2}{3} - \frac{1}{2\lambda})$	101
4.20	K_2K_1 scattering: $t = (\frac{2}{3} - \frac{1}{2\lambda})$ at $\lambda = 2$	103
4.21	K_2K_1 scattering: $t = (\frac{2}{3} - \frac{1}{2\lambda})$ at $\lambda = \frac{9}{4}$	104
4.22	Interpolation of (a)Kink and (b)Anti-kink between vacua	118
4.23	$\mathcal{S}_1(\theta)$: Particle/Antiparticle scattering for $\lambda = 2$	119
4.24	$\mathcal{S}_2(\theta)$: Particle/Antiparticle scattering for $\lambda = 2$	119
5.1	Construction of dual lattice \mathcal{L}_D (dashed lines, empty circles) for lattice \mathcal{L} (solid lines, full circles)	129

5.2	Boundary scattering amplitude $R_a^b(\theta)$	136
5.3	Boundary Yang-Baxter	137
5.4	Boundary unitarity	138
5.5	Boundary ‘cross-unitarity’	139
5.6	Boundary bootstrap	140
5.7	Boundary coupling of bulk bound state	140
5.8	Two particle coupling to boundary	140
5.9	Kink reflection amplitude $R_{ba}^c(\theta)$	141
5.10	Kink boundary Yang-Baxter equations	142
5.11	Kink amplitudes $\mathcal{S}_0(\theta)$ and $\mathcal{S}_1(\theta)$	143
5.12	Kink amplitudes $\mathcal{S}_2(\theta)$, and $\mathcal{S}_3(\theta)$	143
5.13	Kink unitarity condition	144
5.14	Kink ‘cross-unitarity’ condition	144
5.15	Kink boundary bootstrap condition	145
5.16	Boundary coupling of bulk bound state at $\theta = \frac{i\pi}{6}$	145
5.17	Boundary coupling of bulk bound state at $\theta = \frac{i\pi}{2}$	146
5.18	$R_{ba}^a(\theta) = R_1(\theta)$	148
5.19	$R_{ba}^c(\theta) = R_2(\theta)$	148
5.20	Free boundary condition: Yang-Baxter equation 1.	150
5.21	Free boundary condition: Yang-Baxter equation 2.	150
5.22	Free boundary condition: Yang-Baxter equation 3.	151
5.23	Boundary scattering of breather bound states in $R_1(\theta)$	154
5.24	Boundary scattering of kink bound states in $R_2(\theta)$	154
5.25	Coupling of two kinks to boundary	154
5.26	Excited boundary state	156
5.27	Boundary scattering amplitudes $R_1(\theta)$ and $R_1^A(\theta)$	157
5.28	Boundary scattering amplitudes $R_2(\theta)$ and $R_2^A(\theta)$	157

5.29	Boundary Yang-Baxter conditions arising from $\frac{\pi}{2}$ pole in $R(\theta)$	158
A.1	$\mathcal{S}_{K_2K_2}^0: t = (\frac{1}{\lambda})$	166
A.2	Factorised scattering in Figure (A.1)	167

List of Tables

4.1	Poles and zeroes of non-scalar factors	76
4.2	Poles and zeroes of scalar factor $\Pi(\lambda t)$, $t = \frac{\theta}{i\pi}$	77
4.3	Overall pole structure of amplitudes	77
4.4	Bound state poles for $\mathcal{S}_0, \mathcal{S}_1, \mathcal{S}_2$ and \mathcal{S}_3	79
4.5	Pole structure for $K_2 K_2 \rightarrow K_2 K_2$ scattering	91
4.6	Bound state poles for $\mathcal{S}_{K_2 K_2}^0, \mathcal{S}_{K_2 K_2}^1, \mathcal{S}_{K_2 K_2}^2$ and $\mathcal{S}_{K_2 K_2}^3$	101
4.7	Pole structure for $K_2 K_1 \rightarrow K_1 K_2$ scattering	102
4.8	Bound state poles for $\mathcal{S}_{K_2 K_1}^0, \mathcal{S}_{K_2 K_1}^1, \mathcal{S}_{K_2 K_1}^2$ and $\mathcal{S}_{K_2 K_1}^3$	105
4.9	Pole structure of $\mathcal{S}_{B_1 K_2}$	106
4.10	Pole structure of $\mathcal{S}_{B_3 B_1}$	107
4.11	Pole structure of $\mathcal{S}_{B_3 B_3}$	108
4.12	Pole structure of $\mathcal{S}_{B_3 K_1}$	108
4.13	Pole structure of $\mathcal{S}_{B_3 K_2}$	109
4.14	Pole structure of $\mathcal{S}_{B_2 B_1}$	110
4.15	Pole structure of $\mathcal{S}_{B_2 B_2}$	110
4.16	Pole structure of $\mathcal{S}_{B_2 B_3}$	111
4.17	Pole structure of $\mathcal{S}_{B_2 K_1}$	111
4.18	Pole structure of $\mathcal{S}_{B_2 K_2}$	112
4.19	Pole structure of $\mathcal{S}_{B_5 B_1}$	113

4.20	Pole structure of $\mathcal{S}_{B_5 B_2}$	113
4.21	Pole structure of $\mathcal{S}_{B_5 B_2}$ continued	114
4.22	Pole structure of $\mathcal{S}_{B_5 B_3}$	114
4.23	Pole structure of $\mathcal{S}_{B_5 B_3}$ continued	115
4.24	Pole structure of $\mathcal{S}_{B_5 B_5}$	115
4.25	Pole structure of $\mathcal{S}_{B_5 B_5}$ continued	116
4.26	Pole structure of $\mathcal{S}_{B_5 K_1}$	116
4.27	Pole structure of $\mathcal{S}_{B_5 K_2}$	117
5.1	Pole structure of $P(\frac{\lambda\theta}{i\pi})$	152
5.2	Pole structure of $R_1(\theta)$, free boundary conditions	153
5.3	Pole structure of $R_2(\theta)$, free boundary conditions	153

Chapter 1

Statistical mechanics and field theory

The consideration of statistical mechanical models at second order phase transitions and their relation to conformal field theories and their perturbations underpins all the work to be presented in this thesis. Consequently, I shall begin by giving a brief introduction to these two areas by way of a particular example. The example I shall use will be that on which much of the following work is based, namely the q -state Potts model. I will initially approach this model from the point of view of statistical mechanics before moving on to discuss the relevant aspects of quantum field theory. For a more detailed discussion of statistical mechanical models, see [4] and [5]. Quantum field theory and critical phenomena are given an encyclopaedic treatment in [6], while [7] also touches on most of the material covered in this chapter.

1.1 Statistical mechanics

Statistical mechanics is concerned with modelling lumps of matter. In general, any model giving a realistic approximation of some physical system will have to include so many interactions as to be hopelessly intractable. The problem is thus one of constructing models that are simple enough to make calculation of their properties viable, but which do not lose the essential characteristics of the system being modelled. As a result it is considered quite acceptable to restrict attention to models in two dimensions instead of four, and allow only nearest neighbour interactions. As we shall see in the discussion of universality, taking only short range interactions into account may not alter certain properties of the system at all.

The basic object in statistical mechanics is the partition function, from which all thermodynamic properties of a particular system can be derived. For a statistical mechanical system in equilibrium at some finite temperature T , the relative probability of finding different configurations is given by the Boltzmann distribution, where the relative probability of a particular configuration is

$$P(\text{config}) = e^{-\mathcal{E}(\text{config})/k_B T}$$

where k_B is Boltzmann's constant. The partition function is then given by

$$\mathcal{Z} = \sum_{(\text{configs})} P(\text{config}) = \sum_{(\text{configs})} e^{-\mathcal{E}(\text{config})/k_B T}$$

where the sum is over all possible configurations of the system.

To give an example, a magnet can be modelled as a lattice having a spin σ_i associated with each site. These spins interact pairwise, with an

interaction energy of $J(\sigma_i, \sigma_j)$ between spins at neighbouring sites i and j . Each configuration of the system is then characterized by the particular set of values taken by the spins, $\{\sigma\}$, and the energy of a given configuration is thus

$$\mathcal{E}(\{\sigma\}) = \sum_{(i,j)} J(\sigma_i, \sigma_j)$$

Here, the sum is over all pairs of spins. Similarly, the partition function can be expressed as

$$\mathcal{Z} = \sum_{\{\sigma\}} P(\{\sigma\}) = \sum_{\{\sigma\}} e^{-\mathcal{E}(\{\sigma\})/k_B T}$$

Important information about a system is given by its correlation functions. These are the averaged values of quantities for the system at thermal equilibrium. For example, the average value of the spin at site i is given by

$$\langle \sigma_i \rangle = \frac{\sum_{\{\sigma\}} \sigma_i P(\{\sigma\})}{\sum_{\{\sigma\}} P(\{\sigma\})} = \frac{\sum_{\{\sigma\}} \sigma_i e^{-\mathcal{E}(\{\sigma\})/k_B T}}{\sum_{\{\sigma\}} e^{-\mathcal{E}(\{\sigma\})/k_B T}}$$

the factor of $1/\mathcal{Z}$ being necessary to normalize the probabilities. In a similar fashion, the correlation function between spins at sites i and j (the two-point spin correlation function) is

$$\langle \sigma_i, \sigma_j \rangle = 1/\mathcal{Z} \sum_{\{\sigma\}} \sigma_i \sigma_j P(\{\sigma\})$$

From this, the generalisation to n-point correlation functions is obvious. In fact, for such a system, all thermodynamic properties can be expressed in terms of the set of spin correlation functions. The most relevant of these to the following discussion is the correlation length ξ . This is a measure of the distance over which spins exert a significant effect on each other, ie. the value that a given spin σ takes will reflect its interaction with those spins

situated within a distance of order ξ , with those spins further away exerting a negligible effect on σ . When ξ is finite, it is related to the connected two-point function $\langle \sigma_i, \sigma_j \rangle_C$ when the distance r between i and j is large by

$$\langle \sigma_i, \sigma_j \rangle_C = \langle \sigma_i, \sigma_j \rangle - \langle \sigma_i \rangle \langle \sigma_j \rangle = \frac{e^{-r/\xi}}{r^\tau} \quad (1.1)$$

In the following sections I will primarily be concerned with manipulations of this quantity in order to draw out points of interest.

1.1.1 The q -state Potts model

The statistical mechanical model to be considered in this section was first defined by R.B.Potts [8], and the following discussion will draw heavily on that given in [4]. Although the Potts model may be defined in a more general way, I will restrict my discussion to a two-dimensional square lattice \mathcal{L} consisting of N sites. At each site i , there is an associated quantity σ_i which can take any one of q different values, say $1, 2, \dots, q-1, q$. As is usual, I will refer to σ_i as a ‘spin’. The interaction energy between adjacent spins σ_i and σ_j is defined to be $-J\delta(\sigma_i, \sigma_j)$, where

$$\begin{aligned} \delta(\sigma_i, \sigma_j) &= 1 && \text{if } \sigma_i = \sigma_j \\ &= 0 && \text{if } \sigma_i \neq \sigma_j \end{aligned}$$

This can be associated with the edge (i, j) joining the two spins. The total energy is then

$$\mathcal{E} = -J \sum_{(i,j)} \delta(\sigma_i, \sigma_j)$$

where the summation is over all edges. Using this, we can write the partition function as

$$\mathcal{Z}_N = \sum_{\sigma} \exp \left(\frac{J}{k_B T} \sum_{(i,j)} \delta(\sigma_i, \sigma_j) \right)$$

where k_B is Boltzmann's constant, T is the temperature, and the outer sum is over all possible spin combinations (giving q^N terms). This can be rewritten as

$$\mathcal{Z}_N = \sum_{\sigma} \prod_{(i,j)} [1 + K \delta(\sigma_i, \sigma_j)] \quad (1.2)$$

where $K = e^{\frac{J}{k_B T}} - 1$. On expanding the product, we get a sum of 2^N terms, and we can associate a unique graph \mathcal{G} with each term as follows. In a given term, there will be a factor of either 1 or $K \delta(\sigma_i, \sigma_j)$ for each edge (i, j) . If the factor $K \delta(\sigma_i, \sigma_j)$ appears then place a bond on the corresponding edge of \mathcal{L} , leaving all edges where the factor 1 appears empty.

Now consider a general term in the expansion, represented by a graph \mathcal{G} with ν bonds, and C connected components, a connected component being a chain of spins joined by bonds or an isolated site having no bonds associated with it. Such a term will have a factor of K^ν associated with it, the presence of the delta functions meaning that all spins in a connected component must be the same. As each connected component can assume q different spin states the sum over all spin combinations will give a weight of q^C to the term, leading to a total contribution of $K^\nu q^C$ to \mathcal{Z}_N . Summing over all graphs \mathcal{G} which can be drawn on \mathcal{L} we get

$$\mathcal{Z}_N = \sum_{\mathcal{G}} K^\nu q^C \quad (1.3)$$

as was shown by Kasteleyn and Fortuin [9]. Note that in this formulation q need not be integer, and may be taken to be any real number. While this

may be of use formally, the physical interpretation is not immediately clear. If we generalize the above treatment to allow for different couplings J_1 and J_2 in the horizontal and vertical directions respectively, equation (1.3) becomes

$$\mathcal{Z}_N = \sum_{\mathcal{G}} K_1^{\nu_1} K_2^{\nu_2} q^C \quad (1.4)$$

where ν_1 and ν_2 are the number of bonds on horizontal and vertical edges respectively, and

$$K_r = \exp(J_r/k_B T) - 1$$

In what follows, I shall assume that both J_1 and J_2 are positive. As a result the system is ferromagnetic, ie. adjacent spins will tend to align — this being the configuration with lowest interaction energy.

1.1.2 Ice-type formulation and location of the critical point

In order to show that the square-lattice Potts model satisfies a duality relation and hence find the critical point, it is convenient to recast the form of \mathcal{Z}_N . As a preliminary step, we must first change the formulation of \mathcal{Z}_N and consider its representation on the medial lattice instead.

Formulation of \mathcal{Z}_N on the medial lattice \mathcal{L}'

The medial lattice \mathcal{L}' can be defined as follows. Draw polygons around sites of \mathcal{L} such that

1. No polygons overlap, and no polygon surrounds another.
2. Polygons of non-adjacent sites have no common corners.

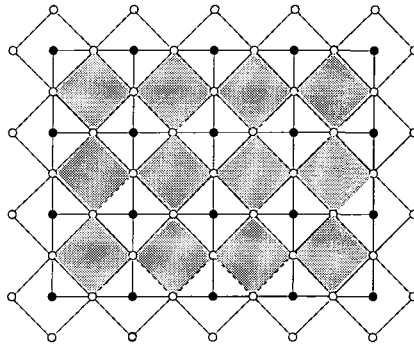


Figure 1.1: Medial lattice \mathcal{L}' (empty circles) around \mathcal{L} (solid circles)

3. Polygons of adjacent sites i and j have one and only one common corner, and this lies on the edge (i, j) .

Take the corners of these polygons to be the sites of \mathcal{L}' — from now on I shall call these polygons ‘basic polygons’. There are two types of site on \mathcal{L}' , internal sites which are common to two basic polygons, and external sites which lie on only one basic polygon. In the case of the square lattice there is an obvious choice for the medial lattice, being that with sites of \mathcal{L}' situated at the midpoint of the edges of \mathcal{L} , and the sites of \mathcal{L} in the middle of the basic polygons. This is shown in figure 1.1. Obviously, we now have two types of internal site on \mathcal{L}' — those situated on horizontal and those on vertical edges of \mathcal{L} — for the case of $J_1 \neq J_2$.

There is a 1 – 1 correspondence between graphs \mathcal{G} on \mathcal{L} and polygon decompositions on \mathcal{L}' : if \mathcal{G} has no bond on an edge (i, j) then separate the basic polygons of \mathcal{L}' that meet at the midpoint of (i, j) , whereas if there is a bond on (i, j) then separate the edges of \mathcal{L} so as to join the two basic polygons together (see figure 1.2). A connected component on \mathcal{L} will therefore become

a joined group of basic polygons having a polygon as an outer perimeter and, if it contains closed loops, one or more internal polygons. A particular decomposition on \mathcal{L}' is thus made up of p distinct polygons where

$$p = C + S, \quad (1.5)$$

denoting the number of connected components of \mathcal{G} by C , and the number of internal polygons by S .

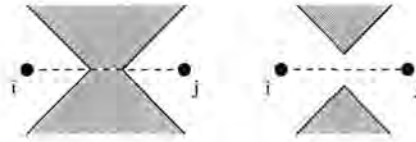


Figure 1.2: Separation of edges for (a) no bond on (i, j) and (b) bond on (i, j)

For a graph \mathcal{G} in the decomposition of \mathcal{Z}_N the quantities S , C , N , and ν are not independent. If \mathcal{G} has no bonds, then $C = N$. If we introduce bonds onto the graph but don't form closed loops, then the number of sites in a connected component C_i = the number of bonds in it $(\nu_i) + 1$. If we now allow closed loops in C_i , then the bond that closes the loop does not introduce a new site, so the number of sites in $C_i = (\nu_i - S_i) + 1$, where S_i is the number of closed loops in C_i . In this most general case, we can see that

$$N = \sum_i (\nu_i - S_i + 1) = \nu - S + C$$

where the sum is over all connected components C_i . Combining this with (1.5) we can express C as

$$C = (p - \nu + N)/2 \quad (1.6)$$

which identity can then be used in equation (1.4) to give

$$\mathcal{Z}_N = q^{N/2} \sum_{p.d.} q^{p/2} x_1^{\nu_1} x_2^{\nu_2} \quad (1.7)$$

where

$$x_i = q^{-1/2} K_i$$

and the sum is over all polygon decompositions on \mathcal{L}' . In this formulation ν_i — the number of bonds of type i on \mathcal{L} — becomes the number of sites of type i on \mathcal{L}' where the edges have been separated to join basic polygons.

The final step in this reformulation is to make all factors in the sum over polygon decompositions independent of global considerations. The x_r already depend solely on the circumstances at each individual site, whereas the factor of $q^{p/2}$ clearly does not. If we now define λ and z such that

$$q^{1/2} = 2 \cosh(\lambda) \quad \text{and} \quad z = e^{\lambda/2\pi}$$

then we can make $q^{p/2}$ local by the following trick. Place arrows on the edges of the polygons on \mathcal{L}' so that there is one arrow pointing towards, and one arrow pointing away from each corner of each polygon. Now, give each corner a weight of z^α , where α is the angle turned to the left when passing around the corner in the direction of the arrows (for the square lattice $\alpha = \pm\frac{\pi}{2}$).

For each polygon, the sum of all angles $\alpha = \pm 2\pi$, depending on whether they form an anti-clockwise or clockwise circuit of the polygon. This means that the product of weights $z^\alpha = z^{\pm 2\pi} = e^{\pm\lambda}$. If we allow both possibilities,

then the total weight associated with each polygon will be $q^{1/2}$ allowing us to write

$$\mathcal{Z}_N = q^{N/2} \sum_{p.d.} x_1^{\nu_1} x_2^{\nu_2} \sum_{a.c.} \prod_m z^{\alpha_m} \quad (1.8)$$

where the inner sum is over all allowed arrow coverings, and the product is over all polygon corners m , with α_m being the corresponding angle.

Ice-type formulation

At each internal site of \mathcal{L}' there are two ways of separating the edges, and for each of these there are four ways of placing arrows. In each case there are two arrows into, and two arrows out of each site, satisfying the ice rule. These are shown in figure 1.3, together with their corresponding contribution to \mathcal{Z}_N .

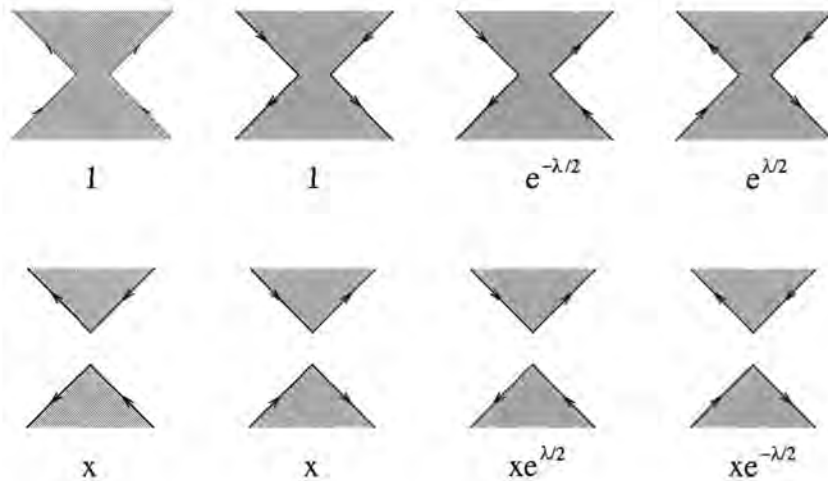


Figure 1.3: Arrow configurations on \mathcal{L}' and their respective weights

Without separating any edges and decomposing into polygons, let us

consider the possible arrangements of arrows satisfying the ice rule at an internal site. There are six distinct arrangements as shown in figure 1.4.

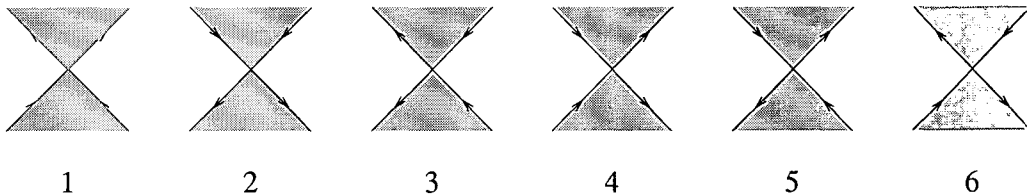


Figure 1.4: Distinct arrow configurations on \mathcal{L}'

Comparing figures 1.3 and 1.4 we can see that arrangements 1 to 4 in 1.4 correspond to unique edge separations and hence unique weights at each site. On the other hand 5 and 6 can appear for both edge separations, so each have two associated weights. The sum over polygon decompositions is thus almost implicit in a sum over all arrow configurations satisfying the ice rule. We can make it so by simply summing the relevant weights for configurations 5 and 6. Now, for a particular arrow covering of \mathcal{L}' , the contribution to \mathcal{Z}_N is a product over all sites of the weight occurring at each site. The composite weights of 5 and 6 ensure that both possible edge separations are taken into account each time they occur. This gives the final formulation of \mathcal{Z}_N as

$$\mathcal{Z}_N = q^{N/2} \sum_{a.c. \text{ sites}} \prod (\text{weights}) \quad (1.9)$$

The sum is now over all arrow coverings satisfying the ice rule at each internal site and with one arrow into and one arrow out of each external site. The product is over all sites of \mathcal{L}' . Each external site contributes a weight of $e^{\pm\lambda/4}$, and each internal site a weight ω_k ($k = 1, \dots, 6$) corresponding to the particular arrow arrangement in figure 1.4. For a site of type r , these weights are $\omega_1, \dots, \omega_6 = 1, 1, x_r, x_r, e^{-\lambda/2} + x_r e^{\lambda/2}, e^{\lambda/2} + x_r e^{-\lambda/2}$. Looking at figure 1.4,

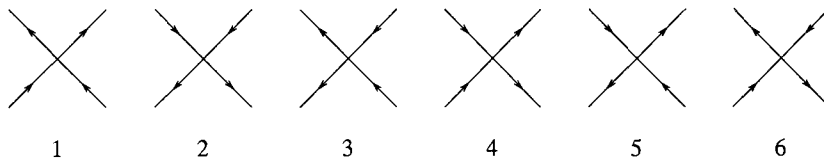
we can see that these weights are for arrow configurations oriented such that the basic polygons are to the left and right of the site. Whilst this is the case for sites of type 1, for type 2 sites the corresponding arrow configurations have to be rotated by 90° . Relabelling the weights so that they depend on the arrow configurations alone, we have

$$\omega_1, \dots, \omega_6 = 1, 1, x_1, x_1, e^{-\lambda/2} + x_1 e^{\lambda/2}, e^{\lambda/2} + x_1 e^{-\lambda/2} \quad (1.10)$$

as before for sites of type 1, and for sites of type 2

$$\omega_1, \dots, \omega_6 = x_2, x_2, 1, 1, e^{\lambda/2} + x_2 e^{-\lambda/2}, e^{-\lambda/2} + x_2 e^{\lambda/2} \quad (1.11)$$

The respective arrow configurations being



Duality relation and location of the critical point

Using the ice-type formulation of \mathcal{Z}_N , it is a simple matter to see that the q -state Potts model satisfies a duality relation on the square lattice. It can be seen that by replacing x_1, x_2 with x_2^{-1}, x_1^{-1} in (1.10) and (1.11), then multiplying all type 1 weights by x_2 and all type 1 weights by x_1 we interchange the two types of weight. Although this may change any boundary conditions imposed on the lattice, we do not expect it to significantly affect the large N limit of \mathcal{Z}_N . Treating \mathcal{Z}_N as a function of x_1 and x_2 we can thus write, for large N ,

$$\mathcal{Z}_N(x_1, x_2) = (x_1 x_2)^N \mathcal{Z}_N(x_2^{-1}, x_1^{-1}) \quad (1.12)$$

This is a duality relation which sets up a correspondence between a high temperature Potts model (x_1 and x_2 small), and a low temperature (x_1 and x_2 large) one. This was first derived by Potts [8]. It is to be expected that at low temperatures the ferromagnetic Potts model will be ordered, with spins predominantly taking one particular value. At high temperatures, we expect the model to exhibit a disordered phase, where no one spin state is dominant on the lattice as a whole — each being equally likely at each individual site. At some critical temperature T_c between these two phases, we expect to see a transition from one phase to the other. This will be characterised by the free energy becoming non-analytic along a line in the (x_1, x_2) plane. The dimensionless free energy per site taken as a function of x_1 and x_2 is defined as

$$\psi(x_1, x_2) = - \lim_{N \rightarrow \infty} N^{-1} \ln \mathcal{Z}_N$$

and we expect it to be analytic everywhere except at such a phase transition. In terms of ψ , equation (1.12) becomes

$$\psi(x_1, x_2) = - \ln(x_1 x_2) + \psi(x_2^{-1}, x_1^{-1}) \quad (1.13)$$

If ψ is non-analytic on a line in the region $x_1 x_2 < 1$, then by equation (1.13) it will also be non-analytic on a line in the region $x_1 x_2 > 1$. The line $x_1 x_2 = 1$ is unique in that it is self-dual, so the simplest solution is that ψ is non-analytic on this line alone. This assumes that there is only a single phase transition which, although true for the model under discussion, is not necessarily the case. In later chapters the isotropic ($J_1 = J_2 = J$) Potts model will be of particular interest. In this case $x_1 = x_2 = x$, and the critical point is located at $K = K_C = \sqrt{q}$.

In going from the high to the low temperature phase, blocks of spins order themselves such that one spin value predominates. The size of these blocks is of order ξ . For $q > 4$, ξ is always finite and the model undergoes a first order phase transition at the critical point [10]. The behaviour of the model is radically altered when ξ becomes infinite at the critical point, as is the case for $q \leq 4$. Such phase transitions, where ξ becomes infinite at the critical point, are denoted second order phase transitions. As we shall see below, these play a very important role in the study of statistical mechanical systems and their related quantum field theories (see, for example, [6]).

1.2 Universality and the renormalization group

Consider the square-lattice Potts model with $q \leq 4$, close to the critical point, and let the number of sites N be large enough that finite size effects can be neglected for the following discussion. Now replace every block of 4 spins with one at their centre, whose value reflects their average. As the model is close to the critical point, ξ will be very large, and the 4 spins in any one block will be highly correlated. Consequently, it is to be expected that the spin distributions of this approximate lattice will, on a large scale, be the same as the original lattice and hence it will have the same macroscopic properties. If we continue with this program of coarse-graining, at some point the properties of the lattice will begin to change, and the spin distributions will look quite different from that of the original lattice. This will happen when the size of the section of the original lattice now blocked into one spin is of the same order as the correlation length. When the model is exactly at its critical point, ξ becomes infinite and all spins are highly correlated. As a result, no matter how many times we coarse grain the lattice, it will always

look the same and have the same macroscopic properties — until, of course, the fact that it is of finite size becomes relevant.

1.2.1 Universality

As we have just seen, when a system is undergoing a second order phase transition its large scale properties are independent of the details of its microscopic interactions. In fact, the properties of such a system — for example its specific heat, correlation length, etc. — have a power law dependence on each other close to the critical point, the exponents of these power laws being denoted critical exponents. This insensitivity to small scale interactions leads to the phenomenon of universality whereby many disparate systems can be grouped into classes through a consideration of their large scale features alone. The systems in a given universality class are described by the same set of critical exponents when in the scaling region close to criticality.

1.2.2 The Renormalization Group

Although the above discussion is very imprecise, it should be enough to get across the basic ideas behind the renormalization group. It should be stressed that although the renormalization group approach only really works for systems with short-range interactions, when it *does* work the precise details of those interactions are unimportant, leading to the phenomenon of universality. I shall now treat this in a (slightly) more detailed fashion.

Essentially we start with the original, unscaled model for which the set of possible spin configurations and the relative probabilities of each appearing is determined by its spin correlation functions. These can in turn be calcu-

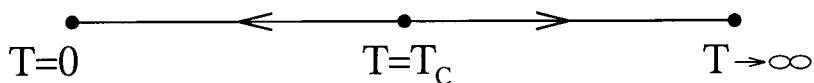
lated from $\mathcal{E}(\{\sigma\})$ as we have seen above. By performing the coarse-graining procedure on a representative set of spin configurations, a new set of configurations would be obtained with its corresponding set of probabilities. We now assume that it is possible to construct a new function $\mathcal{E}'(\{\sigma'\})$ from which this new set of configurations / correlation functions can be calculated, and for which only short-range interactions are important. It is always possible to find an $\mathcal{E}'(\{\sigma'\})$ which will produce the correct set of correlation functions, but in general it will include interactions between spins at arbitrary separations and it is not at all obvious that short range interactions will dominate. In practice one would deal directly with the effect of the chosen coarse-graining procedure on $\mathcal{E}(\{\sigma\})$ without considering the effect on a set of configurations directly. Here, the latter approach is used to convey the underlying physical picture without getting bogged down in technical manipulations of partition functions.

For example, in the treatment of the Potts model \mathcal{E} contained only nearest neighbour interactions with coupling constants J_1 and J_2 . In the scaled model, keeping only nearest neighbour interactions again, there will be a new pair of coupling constants J'_1 and J'_2 which will depend on J_1 and J_2 . The J and J' couplings are related by renormalization group equations, and the procedure of going from the unscaled to the scaled model is denoted a renormalization group transformation.

The use of the renormalization group lies in the location of fixed points of the renormalization group transformation, and the identification of flows between them. As an example, I turn once more to the q -state Potts model for $q \leq 4$. As we have already seen, ξ becomes infinite at the critical point and the resulting spin configurations are invariant under any number of iterations

of the renormalization group transformation. The critical point is thus a fixed point of the transformation and is characterised by the critical temperature T_C which in turn depends on J_1 and J_2 as can be seen from the definition of the x_i following equation (1.7). If instead we start close to T_C , either slightly above or slightly below, then under repeated iterations of the renormalization group transformation the size of the correlation length, measured in terms of the number of lattice sites it spans, decreases and the system moves further and further away from criticality into the high or low temperature region respectively.

The Potts model has two other fixed points under the renormalization group transformation which I have yet to consider. These are the $T \rightarrow 0$ and $T \rightarrow \infty$ limits of the model. As $T \rightarrow 0$, the interaction energy between pairs of spins $-J/k_B T \rightarrow -\infty$ and all spins will become aligned in the same direction. As $T \rightarrow \infty$, $J/k_B T \rightarrow 0$ and the spins effectively become decoupled from each other at high temperatures. In this case each spin has an equal probability of taking any of the allowed values leading to completely uncorrelated spin distributions. For both of these limits the correlation length $\xi = 0$ as can easily be seen from equation (1.1), and thus both are invariant under the scaling procedure of the renormalisation group. If we start with a spin configuration close to either of these fixed points, then iterations of the renormalisation group transformation will drive the configuration closer, so unlike the previous case, these two fixed points are stable under the renormalisation group transformation. We can summarize the above discussion diagrammatically, showing the renormalisation group flow of the model as



1.2.3 Behaviour close to criticality

If we denote the set of couplings of a given model by $\{J_\alpha\}$, then under the coordinate scaling $r \rightarrow r' = b^{-1}r$ these transform to a new set $\{J'_\alpha\}$ given by

$$J'_\alpha = R(\{J_\alpha\})$$

where the function R depends on the scale factor b , and the particular coarse-graining procedure implemented. The critical point is characterized by the set of couplings $\{J_\alpha^*\}$ which are invariant under the renormalisation group transformation:

$$J_\alpha^* = R(\{J_\alpha^*\})$$

Assuming that R is analytic at the fixed point, then in some neighbourhood of this point it can be approximated as

$$J'_\alpha - J_\alpha^* = \sum_\beta T_{\alpha\beta}(J_\beta - J_\beta^*)$$

where $T_{\alpha\beta} = \partial J'_\alpha / \partial J_\beta |_{J=J^*}$. The matrix T will have eigenvectors τ_α^i and corresponding eigenvalues λ^i which satisfy

$$\sum_\alpha \tau_\alpha^i T_{\alpha\beta} = \lambda^i \tau_\beta^i$$

from which we can construct composites of the coupling constants which have a simple behaviour under the renormalisation group transformation close to the fixed point. Defining the scaling variables u_i by

$$u_i = \sum_\alpha \tau_\alpha^i (J_\alpha - J_\alpha^*)$$

then under the renormalisation group transformation

$$u'_i = \sum_{\alpha} \tau_{\alpha}^i (J'_{\alpha} - J_{\alpha}^*) = \sum_{\alpha, \beta} \tau_{\alpha}^i T_{\alpha\beta} (J_{\beta} - J_{\beta}^*) = \sum_{\beta} \lambda^i \tau_{\beta}^i (J_{\beta} - J_{\beta}^*) = \lambda^i u_i$$

Defining the renormalisation group eigenvalues by $\lambda^i = b^{y_i}$ we can classify the scaling variables by their behaviour close to the fixed point as follows.

- If $y_i > 0$ then under repeated iterations of R , u_i will move further and further away from its fixed point value as $J'_{\alpha} - J_{\alpha}^*$ becomes increasingly large. In this case u_i is said to be *relevant*.
- If $y_i < 0$ then u_i will move towards its fixed point value under repeated iterations of R . In this case, u_i is said to be *irrelevant*.
- If $y_i = 0$ then u_i is said to be *marginal*.

In the space of all couplings, the irrelevant scaling variables form the basis of a hypersurface called the critical surface. If the set of coupling constants $\{J_{\alpha}\}$ of a particular model lie on this surface, then under renormalisation group transformations $\{J_{\alpha}\}$ will flow to their critical values $\{J_{\alpha}^*\}$ and the model's large distance behaviour will be determined by that of the fixed point.

If J_{α} is coupled to some function of spins $s_{\alpha}(\sigma)$, then u_i will be coupled to the scaling density ϕ_i defined by

$$\phi_i = \sum_{\alpha} \tau_{\alpha}^i s_{\alpha}(\sigma)$$

and the total energy $\mathcal{E} = \mathcal{E}(\{J_{\alpha} s_{\alpha}(\sigma)\})$ may be expressed as a function of these densities

$$\mathcal{E} = \mathcal{E}(\{u_i \phi_i\}).$$

It is possible to continue the above analysis and to extract more information about a given model such as its critical exponents, but such details are not necessary for the present discussion.

As we have seen, at a second order phase transition a statistical mechanical model becomes correlated over all length scales. If we let the lattice spacing $a \rightarrow 0$, the discrete lattice of spins σ_i becomes a continuous distribution $\sigma(r)$, where r is the position vector. In taking this continuum limit, the correlation length in terms of lattice units ξ_a tends to infinity in such a way that the physical correlation length $\xi = a\xi_a$ remains constant. The system thus approaches the critical surface, becoming invariant under rotations and translations. If we then let $\xi \rightarrow \infty$, the continuum theory acquires an additional invariance under dilatations.

If we allow σ to take a continuous range of values, then in the continuum limit the partition function and spin correlation functions will take the forms

$$\mathcal{Z} = \int [d\sigma] e^{-\mathcal{E}(\sigma)/k_B T} \quad (1.14)$$

$$\langle \sigma(r_1)\sigma(r_2)\dots\sigma(r_n) \rangle = \frac{\int [d\sigma] \sigma(r_1)\sigma(r_2)\dots\sigma(r_n) e^{-\mathcal{E}(\sigma)/k_B T}}{\int [d\sigma] e^{-\mathcal{E}(\sigma)/k_B T}} \quad (1.15)$$

The discrete sum has been replaced by an integration over what is now a continuous set of possible spin distributions, and I have given the general form for the correlation of spins at n points $r_1 \dots r_n$. As we shall see in the next section such models are intimately related to quantum field theories. These will be massive theories for finite ξ (mass being related to correlation length by $m \sim \xi^{-1}$), becoming massless in the limit $\xi \rightarrow \infty$.

1.3 Quantum field theory

1.3.1 Path integrals and quantum mechanics

The state of a quantum mechanical system at any given time is described by a state vector $|\psi\rangle$ belonging to a complex linear vector space \mathcal{H} . The time evolution of $|\psi\rangle$ is determined by a Hamiltonian operator \hat{H} through Schrödinger's equation:

$$i\hbar \frac{d|\psi\rangle}{dt} = \hat{H}|\psi\rangle \quad (1.16)$$

Generally, $|\psi\rangle$ can be written as

$$|\psi\rangle = \sum_n c_n |o_n\rangle$$

where the $|o_n\rangle$ are orthogonal, observable states (eg. position). The probability that we observe the state $|o_n\rangle$ is then $|c_n|^2$, and after $|o_n\rangle$ has been observed the state of the system becomes $|o_n\rangle$.

If the Hamiltonian \hat{H} is time independent, then this has the formal solution

$$|\psi(t)\rangle = e^{-\frac{i}{\hbar}\hat{H}(t-t_0)}|\psi(t_0)\rangle \quad (1.17)$$

For a particle of mass m moving in a potential well $V(x)$, \hat{H} has the form

$$\hat{H} = \frac{\hat{p}^2}{2m} + V(\hat{q})$$

where \hat{p} is the momentum operator and \hat{q} is the position operator. The probability amplitude for such a particle to go from x_a to x_b in a time δt is

$$\langle x_b | e^{-\frac{i}{\hbar}\hat{H}\delta t} | x_a \rangle = \langle x_b | e^{-\frac{i}{\hbar}\frac{\hat{p}^2}{2m}\delta t - \frac{i}{\hbar}V(\hat{q})\delta t} | x_a \rangle \quad (1.18)$$

Here we are working in the basis formed by position eigenstates $|x\rangle$, satisfying

$$\hat{q}|x\rangle = x|x\rangle$$

$$\int dx|x\rangle\langle x| = \hat{I}$$

where \hat{I} is the identity operator, $\hat{I}|\psi\rangle = |\psi\rangle$. For infinitesimal δt , we can write (1.18) as

$$\begin{aligned} \langle x_b|e^{-\frac{i}{\hbar}\frac{\hat{p}^2}{2m}\delta t}e^{O(\delta t^2)}e^{-\frac{i}{\hbar}V(\hat{q})\delta t}|x_a\rangle &= \langle x_b|e^{-\frac{i}{\hbar}\frac{\hat{p}^2}{2m}\delta t}|x_a\rangle e^{-\frac{i}{\hbar}V(x_a)\delta t} \\ &= \left(\frac{2\pi i\hbar\delta t}{m}\right)^{-\frac{1}{2}}e^{-\frac{im}{2\hbar}\frac{(x_b-x_a)^2}{\delta t}}e^{-\frac{i}{\hbar}V(x_a)\delta t} \end{aligned}$$

The first line follows from a general result for operators \hat{a} , \hat{b} with $[\hat{a}, \hat{b}] \neq 0$, which states that $e^{\hat{a}+\hat{b}} = e^{\hat{a}}e^{-\frac{1}{2}[\hat{a}, \hat{b}]}e^{\hat{b}}$. The $\langle x_b|e^{-\frac{i}{\hbar}\frac{\hat{p}^2}{2m}\delta t}|x_a\rangle$ term is just the free particle propagator, which is written explicitly in the second line. In practice, we will want to be able to calculate transition amplitudes from x_a at time t_a to x_b at time t_b where $t_b - t_a$ is finite. By splitting $t_b - t_a$ into n small time intervals (so $t_0 = t_a$, $t_n = t_b$, etc.) we can write $\langle x_b, t_b||x_a, t_a\rangle$ as

$$\langle x_b|e^{-\frac{i}{\hbar}\hat{H}(t_b-t_a)}|x_a\rangle = \lim_{n\rightarrow\infty} \int dx_{n-1} \dots \int dx_1 \langle x_b|e^{-\frac{i}{\hbar}\hat{H}(t_b-t_{n-1})}|x_{n-1}\rangle \dots \langle x_1|e^{-\frac{i}{\hbar}\hat{H}(t_1-t_a)}|x_a\rangle$$

where the integrals ensure that all possible paths from x_a to x_b are taken into account. Using the fact that $\int dx|x\rangle\langle x| = \hat{I}$ the expression for $\langle x_b, t_b||x_a, t_a\rangle$ becomes

$$\lim_{n\rightarrow\infty} \int \prod_{j=1}^{n-1} dx_j \left(\frac{2\pi i\hbar(t_j-t_{j-1})}{m}\right)^{-\frac{1}{2}} \left(\frac{2\pi i\hbar(t_n-t_{n-1})}{m}\right)^{-\frac{1}{2}} e^{\frac{i}{\hbar} \sum_{j=1}^{n-1} \frac{m}{2} \frac{(x_j-x_{j-1})^2}{(t_j-t_{j-1})} - (t_j-t_{j-1})V(x_{j-1})} \quad (1.19)$$

Assuming that this limit exists,

$$\langle x_b, t_b | x_a, t_a \rangle = \int [dx] e^{\frac{i}{\hbar} S} \quad (1.20)$$

where the integration is over all paths $x(t)$ such that $x(t_a) = x_a$ and $x(t_b) = x_b$. S is given by

$$\begin{aligned} S &= \int_{t_a}^{t_b} \left(\frac{m}{2} \left(\frac{dx}{dt} \right)^2 - V(x) \right) dt \\ &= \int_{t_a}^{t_b} \mathcal{L} dt \end{aligned}$$

This is just the classical action for the trajectory $x(t)$. The generalisation to fields $\phi_a(x^\mu)$ in an n -dimensional space-time with coordinates $x^\mu = x^0, x^1, \dots, x^{n-1}$ ($x^0 = t$ as is conventional) is straightforward. The action S will now be a function of the $\phi_a(x^\mu)$, and the integration is now over all field configurations subject to the obvious boundary conditions. Of primary importance in field theory are the time-ordered expectation values of fields, defined by

$$\langle 0 | \mathcal{T} \phi_1(x^{\mu_1}) \phi_2(x^{\mu_2}) \dots \phi_n(x^{\mu_n}) | 0 \rangle = \int [d\phi] e^{\frac{i}{\hbar} S[\phi]} \phi_1 \phi_2 \dots \phi_n \quad (1.21)$$

The integration is over all paths with fields ϕ_α at x^α and the time ordering \mathcal{T} meaning that the ϕ_α on the lefthand side are ordered by increasing value of x^0 from right to left.

1.3.2 Connection with statistical mechanics

Comparing equation (1.15) for the statistical mechanical correlation functions in the infinite volume continuum limit, with equation (1.21) for the expectation values of fields in a quantum mechanical system it can be seen that they are similar in many respects. These are summed up in the table below.

Quantum field theory	Statistical mechanics
<p>system in $1 + N$ dimensions</p> <p>$(x^\mu = x^0(= t), x^1, \dots, x^N)$</p> <p>$\frac{1}{\hbar}$</p> <p>$S[\phi]$</p> <p>generating function $\mathcal{Z} = \int [d\phi] e^{\frac{i}{\hbar} S[\phi]}$</p> <p>time-ordered expectation values</p> <p>ground state</p>	<p>system in $0 + (N + 1)$ dimensions</p> <p>$r = r^1, \dots, r^N, r^{N+1}(= -it)$</p> <p>$\frac{1}{k_B T}$</p> <p>$\mathcal{E}[\sigma]$</p> <p>partition function $\mathcal{Z} = \int [d\sigma] e^{-\frac{1}{k_B T} \mathcal{E}[\sigma]}$</p> <p>correlation functions</p> <p>equilibrium state</p>

In fact, it is possible to construct a statistical mechanical system from a quantum field theory, but not all sets of statistical mechanical correlation functions can be analytically continued to give expectation values of a unitary quantum field theory. For this to be possible, the statistical mechanical model must satisfy various conditions, such as the Osterwalder-Schrader condition (for a discussion of these issues, see Parisi [7]).

Chapter 2

Conformal field theory

2.1 Conformal symmetry

The connection between conformal field theories and statistical mechanical systems at second order phase transitions was first noted by Polyakov in [11]. The ramifications of this link were studied by Belavin, Polyakov and Zamolodchikov [12], laying the foundation for a large body of subsequent work. This chapter will of necessity only touch this work lightly, and more extensive reviews can be found in [13], [14] and [15]. We have already seen that such statistical mechanical systems are invariant under the scaling transformations of the renormalisation group. In the related field theories this manifests as invariance under conformal transformations, being those which leave the metric $\eta_{\mu\nu}(x)$ unchanged up to a local scale transformation ie. under $x \rightarrow x'$ the metric transforms as

$$\eta_{\mu\nu}(x) \rightarrow \eta'_{\mu\nu}(x') = \Omega(x)\eta_{\mu\nu}(x) \quad (2.1)$$

Such transformations preserve the angle θ between vectors as can be checked by performing a conformal transformation on the relation $\cos(\theta) =$

$\frac{v \cdot w}{|v||w|}$. The inner product is defined by $v \cdot w = v^\mu w^\nu \eta_{\mu\nu}$ as usual.

Under infinitesimal coordinate transformations $x^\mu \rightarrow x^\mu + \epsilon^\mu$, the line element $ds^2 = \eta_{\mu\nu} dx^\mu dx^\nu$ transforms as

$$ds^2 \rightarrow ds^2 + (\partial_\mu \epsilon_\nu + \partial_\nu \epsilon_\mu) dx^\mu dx^\nu$$

In order that equation (2.1) is satisfied under such a transformation, we require that

$$\partial_\mu \epsilon_\nu + \partial_\nu \epsilon_\mu = f(x) \eta_{\mu\nu} \quad (2.2)$$

The precise form of $f(x)$ can be fixed by acting on both sides with $\eta^{\mu\nu}$, giving $2\partial \cdot \epsilon = f(x)d$ where d is the number of space-time dimensions ($\eta_{\mu\nu} \eta^{\mu\nu} = d$). Condition (2.2) thus becomes

$$\partial_\mu \epsilon_\nu + \partial_\nu \epsilon_\mu = \frac{2}{d} (\partial \cdot \epsilon) \eta_{\mu\nu} \quad (2.3)$$

In two dimensions with the metric $\eta_{\mu\nu} = \delta_{\mu\nu}$, (2.3) become the Cauchy-Riemann equations

$$\partial_1 \epsilon_1 = \partial_2 \epsilon_2 \quad \partial_1 \epsilon_2 = -\partial_2 \epsilon_1$$

It is therefore natural to introduce complex coordinates z and \bar{z} such that

$$\begin{aligned} z &= x^1 + ix^2 & \bar{z} &= x^1 - ix^2 \\ \epsilon(z) &= \epsilon^1 + i\epsilon^2 & \bar{\epsilon}(\bar{z}) &= \epsilon^1 - i\epsilon^2 \end{aligned}$$

With this choice of coordinates it becomes clear that the group of two dimensional conformal transformations is isomorphic to the group of analytic coordinate transformations

$$z \rightarrow f(z), \quad \bar{z} \rightarrow \bar{f}(\bar{z})$$

which is infinite dimensional. Under such transformations, the line element transforms as

$$ds^2 = dzd\bar{z} \rightarrow \left(\frac{\partial f}{\partial z}\right) \left(\frac{\partial \bar{f}}{\partial \bar{z}}\right) dzd\bar{z} = \left|\frac{\partial f}{\partial z}\right|^2 dzd\bar{z},$$

and so $\Omega = |\partial f/\partial z|^2$. The infinitesimal form of these transformations can be written as

$$z \rightarrow z' = z + \epsilon_n(z) \quad \bar{z} \rightarrow \bar{z}' = \bar{z} + \bar{\epsilon}_n(\bar{z}) \quad (n \in \mathcal{Z})$$

where

$$\epsilon_n(z) = -z^{n+1} \quad \bar{\epsilon}_n(\bar{z}) = -\bar{z}^{n+1}.$$

The corresponding infinitesimal generators are

$$l_n = -z^{n+1}\partial_z \quad \bar{l}_n = -\bar{z}^{n+1}\partial_{\bar{z}} \quad (n \in \mathcal{Z}) \quad (2.4)$$

which satisfy the following sets of commutation relations:

$$[l_m, l_n] = (m - n)l_{m+n} \quad ; \quad [\bar{l}_m, \bar{l}_n] = (m - n)\bar{l}_{m+n} \quad ; \quad [l_m, \bar{l}_n] = 0 \quad (2.5)$$

Since the l_n 's commute with the l_m 's, the algebra (2.5) splits up into a direct sum $\mathcal{A} \oplus \bar{\mathcal{A}}$ of two isomorphic subalgebras generated by the holomorphic $\{l_n : n \in \mathcal{Z}\}$ and the anti-holomorphic $\{\bar{l}_n : n \in \mathcal{Z}\}$ generators respectively. As a result, it is possible to treat z and \bar{z} as independent coordinates, each taking values over the whole complex plane. In order to get back to the physically relevant case, all that has to be done is impose $\bar{z} = z^*$. The physical theory is thus invariant under transformations generated by $(l_n + \bar{l}_n)$ and $i(l_n - \bar{l}_n)$.

The generators (2.4) of the algebra (2.5) are not all well-defined globally on the Riemann sphere $\mathcal{S}^2 = \mathcal{C} \cup \infty$. From (2.4) it can be seen that the set of generators $\{l_n : n \geq -1\}$ are non-singular as $z \rightarrow 0$. Performing the transformation $z = 1/w$, we find

$$l_n = \left(\frac{1}{w}\right)^{n-1} \partial_w$$

which is singular at $w = 0$ ($z \rightarrow \infty$) for $n > 1$. The only infinitesimal generators that are globally well-defined are thus $\{l_{-1}, l_0, l_1\} \cup \{\bar{l}_{-1}, \bar{l}_0, \bar{l}_1\}$. These form the global conformal group in two dimensions. Acting on $z = re^{i\theta}$, l_{-1} and \bar{l}_{-1} generate translations, $(l_0 + \bar{l}_0)$ and $i(l_0 - \bar{l}_0)$ generate dilations and rotations respectively. The remaining two generators, l_1 and \bar{l}_1 , produce special conformal transformations. The finite transformations corresponding to the set of generators $\{l_{-1}, l_0, l_1\}$ form the group of projective conformal transformations $SL(2, \mathcal{C})/\mathcal{Z}_2$ which can be written as

$$z \rightarrow g(z) = \frac{az + b}{cz + d} \tag{2.6}$$

where $a, b, c, d \in \mathcal{C}$ and $ad - bc = 1$. The global conformal algebra can be used to characterize physical states. For instance, it will be found useful to work in the basis of eigenstates of l_0 and \bar{l}_0 with eigenvalues h and \bar{h} respectively. These (real) eigenvalues are known as the ‘left’ and ‘right’ scaling dimensions of the operator. As $(l_0 + \bar{l}_0)$ and $i(l_0 - \bar{l}_0)$ generate dilations and rotations respectively, the scaling dimension Δ and the spin s of the state are defined as $\Delta = h + \bar{h}$ and $s = h - \bar{h}$.

2.2 Conformal theories in 2 dimensions

On the basis of some simple assumptions Belavin, Polyakov and Zamolodchikov [12] found that conformal field theories in two dimensions satisfied the following fundamental properties:

1. There is a (generally infinite) set of fields $\mathcal{A} = \{A_i : i = 1, 2, \dots\}$. If a particular field $A_i(z, \bar{z})$ is present, then so are all of its derivatives.
2. There is a subset $\{\Phi_j\} \subset \{A_i\}$ that transform covariantly under projective conformal transformations $z \rightarrow g(z)$, $\bar{z} \rightarrow \bar{g}(\bar{z})$ (the definition of $\bar{g}(\bar{z})$ being similar to that for $g(z)$ in equation (2.6)) ie.

$$\Phi(z, \bar{z}) \rightarrow \left(\frac{\partial g}{\partial z}\right)^h \left(\frac{\partial \bar{g}}{\partial \bar{z}}\right)^{\bar{h}} \Phi_j(z, \bar{z})$$

Such fields are known as quasi-primary fields.

3. The remaining $\{A_i\}$'s can be expressed as linear combinations of the quasi-primary fields and their derivatives.
4. There is a vacuum state which is invariant under projective conformal transformations.
5. There is a subset $\{\phi_j\} \subset \{\Phi_j\}$ that transform covariantly under any conformal transformation $z \rightarrow f(z)$, $\bar{z} \rightarrow \bar{f}(\bar{z})$ ie.

$$\phi_j(z, \bar{z}) \rightarrow \left(\frac{\partial f}{\partial z}\right)^h \left(\frac{\partial \bar{f}}{\partial \bar{z}}\right)^{\bar{h}} \phi_j(z, \bar{z}) \quad (2.7)$$

Such fields are known as primary fields of ‘left’ and ‘right’ scaling dimensions (h, \bar{h}) .

2.2.1 Correlation functions

The transformation of primary and quasi-primary fields under global conformal transformations can be used to place restrictions on the form taken by correlation functions. Under infinitesimal transformations $z \rightarrow z + \epsilon(z)$, the holomorphic part of these fields transforms as

$$\begin{aligned} \phi(z) &\rightarrow [\partial(z + \epsilon(z))]^h \phi(z + \epsilon(z)) \\ &= (1 + \partial\epsilon(z))^h (\phi(z) + \epsilon(z)\partial\phi(z)) \\ &= (1 + h\partial\epsilon(z) + \epsilon(z)\partial + O(\epsilon(z)^2))\phi(z) \end{aligned}$$

The infinitesimal variation of $\phi(z, \bar{z})$ is thus given by

$$\delta_{\epsilon, \bar{\epsilon}}\phi(z, \bar{z}) = \left((h\partial\epsilon(z) + \epsilon(z)\partial) + (\bar{h}\bar{\partial}\bar{\epsilon}(\bar{z}) + \bar{\epsilon}(\bar{z})\bar{\partial}) \right) \phi(z, \bar{z}) \quad (2.8)$$

The two-point function $G_2(z_i, \bar{z}_i, z_j, \bar{z}_j) = \langle \phi(z_i, \bar{z}_i), \phi(z_j, \bar{z}_j) \rangle$ must then satisfy

$$\begin{aligned} \delta_{\epsilon, \bar{\epsilon}}G_2(z_i, \bar{z}_i, z_j, \bar{z}_j) &= \langle \delta\phi(z_i, \bar{z}_i), \phi(z_j, \bar{z}_j) \rangle + \langle \phi(z_i, \bar{z}_i), \delta\phi(z_j, \bar{z}_j) \rangle \\ &= 0 \end{aligned}$$

leading to the equation

$$(h_i\partial_i\epsilon(z_i) + \epsilon(z_i)\partial_i + h_j\partial_j\epsilon(z_j) + \epsilon(z_j)\partial_j)G_2(z_i, \bar{z}_i, z_j, \bar{z}_j)$$

$$+(\bar{h}_i \bar{\partial}_i \bar{\epsilon}(\bar{z}_i) + \bar{\epsilon}(\bar{z}_i) \bar{\partial}_i + \bar{h}_j \bar{\partial}_j \bar{\epsilon}(\bar{z}_j) + \bar{\epsilon}(\bar{z}_j) \bar{\partial}_j) G_2(z_i, \bar{z}_i, z_j, \bar{z}_j) = 0$$

where $\partial_i = \partial/\partial z_i$, $\bar{\partial}_i = \partial/\partial \bar{z}_i$, etc. Looking for the moment at the holomorphic part alone, the infinitesimal transformations generated by l_{-1}, l_0, l_1 lead to the following constraints on $G_2(z_i, z_j)$:

1. $\epsilon = 1$: $(\partial_i + \partial_j)G_2(z_i, z_j) = 0 \Rightarrow G_2$ depends only on $z_{ij} = z_i - z_j$.
2. $\epsilon = z$: $(h_i + h_j)G_2(z_{ij}) = -z_{ij} \partial G_2(z_{ij}) \Rightarrow G_2(z_{ij}) = \frac{C_{ij}}{z_{ij}^{(h_i+h_j)}}$.
3. $\epsilon = z^2$: $2(h_i z_i + h_j z_j) \frac{C_{ij}}{z_{ij}^{(h_i+h_j)}} = (h_i + h_j) \frac{C_{ij}(z_i^2 - z_j^2)}{z_{ij}^{(h_i+h_j+1)}}$
 $\Rightarrow C_{ij}(h_i - h_j)(z_i - z_j) = 0 \Rightarrow C_{ij} = 0$ unless $h_i = h_j$

Following the same procedure for the anti-holomorphic part, the two-point functions of primary and quasi-primary fields are thus constrained to have the form

$$G_2(z_i, \bar{z}_i, z_j, \bar{z}_j) = \frac{C_{ij}}{z_{ij}^{2h} \bar{z}_{ij}^{2\bar{h}}} \quad (h_i = h_j = h, \bar{h}_i = \bar{h}_j = \bar{h}) \quad (2.9)$$

The three-point correlation function $G_3 = \langle \phi_i(z_i, \bar{z}_i), \phi_j(z_j, \bar{z}_j), \phi_k(z_k, \bar{z}_k) \rangle$ can be similarly constrained, and is found to have the form

$$G_3(z_i, \bar{z}_i, z_j, \bar{z}_j, z_k, \bar{z}_k) = C_{ijk} \frac{1}{z_{ij}^{h_i+h_j-h_k} z_{jk}^{h_j+h_k-h_i} z_{ki}^{h_k+h_i-h_j}} \frac{1}{\bar{z}_{ij}^{\bar{h}_i+\bar{h}_j-\bar{h}_k} \bar{z}_{jk}^{\bar{h}_j+\bar{h}_k-\bar{h}_i} \bar{z}_{ki}^{\bar{h}_k+\bar{h}_i-\bar{h}_j}} \quad (2.10)$$

which again depends upon a single constant, C_{ijk} . Higher correlation functions have too many degrees of freedom to be determined so simply, and other conditions must be imposed in order to fix their forms.

2.2.2 The stress-energy tensor

Invariance of a field theory under a local coordinate transformation $x^\mu \rightarrow x^\mu + \epsilon^\mu$ ($\mu = 0, 1, \dots, N$) leads, via Noether's theorem, to the existence of a conserved current $j^\mu(\epsilon) = T_\nu^\mu \epsilon^\nu$ which satisfies $\partial_\mu j^\mu = 0$. From this we can construct a conserved charge $Q = \int d^N x j^0 = \int d^N x T_\nu^0 \epsilon^\nu$: $\partial_0 Q = 0$. The corresponding infinitesimal transformation of fields ϕ is given by $\phi \rightarrow \phi + \delta\phi$, where $\delta\phi = [\phi, Q]$. In this section, the use of the stress-energy tensor T_ν^μ as the generator of conformal coordinate transformations will reveal many of the basic properties of conformal field theories.

The structure of T_ν^μ is itself constrained by invariance of the theory under the coordinate transformations which it generates. The condition $\partial_\mu j^\mu = 0$ leads to the following properties of T_ν^μ when ϵ^ν corresponds to a translation, rotation, or a dilatation respectively.

$$\begin{aligned} \epsilon^\mu &= a^\mu & : & \quad \partial_\mu (T_\nu^\mu) a^\nu = 0 \Rightarrow T_\nu^\mu \text{ conserved} \\ \epsilon^\mu &= \Omega_\rho^\nu x^\rho & : & \quad T_\nu^\rho \Omega_\rho^\nu = 0 \Rightarrow T_\nu^\mu \text{ symmetric } (\Omega_\mu^\nu \text{ antisymmetric}) \\ \epsilon^\mu &= \lambda x^\mu & : & \quad T_\mu^\mu = 0 \Rightarrow T_\nu^\mu \text{ traceless} \end{aligned}$$

If a theory is invariant under translation, rotations, and dilatations then for a general conformal transformation ϵ^ν (and making use of equation (2.3))

$$\begin{aligned} \partial_\mu (T_\nu^\mu \epsilon^\nu) &= T_\nu^\mu \partial_\mu \epsilon^\nu = T^{\mu\nu} \partial_\mu \epsilon_\nu = \frac{1}{2} T^{\mu\nu} (\partial_\mu \epsilon_\nu + \partial_\nu \epsilon_\mu) \\ &= T^{\mu\nu} \frac{1}{d} \eta_{\mu\nu} \partial_\lambda \epsilon^\lambda = T_\mu^\mu \frac{1}{d} \partial_\lambda \epsilon^\lambda = 0 \end{aligned}$$

and we automatically have invariance under general conformal transformations. For two dimensional conformal field theories, changing to coordinates z and \bar{z} , T_ν^μ takes the form

$$\begin{aligned}
T_{zz} &= \frac{1}{4}(T_{xx} - 2iT_{xy} - T_{yy}) \\
T_{\bar{z}\bar{z}} &= \frac{1}{4}(T_{xx} + 2iT_{xy} - T_{yy}) \\
T_{z\bar{z}} &= \frac{1}{4}(T_{xx} + T_{yy}) = 0
\end{aligned}$$

Where the final equality follows from the tracelessness of T_{ν}^{μ} . Conservation of T_{ν}^{μ} ($\partial^{\mu}T_{\mu\nu} = \eta^{\alpha\mu}\partial_{\alpha}T_{\mu\nu} = 0$) takes the form

$$\begin{aligned}
\bar{\partial}T_{zz} &= 0 \Rightarrow T_{zz} = T(z) \\
\partial T_{\bar{z}\bar{z}} &= 0 \Rightarrow T_{\bar{z}\bar{z}} = T(\bar{z})
\end{aligned}$$

Using the fact that $T_{\mu\nu}$ generates conformal transformations, and the resulting transformation of primary fields given in equation (2.7), the short distance operator product expansion of $T(z)$ with a primary field $\phi(z', \bar{z}')$ must take the form

$$T(z)\phi(z', \bar{z}') = \frac{h}{(z - z')^2}\phi(z', \bar{z}') + \frac{1}{(z - z')} \partial_{z'}\phi(z', \bar{z}') + \dots \quad (2.11)$$

whilst a similar expression holds for the operator product expansion of $\bar{T}(\bar{z})$ with $\phi(z', \bar{z}')$. The non-singular terms in the expansion are fields which, by completeness, must also belong to \mathcal{A} . The set of fields $\mathcal{A} = \{A_i(z, \bar{z})\}$ in a given conformal field theory is complete in the sense that as $z_i \rightarrow z_j$, the operator product expansion of any pair of fields is given by the (convergent) sum

$$A_i(z_i, \bar{z}_i)A_j(z_j, \bar{z}_j) \sim \sum_k C_{ijk}(z_i - z_j, \bar{z}_i - \bar{z}_j)A_k(z_k, \bar{z}_k)$$

where the $C_{ijk}(z_i - z_j, \bar{z}_i - \bar{z}_j)$ are singular coefficients. For two dimensional conformal field theories it is always possible to construct a basis of operators

$\phi_i(z, \bar{z})$ with conformal weights (h_i, \bar{h}_i) . Setting the normalization constants $C_{ij} = 1$ in equation (2.9), their two-point correlation functions take the form

$$\langle \phi_i(z_i, \bar{z}_i) \phi_j(z_j, \bar{z}_j) \rangle = \delta_{ij} \frac{1}{(z_i - z_j)^{2h_i}} \frac{1}{(\bar{z}_i - \bar{z}_j)^{2\bar{h}_i}}.$$

Taking the limit as any two operators approach each other in equation (2.10) for the three-point function $\langle \phi_i \phi_j \phi_k \rangle$, the operator product expansion for any two operators can be expressed as

$$\phi_i(z_i, \bar{z}_i) \phi_j(z_j, \bar{z}_j) \sim \sum_k C_{ijk} \frac{1}{(z_i - z_j)^{(h_k - h_i - h_j)}} \frac{1}{(\bar{z}_i - \bar{z}_j)^{(\bar{h}_k - \bar{h}_i - \bar{h}_j)}} \phi_k(z_k, \bar{z}_k) \quad (2.12)$$

This expansion holds only for primary fields. Any other fields, generally known as secondary fields, will have higher order poles in their operator product expansions. An example of such a field is the stress- energy tensor $T(z)$ whose operator product with itself is given by

$$T(z)T(z') = \frac{c/2}{(z - z')^4} + \frac{2}{(z - z')^2} T(z') + \frac{1}{(z - z')} \partial T(z')$$

where the constant c is known as the central charge, its value depending on the particular conformal theory under consideration. The rest of the expansion is identical to that of a primary field, and marks $T(z)$ as a conformal field of weight $(2, 0)$. The anti-holomorphic part of the stress-energy tensor, $\bar{T}(\bar{z})$ has a similar operator product expansion with a constant \bar{c} appearing. The two constants c and \bar{c} are independent unless additional constraints are imposed on the theory eg. modular invariance.

2.2.3 Virasoro algebra and the structure of \mathcal{A}

Returning to equation (2.11), we may define operators L_{-n} which act on ϕ to generate the fields appearing in the expansion,

$$\begin{aligned} T(z)\phi(z', \bar{z}') &\equiv \sum_{n \geq 0} (z - z')^{n-2} L_{-n} \phi(z', \bar{z}') \quad \star \\ &= \frac{1}{(z - z')^2} L_0 \phi + \frac{1}{(z - z')} L_{-1} \phi + L_{-2} \phi + (z - z') L_{-3} \phi + \dots \end{aligned}$$

This can be inverted to give the descendant fields in terms of $T(z)$ and $\phi(z', \bar{z}')$

$$L_{-n} \phi(z', \bar{z}') = \oint \frac{dz}{2\pi i} \frac{1}{(z - z')^{n-1}} T(z) \phi(z', \bar{z}').$$

From this we can see that the stress-energy tensor $T(z)$ is itself a level 2 descendant of the identity operator

$$L_{-2} I(z') = \oint \frac{dz}{2\pi i} \frac{1}{(z - z')} T(z) I = T(z').$$

The descendant field $L_{-n} \phi(z', \bar{z}')$ will have scaling dimension $(h + n, \bar{h})$. Comparing the above with equation (2.11) we see that

$$L_0 \phi = h\phi \quad L_{-1} \phi = \partial\phi$$

The expansion of $\bar{T}(\bar{z})$ with $\phi(z', \bar{z}')$ may be treated in the same manner, leading to an analogous definition of operators \bar{L}_{-n} . The L_n and \bar{L}_n satisfy commutation relations

$$[L_n, L_m] = (n - m)L_{n+m} + \frac{c}{12}n(n^2 - 1)\delta_{n+m,0} \quad (2.13)$$

$$[\bar{L}_n, \bar{L}_m] = (n - m)\bar{L}_{n+m} + \frac{\bar{c}}{12}n(n^2 - 1)\delta_{n+m,0} \quad (2.14)$$

$$[L_n, \bar{L}_m] = 0 \quad (2.15)$$

It is possible to generate a whole family of descendant fields from a primary field ϕ through repeated short distance expansions with $T(z)$ and $\bar{T}(\bar{z})$. Such descendants will have the form

$$\phi^{\{-m_1 \dots -m_k; -n_1 \dots -n_l\}} = \bar{L}_{-m_1} \dots \bar{L}_{-m_k} L_{-n_1} \dots L_{-n_l} \phi \quad m_i, n_j > 0$$

and scaling dimensions given by

$$\begin{aligned} L_0 \phi^{\{-m_1 \dots -m_k; -n_1 \dots -n_l\}} &= (h + \sum_{i=1}^l n_i) \phi^{\{-m_1 \dots -m_k; -n_1 \dots -n_l\}} \\ \bar{L}_0 \phi^{\{-m_1 \dots -m_k; -n_1 \dots -n_l\}} &= (h + \sum_{i=1}^k m_i) \phi^{\{-m_1 \dots -m_k; -n_1 \dots -n_l\}}. \end{aligned}$$

The fields in a conformal field theory may thus be grouped into families $[\phi_n]$, each containing a single primary field $\phi_n(z, \bar{z})$ and an infinite number of secondary fields, called its descendants. As all fields in the theory are either primary, or descendants of a primary field, \mathcal{A} may be written as a direct sum over conformal families:

$$\mathcal{A} = \bigoplus_n [\phi_n]$$

As we have seen, there are two mutually commuting copies of the Virasoro algebra, so each conformal family may be considered as a direct product

$$[\phi_n] = \Phi_n \otimes \bar{\Phi}_n$$

where Φ_n is the space of descendants of ϕ_n generated by the action of $\{L_n : n < 0\}$ on ϕ . As the ‘left’ and ‘right’ commute, it is possible to treat them more or less independently. In the following sections only the ‘left’ algebra will be considered, it being understood that analogous arguments will hold for the ‘right’ algebra.

2.2.4 Integrals of motion

Let us consider for the moment the identity operator I . It is the unique primary field with scaling dimensions $(0, 0)$, and its conformal family may be written as

$$[I] = \Lambda \otimes \bar{\Lambda}.$$

The space Λ is composed of all analytic fields descended from I , and may be decomposed into eigenspaces of L_0

$$\Lambda = \bigoplus_{s=0}^{\infty} \Lambda_s$$

where

$$L_0 \Lambda_s = s \Lambda_s \quad ; \quad \bar{L}_0 \Lambda_s = 0,$$

so all fields in Λ_s will have scaling dimensions $(s, 0)$. In particular, $T = L_{-2}I \in \Lambda_2$. As the fields in Λ are analytic, they each give rise to a conserved quantity. There are thus an infinite number of integrals of motion which are generated from I by combinations of the Virasoro operators.

2.2.5 Unitarity and crossing symmetry

All information about a given conformal field theory is contained in its correlation functions. Using the formalism developed above, it is possible to obtain expressions for the correlation functions of any set of fields in terms of those for primary fields, which are in turn determined once we know their conformal weights and operator product coefficients C_{ijk} . The values that these can take are further constrained by imposing conditions such as crossing symmetry and unitarity. Requiring both crossing symmetry and unitarity

has been shown to limit the possible conformal field theories. Such theories may occur when the central charge takes values in the discrete series

$$c = 1 - \frac{6}{m(m+1)} \quad m = 3, 4, \dots$$

For each such value of c , primary fields of weight h are allowed, where

$$h_{p,q}(m) = \frac{[(m+1)p - mq]^2 - 1}{4m(m+1)} \quad 1 \leq p \leq m-1 \quad 1 \leq q \leq p$$

For example, the Ising (2-state Potts) model corresponds to $c = \frac{1}{2}$ ($m = 3$) and the allowed primary fields are of weight $0, \frac{1}{2}$ and $\frac{1}{16}$.

2.3 Perturbations of Conformal Field Theories

Having considered conformally invariant theories in two dimensions, it is natural to ask whether it is possible to break this symmetry, and move away from the renormalization group fixed point, whilst retaining a large enough subset of the integrals of motion to make the resulting theory tractable. In [16], Zamolodchikov showed that this is indeed possible, and the remainder of this chapter will be spent in a brief summary of this work. It should be noted that, on breaking conformal symmetry, the correlation length ξ becomes finite, so perturbation of a conformal field theory will tend to result in a massive field theory.

Consider a conformal field theory with Hamiltonian \mathcal{H}_{CFT} perturbed by a field $\Phi(z, \bar{z})$ of conformal weights (h, h) . The perturbed Hamiltonian is given by

$$\mathcal{H}_\lambda = \mathcal{H}_{CFT} + \lambda \int \Phi(z, \bar{z}) d^2z$$

where the coupling constant λ has dimensions $(1-h, 1-h)$. In order that the resulting perturbation be relevant, it is necessary that $h < 1$. On breaking conformal symmetry, the space of fields may no longer be split into holomorphic and antiholomorphic subspaces. If T_s is a field in Λ_s , then it no longer satisfies $\partial_{\bar{z}}T_s = 0$, but rather

$$\partial_{\bar{z}}T_s = \lambda R_{s-1}^{(1)} + \lambda^2 R_{s-1}^{(2)} + \dots \quad (2.16)$$

where $R_{s-1}^{(n)}$ are some local fields in \mathcal{A} of dimension $(s - n(1-h), 1 - n(1-h))$ (as $\partial_{\bar{z}}T$ has dimensions $(s,1)$). For a unitary conformal field theory all dimensions are positive, so the series (2.16) must be finite. In fact, the term $\lambda^n R_{s-1}^{(n)}$ for $n > 1$ must vanish unless

$$1 - n(1-h) = h_r \quad (2.17)$$

for some scaling dimension h_r in the unperturbed theory, otherwise there is no corresponding field in \mathcal{A} (for $n = 1$, $h_r = h$). In many cases there are no further terms, and

$$\partial_{\bar{z}}T_s = \lambda R_{s-1}^{(1)}$$

where $R_{s-1}^{(1)}$ is a left descendant of Φ with dimensions $(s-1+h, h)$. The space of left descendants of Φ may be decomposed in the same manner as Λ in the previous section:

$$\Phi = \bigoplus_{s=0}^{\infty} \Phi_s$$

where

$$L_0\Phi_s = (h+s)\Phi_s \quad ; \quad \bar{L}_0\Phi_s = h\Phi_s.$$

$R_{s-1}^{(1)}$ thus belongs to Φ_{s-1} , and $\partial_{\bar{z}}$ may be considered as a linear operator

$$\partial_{\bar{z}} : \Lambda_s \rightarrow \Phi_{s-1}.$$

Now, the integrals of motion generated by fields $T \in \Lambda$ are not all linearly independent as some fields will be total derivatives. In order to treat only linearly independent fields it is necessary to consider the factor space $\hat{\Lambda} = \Lambda/L_{-1}\Lambda$ instead of Λ . $\hat{\Lambda}$ may also be decomposed as

$$\hat{\Lambda} = \bigoplus_{s=0}^{\infty} \hat{\Lambda}_s \quad ; \quad L_0\Lambda_s = s\Lambda_s.$$

Defining $\hat{\Phi}$ in a similar manner, the action of $\partial_{\bar{z}}$ is such that

$$\partial_{\bar{z}} : \hat{\Lambda}_s \rightarrow \hat{\Phi}_{s-1}. \tag{2.18}$$

In order that T_s remain a conserved current, R_{s-1} must be a z -derivative and thus $R_{s-1} \in L_{-1}\Phi$. If $\dim(\hat{\Phi}_{s-1}) < \dim(\hat{\Lambda}_s)$, then some T_s must remain in the perturbed theory. For minimal models, the dimensions of these spaces may be obtained from the corresponding character formula. This argument was used [16] to show the presence of integrals of motion in many massive field theories. In particular, when the fields $\Phi_{(1,3)}$, $\Phi_{(1,2)}$ or $\Phi_{(2,1)}$ provide relevant perturbations, it was shown that there exist whole series of conserved charges. Of these, it is the $\Phi_{(1,2)}$ and $\Phi_{(2,1)}$ perturbations that will concern us throughout the rest of this thesis.

Chapter 3

S-matrices for integrable 2-d theories

In this chapter we turn our attention to a field theoretic treatment of the scaling region close to criticality. The study of this region not only provides a model of behaviour near criticality, but may also be used to compute universal quantities characteristic of the critical point itself [3]. This domain is populated by massive, 1 + 1 dimensional field theories which result from perturbation of the conformally invariant theory describing the critical point. The basic object to be studied is the S-matrix, which arises in the calculation of scattering amplitudes. Suppose we wish to calculate the probability \mathcal{P}_{fi} of going from an initial state $|i\rangle$ consisting of a collection of asymptotically free particles as $t \rightarrow -\infty$, to a final state $\langle f|$ of asymptotically free particles as $t \rightarrow \infty$. The corresponding S-matrix element is defined by

$$\mathcal{S}_{fi} = \langle f | \mathcal{S} | i \rangle,$$

in terms of which the probability \mathcal{P}_{fi} is given by

$$\mathcal{P}_{fi} = (\mathcal{S}_{fi})^\dagger \mathcal{S}_{fi}.$$

\mathcal{S}_{fi} is thus the probability amplitude of such a transition. In general the S-matrix of a massive two-dimensional theory can be quite complicated, but for the case of integrable theories it simplifies considerably (see for example [17], [16], [18] [19], [20]). As we shall see later, the presence of conserved quantities means that a general, multiparticle S-matrix element can be factorized into a product of two-particle ones.

Consider a relativistic field theory with n types of particles A_a ($a = 1, \dots, n$) of mass m_a . The two-momentum of a particle satisfies

$$p_\mu p^\mu = p\bar{p} = m^2$$

and will be given in terms of its corresponding rapidity θ , defined by

$$\begin{aligned} p &= p_0 + p_1 = me^\theta \\ \bar{p} &= p_0 - p_1 = me^{-\theta} \end{aligned}$$

The asymptotic states of the theory are generated by non-commuting particle creation operators $A_a(\theta)$:

$$|A_{a_1}(\theta_1)A_{a_2}(\theta_2)\dots A_{a_N}(\theta_N)\rangle = A_{a_1}(\theta_1)A_{a_2}(\theta_2)\dots A_{a_N}(\theta_N)|0\rangle$$

Such states are interpreted as in-states if $\theta_1 > \theta_2 > \dots > \theta_N$, and as out-states if $\theta_1 < \theta_2 < \dots < \theta_N$. The S-matrix is then the unitary transformation relating the in and out bases. In particular, the two-particle S-matrix elements are defined by the commutation relations of the $A_a(\theta)$'s:

$$A_{a_1}(\theta_1)A_{a_2}(\theta_2) = \mathcal{S}_{a_1 a_2}^{b_1 b_2}(\theta_1 - \theta_2)A_{b_1}(\theta_1)A_{b_2}(\theta_2) \quad (3.1)$$

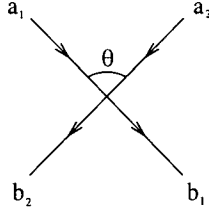


Figure 3.1: $\mathcal{S}_{a_1 a_2}^{b_1 b_2}(\theta)$

The element $\mathcal{S}_{a_1 a_2}^{b_1 b_2}(\theta)$ is interpreted as the 2-particle scattering amplitude for $A_{a_1}(\theta_1)A_{a_2}(\theta_2) \rightarrow A_{b_1}(\theta_1)A_{b_2}(\theta_2)$. This is shown diagrammatically below.

Assuming the theory is \mathcal{C}, \mathcal{P} and \mathcal{T} symmetric, then

$$\mathcal{S}_{a_1 a_2}^{b_1 b_2}(\theta) = \mathcal{S}_{\bar{a}_1 \bar{a}_2}^{\bar{b}_1 \bar{b}_2}(\theta) = \mathcal{S}_{a_2 a_1}^{b_2 b_1}(\theta) = \mathcal{S}_{\bar{b}_2 \bar{b}_1}^{\bar{a}_2 \bar{a}_1}(\theta)$$

where \bar{a} denotes the antiparticle of A_a ($A_{\bar{a}} = \mathcal{C}A_a$). In the models to be studied later on all the particles are neutral, so in the following discussion it will be assumed that $A_{\bar{a}} = A_a$. The above conditions now become

$$\mathcal{S}_{a_1 a_2}^{b_1 b_2}(\theta) = \mathcal{S}_{a_2 a_1}^{b_2 b_1}(\theta) = \mathcal{S}_{b_2 b_1}^{a_2 a_1}(\theta)$$

Integrability of the theory comes from the presence of an infinite set of mutually commuting integrals of the motion P_s and \bar{P}_s ($s = s_1, s_2, \dots$) which commute with the S-matrix. The counting argument due to Zamolodchikov [16] (described in the last chapter) often gives such a set of conserved charges. The asymptotic particle states diagonalize these integrals of the motion, with eigenvalues given by

$$P_s|0\rangle = 0 \quad ; \quad \bar{P}_s|0\rangle = 0$$

$$[P_s, A_a(\theta)] = \gamma_a^{(s)} e^{s\theta} A_a(\theta) \quad ; \quad [\bar{P}_s, A_a(\theta)] = \gamma_a^{(s)} e^{-s\theta} A_a(\theta)$$

In particular, for $s = 1$ we have energy momentum conservation:

$$P_1|A_a(\theta)\rangle = m_a e^\theta |A_a(\theta)\rangle \quad ; \quad \bar{P}_1|A_a(\theta)\rangle = m_a e^\theta |A_a(\theta)\rangle.$$

The presence of such integrals of motion has several important consequences:

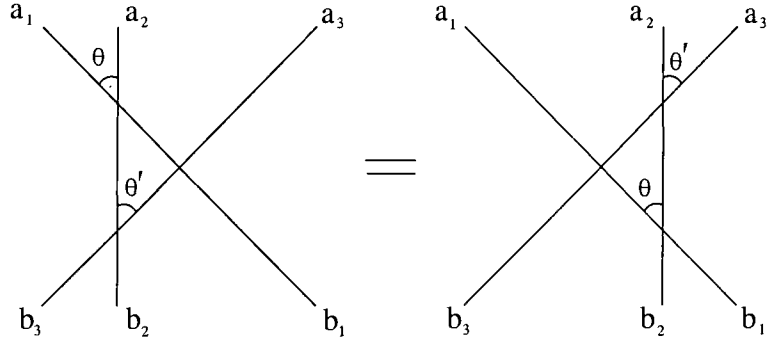
1. Scattering is purely elastic, ie. the number of particles and the set of their momenta are conserved asymptotically. This means that $\mathcal{S}_{a_1 a_2}^{b_1 b_2}(\theta) = 0$ unless $m_{a_1} = m_{b_1}$ and $m_{a_2} = m_{b_2}$.
2. Transition amplitudes between in and out states are unchanged by translation of the initial particles relative to each other.

It is the second condition that leads (see [21] and [22]) to the factorization of multiparticle S-matrix elements mentioned earlier. Indeed, the presence of only two independent integrals of motion is required for the S-matrix to be factorizable as was shown by Parke [22].

3.1 Conditions on $\mathcal{S}_{a_1 a_2}^{b_1 b_2}(\theta)$

Due to the factorization of multiparticle S-matrix elements $\mathcal{S}_{a_1 a_2}^{b_1 b_2}(\theta)$ becomes the basic object describing the theory, and it is required to satisfy some general conditions:

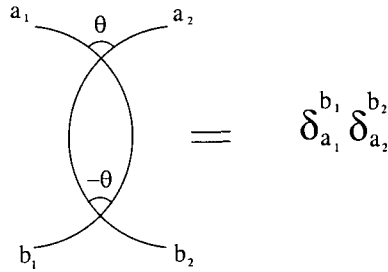
1. Yang-Baxter Equation: This follows from the invariance under translation of initial states mentioned above, and can be seen as the requirement that the algebra (3.1) be associative.



$$\mathcal{S}_{a_1 a_2}^{c_1 c_2}(\theta) \mathcal{S}_{c_1 a_3}^{b_1 c_3}(\theta + \theta') \mathcal{S}_{c_2 c_3}^{b_2 b_3}(\theta') = \mathcal{S}_{a_2 a_3}^{c_2 c_3}(\theta') \mathcal{S}_{a_1 c_3}^{c_1 b_3}(\theta + \theta') \mathcal{S}_{c_1 c_2}^{b_1 b_2}(\theta)$$

(summation over repeated indices assumed.)

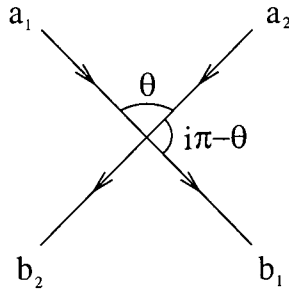
2. Unitarity: This can be seen as the consistency condition of the algebra (3.1), applying it twice.



$$\mathcal{S}_{a_1 a_2}^{c_1 c_2}(\theta) \mathcal{S}_{c_1 c_2}^{b_1 b_2}(-\theta) = \delta_{a_1}^{b_1} \delta_{a_2}^{b_2}$$

3. Analyticity/Crossing Symmetry: In the treatment given above, the rapidity θ is real for physical processes. It is postulated that $\mathcal{S}_{a_1 a_2}^{b_1 b_2}(\theta)$ can be analytically continued to a meromorphic function of θ in the so-called 'physical strip': $0 < \text{Im}\theta < \pi$. Physical scattering amplitudes in the 'direct channel' $A_{a_1} A_{a_2} \rightarrow A_{b_1} A_{b_2}$ are given by the values of $\mathcal{S}_{a_1 a_2}^{b_1 b_2}$

for $Im\theta = 0$ and $Re\theta > 0$. In the ‘cross channel’ $A_{a_2}A_{b_1} \rightarrow A_{b_2}A_{a_1}$ physical amplitudes are given by the values of $\mathcal{S}_{a_2b_1}^{b_2a_1}$ for $Im\theta = 0$ and $Re\theta < 0$. Crossing symmetry relates these two amplitudes.



$$\mathcal{S}_{a_1a_2}^{b_1b_2}(\theta) = \mathcal{S}_{a_2b_1}^{b_2a_1}(i\pi - \theta)$$

4. Bootstrap Condition: As all real scattering processes in these theories conserve particle number and momentum, the only singularities allowed in $\mathcal{S}_{a_1a_2}^{b_1b_2}(\theta)$ are poles at $Re\theta = 0$. Simple poles are usually interpreted ([16], [23]) as bound states in either the direct or cross channel. As we shall see in the next chapter, this is not always the case, but the treatment of such exceptions will be left until then. The bound states are stable particles, and must therefore be found amongst the A_a . Suppose the particle A_c appears as a bound state in the direct channel of $\mathcal{S}_{a_1a_2}^{b_1b_2}(\theta)$ at rapidity $\theta = iu_{a_1a_2}^c$ (shown in figure 3.2).

Its momentum will be given by

$$\begin{aligned} p_c^2 &= (p_{a_1} + p_{a_2})^2 \\ \Rightarrow m_c^2 &= m_{a_1}^2 + m_{a_2}^2 + 2m_{a_1}m_{a_2} \cos u_{a_1a_2}^c. \end{aligned} \quad (3.2)$$

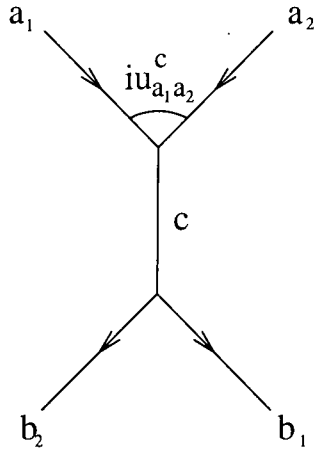


Figure 3.2: A_c bound state in $\mathcal{S}_{a_1 a_2}^{b_1 b_2}(\theta)$

The angle $u_{a_1 a_2}^c$ is known as the fusing angle for the fusion process $A_{a_1} A_{a_2} \rightarrow A_c$. Through equation (3.2) it can be seen that the fusing angle $u_{a_1 a_2}^c$ has a simple geometrical interpretation as the outside angle of a ‘mass triangle’ of sides m_{a_1} , m_{a_2} and m_c (figure 3.3), from which it follows that

$$u_{a_1 a_2}^c + u_{a_2 c}^{a_1} + u_{c a_1}^{a_2} = 2\pi \tag{3.3}$$

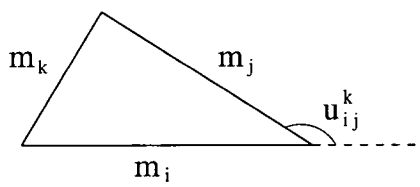


Figure 3.3: Geometrical interpretation of fusing angles

and also

$$\frac{m_{a_1}}{\sin(u_{a_2 c}^{a_1})} = \frac{m_{a_2}}{\sin(u_c^{a_2 a_1})} = \frac{m_c}{\sin(u_{a_1 a_2}^c)}. \quad (3.4)$$

A 3-particle coupling can be associated with the vertex:

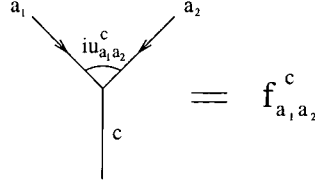
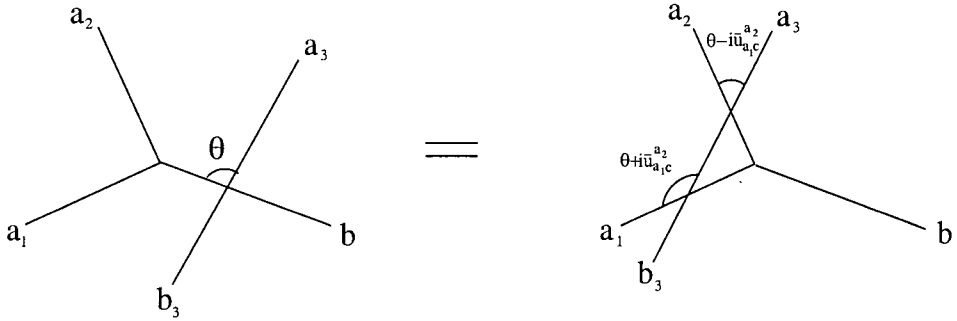


Figure 3.4: $A_{a_1} A_{a_2} \rightarrow A_c$ vertex

with the pole term being given by

$$\mathcal{S}_{a_1 a_2}^{b_1 b_2}(\theta) \simeq i \frac{f_{a_1 a_2}^c f_c^{b_1 b_2}}{(\theta - i u_{a_1 a_2}^c)}$$

When a bound state exists, $\mathcal{S}_{a_1 a_2}^{b_1 b_2}(\theta)$ must satisfy the bootstrap condition:



$$f_{a_1 a_2}^c \mathcal{S}_{c a_3}^{b b_3}(\theta) = f_{c_1 c_2}^b \mathcal{S}_{a_1 c_3}^{c_1 b_3}(\theta + i \bar{u}_{a_1 c}^{a_2}) \mathcal{S}_{a_2 a_3}^{c_2 c_3}(\theta - i \bar{u}_{a_2 c}^{a_1})$$

where $\bar{u} = i\pi - u$.

Taken together, the Yang-Baxter equation, unitarity and crossing symmetry determine $\mathcal{S}_{a_1 a_2}^{b_1 b_2}(\theta)$ up to the CDD ambiguity

$$\mathcal{S}_{a_1 a_2}^{b_1 b_2}(\theta) \rightarrow \mathcal{S}_{a_1 a_2}^{b_1 b_2}(\theta)\Phi(\theta)$$

where the CDD factor $\Phi(\theta)$ is any function satisfying

$$\Phi(\theta) = \Phi(i\pi - \theta) \quad ; \quad \Phi(\theta)\Phi(-\theta) = 1.$$

As we shall see, physical symmetries and the bootstrap condition may impose further constraints allowing the two-particle S-matrix to be completely determined.

3.2 Bulk S-matrix for q -state Potts model

In this section, I shall review the construction of the factorized S-matrix for an integrable perturbation of the q -state Potts model. In [1], Chim and Zamolodchikov considered the massive field obtained by perturbing the q -state Potts model ($0 < q < 4$) with the relevant operator $\Phi_{(2,1)}$. In this paper, they put forward a conjecture for the particle content and corresponding S-matrix elements. The remainder of this section will be devoted to a review of this work in preparation for the next chapter where modifications to their initial conjecture are presented.

As was mentioned in chapter 1, the isotropic q -state Potts model undergoes a second order phase transition for $q \leq 4$. The critical point is located at $K = K_C = \sqrt{q}$ where

$$K = e^{\frac{J}{k_B T}} - 1.$$

This model has a high temperature ($K < K_C$), disordered phase for which the equilibrium state will be S_q symmetric. It also has a low temperature ($K > K_C$), ordered phase which possesses q degenerate equilibrium states. It must be remembered that q will be treated formally as any real number.

The conformal field theory associated with the critical point has been identified by Dotsenko and Fateev in [24] and [25]. Its Virasoro central charge is given by

$$c = 1 - \frac{6}{p(p+1)} \quad \text{where} \quad \sqrt{q} = 2 \sin \left(\frac{\pi (p-1)}{2(p+1)} \right).$$

The primary field $\Phi_{(2,1)}$ corresponds to the energy-density of the model, and will be labelled $\epsilon(x)$ from now on. The conformal dimension Δ_ϵ of $\epsilon(x)$ is given by

$$\Delta_\epsilon = \frac{1}{4} + \frac{3}{4p}.$$

The scaling domain $|(K_C - K)/K_C| \ll 1$ around the critical point $K = K_C$ is therefore described by the perturbed conformal field theory

$$\mathcal{A}_{q,\tau} = \mathcal{A}_{CFT} + \tau \int \epsilon(x) d^2x, \quad (3.5)$$

where

$$\tau = \frac{K_C - K}{K_C} \ll 1$$

and \mathcal{A}_{CFT} denotes the action of the critical point conformal field theory. The integrability of $\Phi_{(2,1)}$ perturbations, noted in the previous chapter, implies that the resulting massive quantum field theory $\mathcal{A}_{q,\tau}$ possesses non-trivial local integrals of motion. As we have seen, this means that the corresponding

S-matrix is factorizable. In what follows, I will consider the low temperature phase ($K > K_C$, $\tau < 0$) where there are q degenerate vacua. The particle content in this phase must contain kinks $K_{ab}(\theta)$ ($a, b = 1, \dots, q; a \neq b$) which correspond to the domain walls separating vacua a and b (see figure 3.5). Obviously these kinks will have the same mass m . The energy-momentum of such kinks can then be characterized as usual by m and rapidity θ through

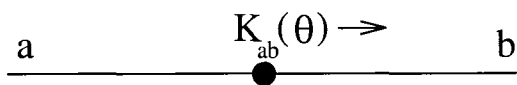


Figure 3.5: Kink interpolating between vacua a and b

$$p^\mu = (m \cosh(\theta), m \sinh(\theta)),$$

and asymptotic n -kink states are associated with the products

$$K_{a_0 a_1}(\theta_1) K_{a_1 a_2}(\theta_2) \dots K_{a_{n-1} a_n}(\theta_n)$$

where ($a_i \neq a_{i+1}, i = 0 \dots n-1$). The K_{ab} satisfy the commutation relations

$$K_{ab}(\theta_1) K_{bc}(\theta_2) = \sum_{d \neq a, c} \mathcal{S}_{ac}^{bd}(\theta_{12}) K_{ad}(\theta_2) K_{dc}(\theta_1), \quad (3.6)$$

where the \mathcal{S}_{ac}^{bd} are the two-particle S-matrix elements. \mathcal{S}_{ac}^{bd} can be represented pictorially as in figure 3.6.

S_q invariance of the S-matrix restricts the number of distinct two-particle elements to four, and equation (3.6) has only two possible forms

$$\begin{aligned} K_{ac}(\theta_1) K_{cb}(\theta_2) &= \mathcal{S}_0(\theta_{12}) \sum_{d \neq a, b, c} K_{ad}(\theta_2) K_{db}(\theta_1) + \mathcal{S}_1(\theta_{12}) K_{ac} K_{cb} & a \neq b \\ K_{ac}(\theta_1) K_{ca}(\theta_2) &= \mathcal{S}_2(\theta_{12}) \sum_{d \neq a, c} K_{ad}(\theta_2) K_{da}(\theta_1) + \mathcal{S}_3(\theta_{12}) K_{ac} K_{ca}. \end{aligned}$$

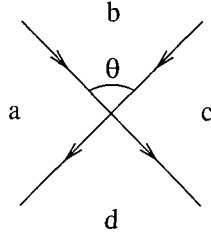


Figure 3.6: $\mathcal{S}_{ac}^{bd}(\theta)$

The four independent amplitudes \mathcal{S}_0 , \mathcal{S}_1 , \mathcal{S}_2 , and \mathcal{S}_3 are shown in figures 3.7 and 3.8. These amplitudes must satisfy the conditions set out in section (3.1). Crossing symmetry leads to the relations

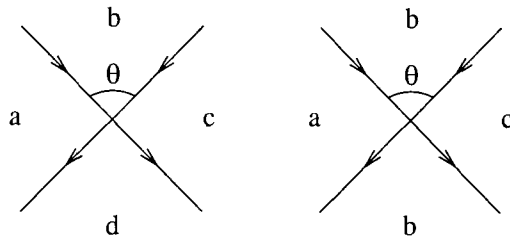


Figure 3.7: Kink amplitudes $\mathcal{S}_0(\theta)$ and $\mathcal{S}_1(\theta)$

$$\mathcal{S}_0(\theta) = \mathcal{S}_0(i\pi - \theta),$$

$$\mathcal{S}_1(\theta) = \mathcal{S}_2(i\pi - \theta),$$

$$\mathcal{S}_3(\theta) = \mathcal{S}_3(i\pi - \theta),$$

and the unitarity conditions now become

$$(q - 2)\mathcal{S}_2(\theta)\mathcal{S}_2(-\theta) + \mathcal{S}_3(\theta)\mathcal{S}_3(-\theta) = 1,$$

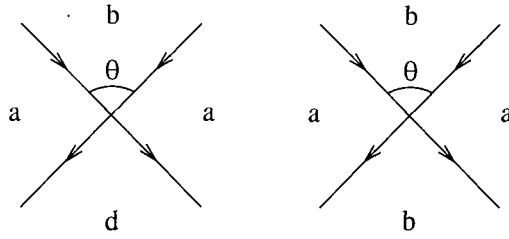
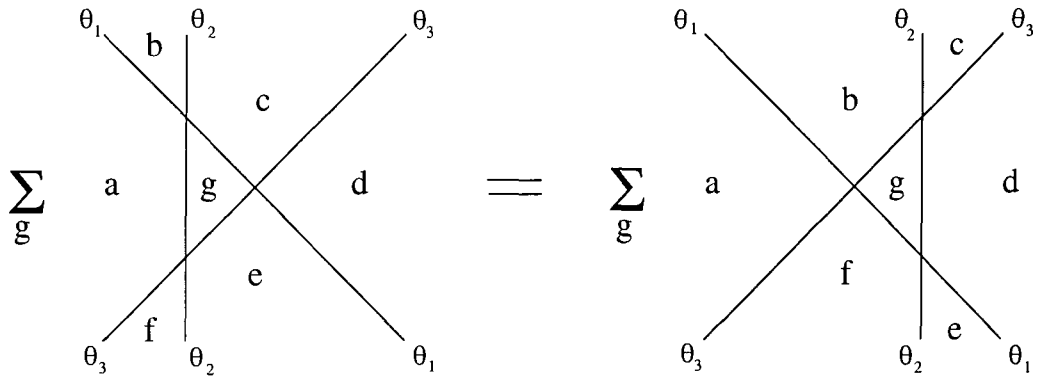


Figure 3.8: Kink amplitudes $\mathcal{S}_2(\theta)$, and $\mathcal{S}_3(\theta)$

$$\begin{aligned}
 (q-3)\mathcal{S}_0(\theta)\mathcal{S}_0(-\theta) + \mathcal{S}_1(\theta)\mathcal{S}_1(-\theta) &= 1, \\
 (q-3)\mathcal{S}_2(\theta)\mathcal{S}_2(-\theta) + \mathcal{S}_2(\theta)\mathcal{S}_3(-\theta) + \mathcal{S}_3(\theta)\mathcal{S}_2(-\theta) &= 0, \\
 (q-4)\mathcal{S}_0(\theta)\mathcal{S}_0(-\theta) + \mathcal{S}_0(\theta)\mathcal{S}_1(-\theta) + \mathcal{S}_1(\theta)\mathcal{S}_0(-\theta) &= 0.
 \end{aligned}$$

There are eight independent Yang-Baxter equations which I shall not give explicitly, but which may be represented pictorially as



The above set of conditions are not enough to specify the four amplitudes completely, and we must turn to a consideration of the bound-state structure and the resulting bootstrap equations to finish the job. In [1], Chim and Zamolodchikov reasoned as follows. Assuming that the field theory contains no particles other than the kinks K_{ab} then all bound-state poles must correspond to the same set of kinks. For example, the kink K_{ab} can

appear as a bound-state in the two-particle scattering process arising from the initial asymptotic state $K_{ac}K_{cb}$ with $a \neq b$. We therefore expect the corresponding S-matrix elements $\mathcal{S}_0(\theta)$ and $\mathcal{S}_1(\theta)$ to exhibit a bound-state pole at $\theta = 2\pi i/3$ (θ can be calculated using the momentum conservation equation (3.2), and the fact that all kinks have the same mass) associated with the pole diagrams (3.10). Crossing symmetry then implies that $\mathcal{S}_0(\theta)$ and $\mathcal{S}_2(\theta)$ must each have a cross-channel pole located at $\theta = i\pi/3$ as shown in diagrams (3.11). Similarly, $\mathcal{S}_2(\theta)$ and $\mathcal{S}_3(\theta)$ must not possess poles at $\theta = 2\pi i/3$ as there are no appropriate particle states corresponding to such poles. Here, crossing symmetry implies that $\mathcal{S}_1(\theta)$ and $\mathcal{S}_3(\theta)$ cannot possess the related cross-channel poles at $\theta = i\pi/3$. Finally, the bootstrap equations arising from these bound-states must be satisfied. The bootstrap equations can be written symbolically as in figure 3.9.

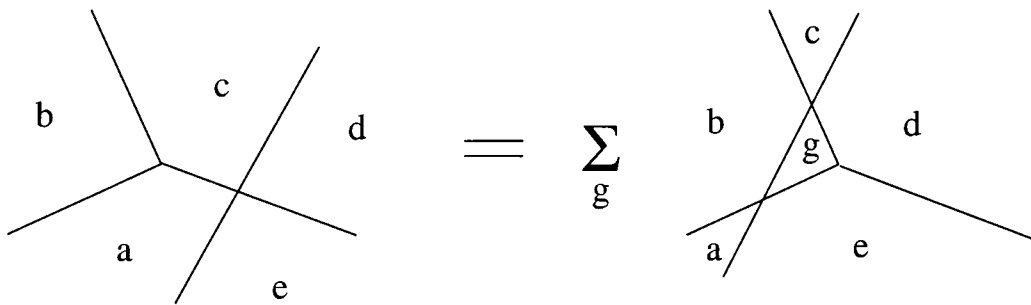


Figure 3.9: $KK \rightarrow K$ bootstrap

These constraints were used in [1] to obtain the following expressions for the four amplitudes

$$\mathcal{S}_0 = \frac{\sinh(\lambda\theta) \sinh[\lambda(i\pi - \theta)]}{\sinh\left[\lambda\left(\theta - \frac{2\pi i}{3}\right)\right] \sinh\left[\lambda\left(\frac{i\pi}{3} - \theta\right)\right]} \Pi\left(\frac{\lambda\theta}{i\pi}\right), \quad (3.7)$$

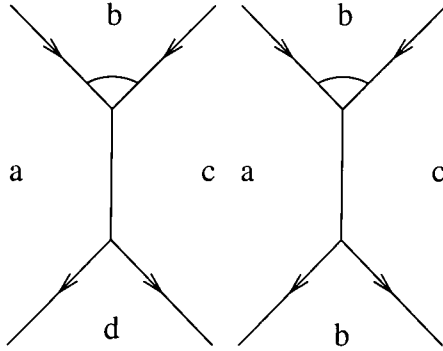


Figure 3.10: Direct channel $KK \rightarrow K$ bound state

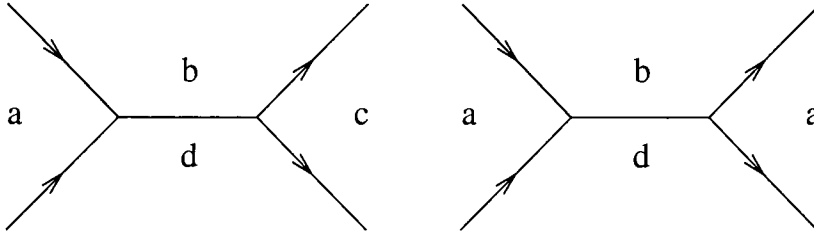


Figure 3.11: Cross channel $KK \rightarrow K$ bound state

$$\mathcal{S}_1 = \frac{\sin(\frac{2\pi\lambda}{3}) \sinh[\lambda(i\pi - \theta)]}{\sin(\frac{\pi\lambda}{3}) \sinh[\lambda(\frac{2\pi i}{3} - \theta)]} \Pi\left(\frac{\lambda\theta}{i\pi}\right), \quad (3.8)$$

$$\mathcal{S}_2 = \frac{\sin(\frac{2\pi\lambda}{3}) \sinh(\lambda\theta)}{\sin(\frac{\pi\lambda}{3}) \sinh[\lambda(\theta - \frac{i\pi}{3})]} \Pi\left(\frac{\lambda\theta}{i\pi}\right), \quad (3.9)$$

$$\mathcal{S}_3 = \frac{\sin(\lambda\pi)}{\sin(\frac{\pi\lambda}{3})} \Pi\left(\frac{\lambda\theta}{i\pi}\right), \quad (3.10)$$

where λ is related to q by

$$\sqrt{q} = 2 \sin\left(\frac{\pi\lambda}{3}\right) \quad (3.11)$$

and

$$\begin{aligned} \Pi(x) &= -\frac{\Gamma(1-x)\Gamma(1-\lambda+x)\Gamma(\frac{7}{3}\lambda-x)\Gamma(\frac{4}{3}\lambda+x)}{\Gamma(1+x)\Gamma(1+\lambda-x)\Gamma(\frac{1}{3}\lambda+x)\Gamma(\frac{4}{3}\lambda-x)} \prod_{k=1}^{\infty} \Pi_k(x)\Pi_k(\lambda-x), \\ \Pi_k(x) &= \frac{\Gamma(1+2k\lambda-x)\Gamma(2k\lambda-x)\Gamma[1+(2k-\frac{1}{3})\lambda-x]\Gamma[(2k+\frac{7}{3})\lambda-x]}{\Gamma[1+(2k+1)\lambda-x]\Gamma[(2k+1)\lambda-x]\Gamma[1+(2k-\frac{4}{3})\lambda-x]\Gamma[(2k+\frac{4}{3})\lambda-x]} \end{aligned}$$

3.2.1 Particle content for $3 < q < 4$ ($1 < \lambda < \frac{3}{2}$)

For $q < 3$, all poles of these S-matrix elements located in the physical strip $0 < \text{Im}\theta < \pi$ correspond to kink bound-states. However, for $q > 3$ Chim and Zamolodchikov found that poles of $\Pi\left(\frac{\lambda\theta}{i\pi}\right)$ located at $\theta = i2\pi\kappa$ and $\theta = i\pi(1 - 2\kappa)$, where

$$\kappa = \frac{1}{2} \left(1 - \frac{1}{\lambda}\right),$$

enter the physical strip. This means that the theory for $q > 3$ involves particles other than the basic kinks K_{ab} . The pole at $\theta = i2\pi\kappa$ appears in $\mathcal{S}_2(\theta)$ and $\mathcal{S}_3(\theta)$, and the pole at $\theta = i\pi(1 - 2\kappa)$ appears in $\mathcal{S}_1(\theta)$ and $\mathcal{S}_3(\theta)$, so $\mathcal{S}_0(\theta)$ alone exhibits no new poles. The resulting kink-kink bound-state was thus interpreted as a new particle B propagating through a single vacuum with the $\theta = i2\pi\kappa$ and $\theta = i\pi(1 - 2\kappa)$ poles corresponding to the direct (diagram 3.12) and cross (diagram 3.13) channels respectively.

The mass m_B of the new particle is found through equation (3.2) which gives

$$m_B = 2m \cos(\pi\kappa),$$

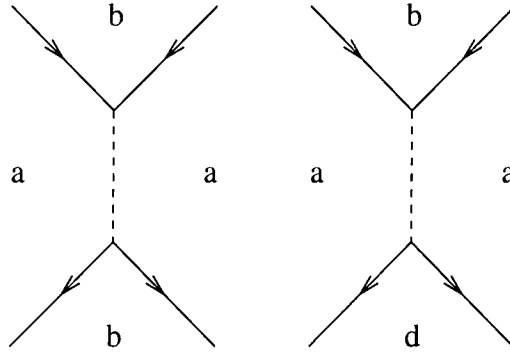


Figure 3.12: Direct channel $KK \rightarrow B$ bound state

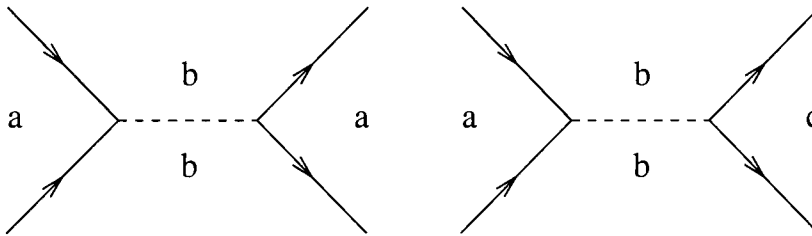


Figure 3.13: Cross channel $KK \rightarrow B$ bound state

where m is the kink mass. There are two possible scattering processes involving B being $BK \rightarrow KB$ and $BB \rightarrow BB$ as shown below.

The corresponding S-matrix elements can be calculated using the bootstrap equations

$$\mathcal{S}_{BK}(\theta) = (q - 2)\mathcal{S}_2(\theta - i\kappa)\mathcal{S}_1(\theta + i\kappa) + \mathcal{S}_3(\theta + i\kappa)\mathcal{S}_3(\theta - i\kappa)$$

$$\mathcal{S}_{BB}(\theta) = \mathcal{S}_{BK}(\theta - i\kappa)\mathcal{S}_{BK}(\theta + i\kappa)$$

which can be represented diagrammatically as

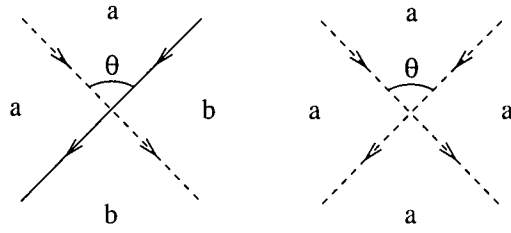
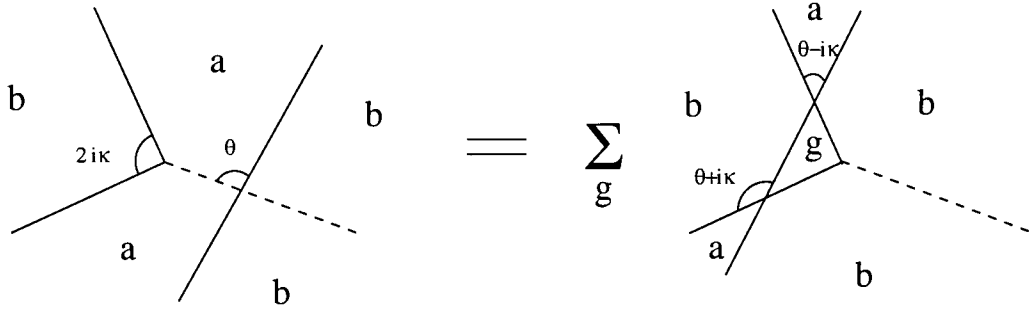
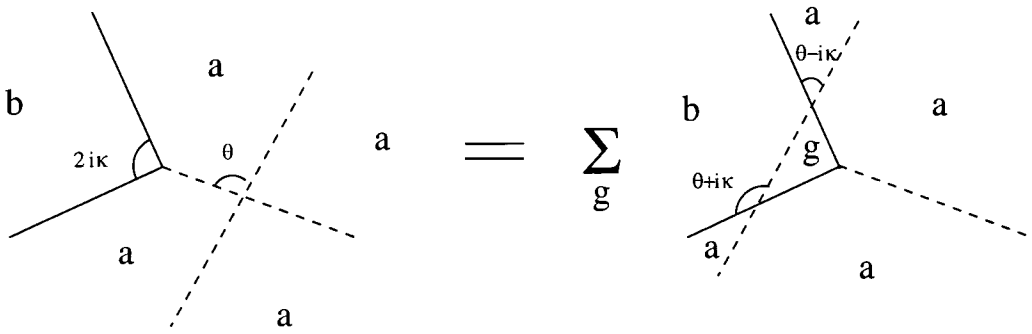


Figure 3.14: $BK \rightarrow KB$ and $BB \rightarrow BB$ scattering



and



These give

$$S_{BK}(\theta) = \frac{\sinh \theta + i \sin \pi \kappa}{\sinh \theta - i \sin \pi \kappa} \frac{\sinh \theta + i \sin(\pi \kappa + \frac{\pi}{3})}{\sinh \theta - i \sin(\pi \kappa + \frac{\pi}{3})} \quad (3.12)$$

$$\mathcal{S}_{BB}(\theta) = \frac{\sinh \theta + i \sin \frac{\pi}{3} \sinh \theta + i \sin(2\pi\kappa) \sinh \theta + i \sin(\frac{\pi}{3} + 2\pi\kappa)}{\sinh \theta - i \sin \frac{\pi}{3} \sinh \theta - i \sin(2\pi\kappa) \sinh \theta - i \sin(\frac{\pi}{3} + 2\pi\kappa)} \quad (3.13)$$

These amplitudes in turn have poles that may be interpreted as new particles. Chim and Zamolodchikov associated these with an ‘excited kink’ K' and a heavier excitation B' of a single vacuum with masses

$$m_{K'} = 2m \cos(\pi\kappa - \frac{\pi}{6}) \quad \text{and} \quad m_{B'} = 4m \cos(\pi\kappa) \cos(\frac{\pi}{3} - \pi\kappa). \quad (3.14)$$

Although the S-matrix elements (3.7)-(3.10) were conjectured to be the exact S-matrix of the field theory (3.5) for $0 < q < 4$ ($0 < \lambda < \frac{3}{2}$), they continue to be well-behaved functions for λ outside this range. In [1], it was proposed that in the domain $\frac{3}{2} \leq \lambda \leq 3$ the complete S-matrix (obtained by completing the bootstrap procedure) described the ‘thermal’ perturbation of the tricritical q -state Potts model fixed-point conformal field theory

$$\mathcal{A}_{q,\tau'} = \mathcal{A}'_{CFT} + \tau' \int \epsilon'(x) d^2x. \quad (3.15)$$

In this case the central charge c' and q are related by

$$\begin{aligned} c' &= 1 - \frac{6}{p'(p'+1)} \\ \sqrt{q} &= 2 \sin\left(\frac{\pi p' + 2}{2 p'}\right). \end{aligned}$$

The energy-density operator $\epsilon'(x)$ is identified with the degenerate field $\Phi_{(1,2)}(x)$ of conformal dimension

$$\Delta_{\epsilon'(x)} = \frac{1}{4} - \frac{3}{4(p'+1)}.$$

It was conjectured that the integrable field theory defined by action (3.15) is described by the S-matrix elements (3.7)-(3.10) with

$$\lambda = \frac{3p' + 2}{2p'}.$$

This would imply that for $\lambda = 2$ and $\lambda = \frac{9}{4}$ (giving $q = 3$ and $q = 2$ respectively), the S-matrix should reduce to the E_6 and E_7 S-matrices which had already appeared in [19]. No attempt was made in [1] to continue the bootstrap program beyond the point reached above in order to check that the particle spectrum was finite and self consistent (known as closure of the bootstrap). This work forms the substance of the next chapter.

Chapter 4

Particle spectra and the generalized bootstrap principle

In this chapter I will take a closer look at the pole structure and particle content of the massive, integrable field theories discussed in the previous chapter. Some of the material from the end of the last chapter will be duplicated, but it will be treated in a slightly more detailed manner. Starting with a discussion of the particle spectrum and closure of the bootstrap for $0 < \lambda < \frac{3}{2}$ ($0 < q < 4$ in the $\Phi_{(2,1)}$ perturbation of the q -state Potts model) I will go on to discuss the problems arising for $\frac{3}{2} \leq \lambda \leq 3$ ($4 \geq q \geq 0$ for the $\Phi_{(1,2)}$ perturbation of the tricritical q -state Potts model). For this latter range it will also be shown that not only does the S-matrix reduce to the E_6 and E_7 S-matrices for $\lambda = 2$ and $\lambda = \frac{9}{4}$ but that the E_8 S-matrix is reproduced for $\lambda = \frac{5}{2}$ ($q = 1$). The labelling of the particles has been changed as the notation used in the last chapter becomes cumbersome for larger numbers of particles. In particular, the excitations over a single vacuum (which will be referred to as ‘breathers’) have been labelled as they appear in the E_8 model.

Where changes have been made, they are related to the relevant quantities in the last chapter.

4.1 $0 < \lambda < 1$: Pole structure of $\mathcal{S}_0, \dots, \mathcal{S}_3$

For ease of reference, the four amplitudes are given again below:

$$\mathcal{S}_0 = \frac{\sinh(\lambda\theta) \sinh[\lambda(i\pi - \theta)]}{\sinh\left[\lambda\left(\theta - \frac{2\pi i}{3}\right)\right] \sinh\left[\lambda\left(\frac{i\pi}{3} - \theta\right)\right]} \Pi\left(\frac{\lambda\theta}{i\pi}\right), \quad (4.1)$$

$$\mathcal{S}_1 = \frac{\sin\left(\frac{2\pi\lambda}{3}\right) \sinh[\lambda(i\pi - \theta)]}{\sin\left(\frac{\pi\lambda}{3}\right) \sinh\left[\lambda\left(\frac{2\pi i}{3} - \theta\right)\right]} \Pi\left(\frac{\lambda\theta}{i\pi}\right), \quad (4.2)$$

$$\mathcal{S}_2 = \frac{\sin\left(\frac{2\pi\lambda}{3}\right) \sinh(\lambda\theta)}{\sin\left(\frac{\pi\lambda}{3}\right) \sinh\left[\lambda\left(\theta - \frac{i\pi}{3}\right)\right]} \Pi\left(\frac{\lambda\theta}{i\pi}\right), \quad (4.3)$$

$$\mathcal{S}_3 = \frac{\sin(\lambda\pi)}{\sin\left(\frac{\pi\lambda}{3}\right)} \Pi\left(\frac{\lambda\theta}{i\pi}\right) = -(q-3) \Pi\left(\frac{\lambda\theta}{i\pi}\right). \quad (4.4)$$

$$\Pi(x) = -\frac{\Gamma(1-x)\Gamma(1-\lambda+x)\Gamma\left(\frac{7}{3}\lambda-x\right)\Gamma\left(\frac{4}{3}\lambda+x\right)}{\Gamma(1+x)\Gamma(1+\lambda-x)\Gamma\left(\frac{1}{3}\lambda+x\right)\Gamma\left(\frac{4}{3}\lambda-x\right)} \prod_{k=1}^{\infty} \Pi_k(x) \Pi_k(\lambda-x),$$

$$\Pi_k(x) = \frac{\Gamma(1+2k\lambda-x)\Gamma(2k\lambda-x)\Gamma\left[1+(2k-\frac{1}{3})\lambda-x\right]\Gamma\left[(2k+\frac{7}{3})\lambda-x\right]}{\Gamma[1+(2k+1)\lambda-x]\Gamma[(2k+1)\lambda-x]\Gamma\left[1+(2k-\frac{4}{3})\lambda-x\right]\Gamma\left[(2k+\frac{4}{3})\lambda-x\right]}$$

These can be conveniently split into a scalar part consisting of the infinite product $\Pi\left(\frac{\lambda\theta}{i\pi}\right)$, and a non-scalar part. The poles and zeroes of the non-scalar factors, given in Table (4.1), correspond to vanishing of the sinh functions and can easily be found. Similarly, the poles and zeroes of the scalar factor occur when $\Gamma(n)$ becomes infinite (ie. $n = 0, -1, -2, \dots$) and are given in Table (4.2). Where possible these have been collected into direct and cross

$t = \theta/i\pi$	Poles: $t =$	Zeroes: $t =$		Poles: $t =$	Zeroes: $t =$
$\mathcal{S}_0(\theta):$	$\frac{1}{3}$ $\frac{2}{3}$	$\frac{1}{\lambda}$ $1 - \frac{1}{\lambda}$	$\mathcal{S}_1(\theta):$	$\frac{2}{3}$	$1 - \frac{1}{\lambda}$
	$\frac{1}{3} + \frac{1}{\lambda}$ $\frac{2}{3} - \frac{1}{\lambda}$	$\frac{2}{\lambda}$ $1 - \frac{2}{\lambda}$		$\frac{2}{3} - \frac{1}{\lambda}$	$1 - \frac{2}{\lambda}$
	$\left(\frac{1}{3} + \frac{2}{\lambda}\right)$ $\left(\frac{2}{3} - \frac{2}{\lambda}\right)$	$\left(\frac{3}{\lambda}\right)$ $\left(1 - \frac{3}{\lambda}\right)$		$\left(\frac{2}{3} - \frac{2}{\lambda}\right)$	$\left(1 - \frac{3}{\lambda}\right)$
$\mathcal{S}_2(\theta):$	$\frac{1}{3}$	$\frac{1}{\lambda}$	$\mathcal{S}_3(\theta):$	none	
	$\frac{1}{3} + \frac{1}{\lambda}$	$\frac{2}{\lambda}$			
	$\left(\frac{1}{3} + \frac{2}{\lambda}\right)$	$\left(\frac{3}{\lambda}\right)$			

Table 4.1: Poles and zeroes of non-scalar factors

channel pairs (ie. $t = a$ and $t = 1 - a$), although no claims have yet been made about which is which. The values enclosed in brackets do not enter the physical strip for $\lambda < 3$ and so can be ignored. Combining these we see that all the physical strip zeroes disappear, leaving the overall pole structure as found in Table (4.3).

Treating each pole as corresponding to a bound state particle in either the direct or cross channel, they can be classified as follows. All poles appearing in \mathcal{S}_0 must correspond to kink type particles, but which are direct and which are cross channel poles cannot be determined by looking at \mathcal{S}_0 alone. On

Poles: $t =$		Zeroes: $t =$	
$\frac{1}{\lambda}$	$1 - \frac{1}{\lambda}$		
$\frac{2}{\lambda}$	$1 - \frac{2}{\lambda}$	$(\frac{2}{3} + \frac{1}{\lambda})$	$(\frac{1}{3} - \frac{1}{\lambda})$
$(\frac{3}{\lambda})$	$(1 - \frac{3}{\lambda})$		

Table 4.2: Poles and zeroes of scalar factor $\Pi(\lambda t)$, $t = \frac{\theta}{i\pi}$

$t = \theta/i\pi$	Poles: $t =$			Poles: $t =$			Poles: $t =$	
$\mathcal{S}_0(\theta):$	$\frac{2}{3}$	$\frac{1}{3}$	$\mathcal{S}_1(\theta):$	$\frac{2}{3}$	$\mathcal{S}_2(\theta):$	$\frac{1}{3}$		
	$\frac{2}{3} - \frac{1}{\lambda}$	$\frac{1}{3} + \frac{1}{\lambda}$		$\frac{2}{3} - \frac{1}{\lambda}$		$\frac{1}{3} + \frac{1}{\lambda}$		
$\mathcal{S}_3(\theta):$	$\frac{1}{\lambda}$	$1 - \frac{1}{\lambda}$		$\frac{1}{\lambda}$		$1 - \frac{1}{\lambda}$		
	$\frac{2}{\lambda}$	$1 - \frac{2}{\lambda}$		$\frac{2}{\lambda}$		$1 - \frac{2}{\lambda}$		

Table 4.3: Overall pole structure of amplitudes

examination of \mathcal{S}_0 we see that one out of each pair of poles appears in \mathcal{S}_1 and the other in \mathcal{S}_2 . In order to be consistent, the pole appearing in \mathcal{S}_1 must be the direct channel pole and the in \mathcal{S}_2 the cross channel pole. Similarly, all poles in \mathcal{S}_3 must correspond to excitations over a single vacuum — ‘breathers’. This time, all poles which also appear in \mathcal{S}_2 must be direct channel poles, and \mathcal{S}_1 must have the appropriate cross channel poles. The masses of these particles may be calculated using equation (3.2) as before, and the resultant particle spectrum is shown in Table (4.4). Here, only the direct channel poles are listed. For $0 < t < 1$ the corresponding pole appears in the physical strip $0 < Im\theta < \pi$ and this leads, according to Chim and Zamolodchikov, to the appearance of a new particle in the particle spectrum. As we shall see shortly, such an interpretation is not always self-consistent and must be modified.

The fusion angles can easily be calculated using equation (3.3), and are summarised in figure(4.1).

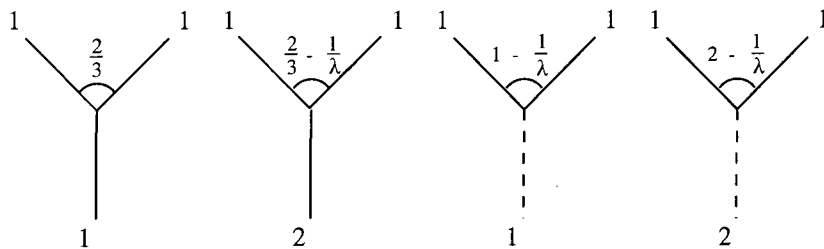


Figure 4.1: K_1K_1 fusion vertices

Pole: $t =$	$\frac{2}{3}$	$\frac{2}{3} - \frac{1}{\lambda}$	$1 - \frac{1}{\lambda}$	$1 - \frac{2}{\lambda}$
$0 < t < 1$	$\forall \lambda$	$\lambda > \frac{3}{2}$	$\lambda > 1$	$\lambda > 2$
Mass:	m	$2m \cos\left(\frac{\pi}{3} - \frac{\pi}{2\lambda}\right)$ $= m_{K_2}$	$2m \cos\left(\frac{\pi}{2} - \frac{\pi}{2\lambda}\right)$ $= m_{B_1}$	$2m \cos\left(\frac{\pi}{2} - \frac{\pi}{\lambda}\right)$ $= m_{B_2}$
Particle:	$K_1 (= K)$	$K_2 (= K')$	$B_1 (= B)$	B_2

Table 4.4: Bound state poles for $\mathcal{S}_0, \mathcal{S}_1, \mathcal{S}_2$ and \mathcal{S}_3

4.2 Closure of bootstrap for $1 < \lambda < \frac{3}{2}$

The region $0 < \lambda < \frac{3}{2}$ corresponds to the $\Phi_{(2,1)}$ perturbation of the q -state Potts model for ($0 < q < 4$). From Table (4.4) we see that the only bound-state particles appearing in the basic kink scattering $K_1 K_1 \rightarrow K_1 K_1$ are K_1 itself, and the first breather B_1 . As mentioned in section (3.2.1), the scattering amplitudes $\mathcal{S}_{B_1 K_1}: B_1 K_1 \rightarrow K_1 B_1$ and $\mathcal{S}_{B_1 B_1}: B_1 B_1 \rightarrow B_1 B_1$ were calculated by Chim & Zamolodchikov. Using the relation

$$\frac{\sinh(\theta) + i \sinh(\pi a)}{\sinh(\theta) - i \sinh(\pi a)} = (a)(1 - a) \quad \text{where} \quad (a) = \frac{\sinh\left(\frac{\theta}{2} + \frac{i\pi a}{2}\right)}{\sinh\left(\frac{\theta}{2} - \frac{i\pi a}{2}\right)},$$

equations (3.12) and (3.13) can be rewritten as

$$\mathcal{S}_{B_1 K_1} = \left(\frac{1}{2} - \frac{1}{2\lambda}\right)\left(\frac{1}{2} + \frac{1}{2\lambda}\right)\left(\frac{5}{6} - \frac{1}{2\lambda}\right)\left(\frac{1}{6} + \frac{1}{2\lambda}\right)$$

$$\mathcal{S}_{B_1 B_1} = \left(\frac{1}{3}\right)\left(\frac{2}{3}\right)\left(1 - \frac{1}{\lambda}\right)\left(\frac{1}{\lambda}\right)\left(\frac{4}{3} - \frac{1}{\lambda}\right)\left(\frac{1}{\lambda} - \frac{1}{3}\right).$$

It is to be expected that all poles will automatically appear in direct and cross channel pairs $(a)(1 - a)$ in any two particle S-matrix element involving at least one breather. As a result, it proves convenient to define $[a] = (a)(1 - a)$. Using this notation $\mathcal{S}_{B_1 K_1}$ and $\mathcal{S}_{B_1 B_1}$ become

$$\mathcal{S}_{B_1 K_1} = \left[\frac{1}{2} + \frac{1}{2\lambda}\right]\left[\frac{1}{6} + \frac{1}{2\lambda}\right] \quad (4.5)$$

$$\mathcal{S}_{B_1 B_1} = \left[\frac{2}{3}\right]\left[\frac{1}{\lambda}\right]\left[\frac{1}{\lambda} - \frac{1}{3}\right]. \quad (4.6)$$

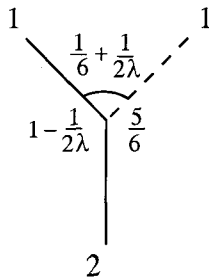


Figure 4.2: $K_1 B_1 \rightarrow K_2$ vertex

4.2.1 $\mathcal{S}_{B_1 K_1}$

Looking first at $\mathcal{S}_{B_1 K_1}$, the $(\frac{1}{2} - \frac{1}{2\lambda})$ and $(\frac{1}{2} + \frac{1}{2\lambda})$ poles can immediately be recognised as the original kink K_1 appearing as a bound state particle by referring to the corresponding vertex in figure (4.1). This also singles out $(\frac{1}{2} + \frac{1}{2\lambda})$ as the direct channel pole. The other pair of poles provide us with a few more problems. The bound state particle for this pole must be an excited kink of some sort, and calculating the mass we find

$$m = 2m \cos(\frac{\pi}{3} - \frac{1}{2\lambda}) = m_{K_2}.$$

As all particles in this theory are neutral ($A_{\bar{a}} = A_a$), the bound state particle must be K_2 . Unlike the K_2 bound state in \mathcal{S}_0 and \mathcal{S}_1 which enters the physical strip for $\lambda > \frac{3}{2}$, the $(\frac{5}{6} - \frac{1}{2\lambda})(\frac{1}{6} + \frac{1}{2\lambda})$ poles in $\mathcal{S}_{B_1 K_1}$ are already located in the physical strip when B_1 appears. As we shall see later on, for $\lambda = 2$ B_1 and K_2 correspond to particles appearing in the E_6 model. From this it is possible to identify $(\frac{1}{6} + \frac{1}{2\lambda})$ as the direct channel pole. Using equation (3.4) the fusion angles for this vertex can be calculated, and these are shown in figure 4.2. Although this would seem to imply that K_2 enters the particle spectrum for

$\lambda > 1$, things turn out to be a bit more complicated. On closer examination it becomes apparent that the following scattering process is allowed and must therefore be accounted for:

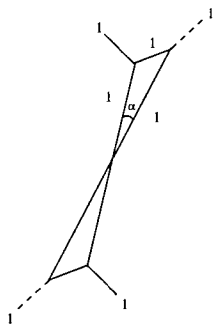


Figure 4.3: $K_1 B_1$ scattering: $t = (\frac{1}{6} + \frac{1}{2\lambda})$, $\lambda < \frac{3}{2}$

The angle between the incoming particles K_1 and B_1 is $\theta = i\pi(\frac{1}{6} + \frac{1}{2\lambda})$ and the internal scattering angle $\alpha = i\pi(\frac{1}{\lambda} - \frac{2}{3})$. The diagram will remain closed for $0 < Im\theta < \pi$ which translates as $\lambda < \frac{3}{2}$. Using the arguments of Coleman and Thun it would be expected that the above diagram should give rise to a double pole. In [26], such graphs are evaluated using the Cutkosky rules [27]: evaluate the graph as if was a Feynman diagram, but replace point interactions with the appropriate S matrix element (ie. \mathcal{S}_{ab}^{cd} for two particle scattering, or a three particle coupling f_{ab}^c for a vertex), and substitute on-shell delta-functions $\theta(p^0)\delta(p^2 - m^2)$ for the Feynman propagators of internal lines. In the present case there are six internal lines and two loops, giving a four dimensional integral over six delta-functions. There are thus two delta-functions left over, leading to a double pole. We know that $\mathcal{S}_{B_1 K_1}$ only has a simple pole at this point, so we must now turn to the factor contributed by the S matrix elements in order to clarify the situation. Looking at the

scattering process, it can be seen that this factor is composed of four, three-particle couplings multiplying a sum over two-particle amplitudes. Denoting this sum by \mathcal{A} , we have

$$\begin{aligned}
\mathcal{A} &= (q-2)[\mathcal{S}_1(\alpha) + (q-3)\mathcal{S}_0(\alpha)] \\
&= \frac{(q-2)\sinh[\lambda(i\pi - \alpha)]}{\sinh[\lambda(\frac{2\pi i}{3} - \alpha)]} \left[\frac{\sin(\lambda\frac{2\pi}{3})}{\sin(\lambda\frac{\pi}{3})} - (q-3)\frac{\sinh(\lambda\alpha)}{\sinh[\lambda(\frac{i\pi}{3} - \alpha)]} \right] \Pi\left(\frac{\lambda\alpha}{i\pi}\right) \\
&= \frac{(q-2)\sin[\lambda\pi(1-t)]\Pi(\lambda t)}{\sin[\lambda\pi(\frac{2}{3}-t)]\sin[\lambda\pi(\frac{1}{3}-t)]\sin(\lambda\frac{\pi}{3})} (\sin(\lambda\frac{2\pi}{3})\sin[\lambda\pi(\frac{1}{3}-t)] + \sin(\lambda\pi)\sin(\lambda\pi t))
\end{aligned}$$

where $t = \frac{\alpha}{i\pi}$ and use has been made of equation (3.11). Substituting in $t = \frac{1}{\lambda} - \frac{2}{3}$ we find that

$$\mathcal{A} = -\frac{(q-2)\sin(\lambda\frac{\pi}{3})\Pi(\lambda t)}{\sin(\lambda\frac{4\pi}{3})\sin(\lambda\pi)\sin(\lambda\frac{\pi}{3})} [-\sin(\lambda\frac{2\pi}{3})\sin(\lambda\pi) + \sin(\lambda\pi)\sin(\lambda\frac{2\pi}{3})] = 0$$

having checked Table (4.2) to ensure that $\Pi(\lambda t)$ does not have any poles or zeroes at this point. The vanishing of \mathcal{A} at $\theta = i\pi(\frac{1}{6} + \frac{1}{2\lambda})$, $\alpha = i\pi(\frac{1}{\lambda} - \frac{2}{3})$ reduces the singularity associated with diagram 4.3 to a simple pole, the presence of which delays the appearance of K_2 in the particle spectrum until $\lambda = \frac{3}{2}$. Beyond this point, the scattering process shown in figure 4.3 can no longer take place and K_2 appears as a bound state in $\mathcal{S}_{B_1K_1}$ as well as \mathcal{S}_0 and \mathcal{S}_1 . This type of generalised bootstrap behaviour has previously been reported in connection with the S-matrices of non-simply-laced affine Toda field theories by Corrigan, Dorey and Sasaki [28].

4.2.2 $\mathcal{S}_{B_1 B_1}$

Looking now at $\mathcal{S}_{B_1 B_1}$, the pair of poles $(\frac{2}{3})(\frac{1}{3})$ can be identified as B_1 appearing as a bound state in the direct and cross channel respectively. Calculating the bound state masses for the other two pairs of poles, and comparing the positions of the poles for $\lambda = \frac{5}{2}$ with those predicted in the E_8 model (see section (4.5.3)), it is possible to identify $(\frac{1}{\lambda})$ as the direct channel bound-state of B_2 and $(\frac{1}{\lambda} - \frac{1}{3})$ as the direct channel bound-state of a new particle B_3 with mass

$$m_{B_3} = 2m_{B_1} \cos(\frac{\pi}{6} + \frac{\pi}{2\lambda}) = 4m \cos(\frac{\pi}{2} - \frac{\pi}{2\lambda}) \cos(\frac{\pi}{2\lambda} - \frac{\pi}{6}).$$

Referring to equation (3.14), B_3 can be identified with B' . Both of these poles are located in the physical strip for $\lambda > 1$ when B_1 appears, but the question of whether or not these particles actually appear at this point must now be considered in the light that the generalized bootstrap principle may be operating. Indeed, at $\theta = (\frac{1}{\lambda})$ it is possible to construct diagram 4.4. The internal scattering angle $\alpha = i\pi(\frac{2}{\lambda} - 1)$ lies in the physical strip for $\lambda < 2$ so it is to be hoped that the S matrix elements once again conspire to reduce the double pole. Calculating \mathcal{A} we find

$$\begin{aligned} \mathcal{A} &= (q-1) [\mathcal{S}_3(\alpha) + (q-2)\mathcal{S}_1(\alpha)] \\ &= (q-1) \frac{\Pi(\lambda t)}{\sin(\lambda \frac{\pi}{3}) \sin[\lambda\pi(\frac{2}{3}-t)]} [\sin(\lambda\pi) \sin[\lambda\pi(\frac{2}{3}-t)] + (q-2) \sin(\lambda \frac{2\pi}{3}) \sin[\lambda\pi(1-t)]] \end{aligned}$$

where once again $t = \frac{\alpha}{i\pi}$. For $t = \frac{2}{\lambda} - 1$, the expression enclosed in brackets does the honourable thing and vanishes. The overall singularity is thus reduced to a simple pole and the resulting scattering process delays the appearance of the B_2 bound state until $\lambda = 2$ where it also appears in \mathcal{S}_2 and \mathcal{S}_3 .

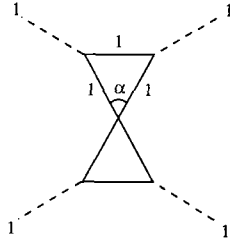


Figure 4.4: B_1B_1 scattering: $t = (\frac{1}{\lambda})$, $\lambda < 2$

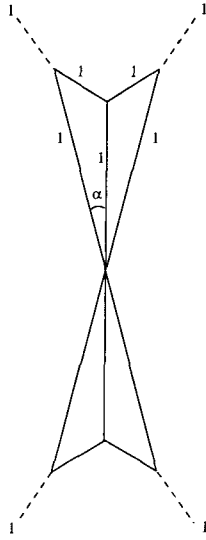


Figure 4.5: B_1B_1 scattering: $t = (\frac{1}{\lambda} - \frac{1}{3})$, $\lambda < \frac{3}{2}$

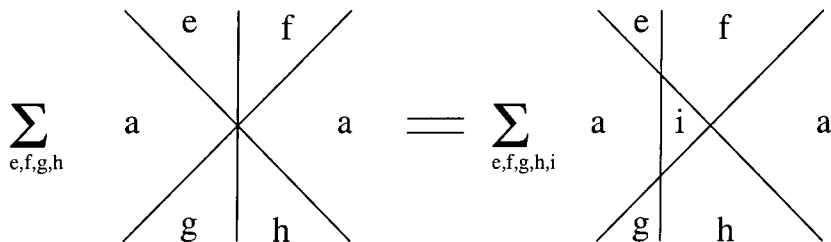


Figure 4.6: Factorised scattering in Figure (4.5)

The appearance of the B_3 bound state is also delayed, but in a slightly more complicated fashion. After some trial and error, it proved possible to construct diagram 4.5. It is not immediately clear what order of pole this diagram represents, but using translational invariance to factorise the three particle interaction as in figure 4.6 we see that naively this is a third order pole. The internal scattering angle $\alpha = i\pi(\frac{1}{\lambda} - \frac{2}{3})$ is physical for $\lambda < \frac{3}{2}$ so we must now look for a double zero to make sense of the process. In the calculation of \mathcal{A} care must be taken in keeping track of all possible combinations (although in comparison to some of the graphs found later on this is a fairly simple matter), after which it is found that

$$\mathcal{A} = (q-1)(q-2) (\mathcal{S}_1(\alpha) + (q-3)\mathcal{S}_0(\alpha))^2 [\mathcal{S}_1(2\alpha) + (q-3)\mathcal{S}_0(2\alpha)].$$

We have already seen that $\mathcal{S}_1(\alpha) + (q-3)\mathcal{S}_0(\alpha) = 0$ for $\alpha = i\pi(\frac{1}{\lambda} - \frac{2}{3})$ in the treatment of $\mathcal{S}_{B_1K_1}$, and a simple calculation shows that the rest of the function is finite and non-zero at this point. So, remarkably enough, the graph does reduce to a simple pole and B_3 does not show up as a bound state until $\lambda = \frac{3}{2}$.

In summary, the operation of the generalized bootstrap principle means that the only particles to appear for $0 < \lambda < \frac{3}{2}$ are K_1 which is present

for all λ , and B_1 which appears for $\lambda > 1$. The two excited states K_2 and B_3 found by Chim and Zamolodchikov do not put in an appearance until $\lambda > \frac{3}{2}$, at which point all their bound states appear at once. The fact that the generalized bootstrap delays their arrival until all their bound state poles enter the physical strip is quite curious in itself. A new particle B_2 was also found, its appearance being postponed until $\lambda > 2$. Although I have only explicitly treated direct channel poles in the above discussion, the cross channel poles are implicitly covered. For \mathcal{S}_0 and \mathcal{S}_3 type scattering, the appropriate diagrams are the cross channels of those given for the direct scattering process, whereas the cross channel poles of \mathcal{S}_1 type scattering are covered by the cross channel of the corresponding \mathcal{S}_2 direct channel graph and vice versa.

4.3 $\frac{3}{2} \leq \lambda < 2$

For the rest of this chapter, I will tend to work in terms of $t = \frac{\theta}{i\pi}$ for convenience and effectively drop a factor of $i\pi$ from all given angles. At $\lambda = \frac{3}{2}$, K_2 and B_3 enter the particle spectrum, and their scattering amplitudes must now be calculated.

4.3.1 Scattering amplitudes for K_2 and B_3

Starting with K_2 , the simplest element to calculate is $\mathcal{S}_{B_1 K_2}$. Applying the bootstrap procedure to the K_2 bound state appearing at $t = \frac{2}{3} - \frac{1}{\lambda}$ in \mathcal{S}_0 , we find that

$$\mathcal{S}_{B_1 K_2}(\theta) = \mathcal{S}_{B_1 K_1}(\theta - i\pi(\frac{1}{3} - \frac{1}{2\lambda}))\mathcal{S}_{B_1 K_1}(\theta + i\pi(\frac{1}{3} - \frac{1}{2\lambda}))$$

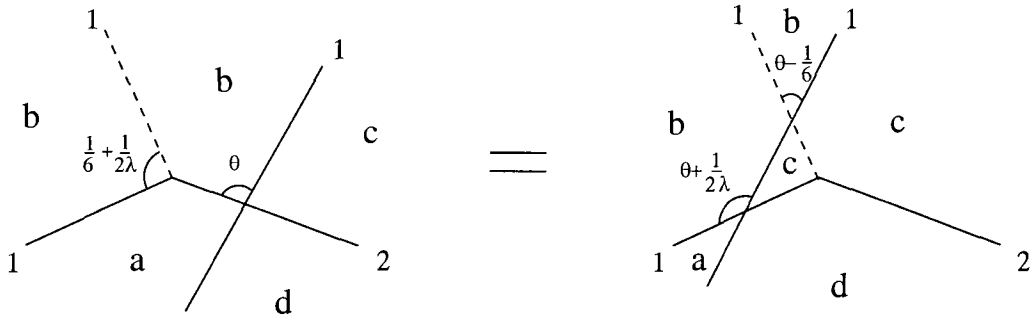


Figure 4.7: $\mathcal{S}_{K_1 K_2}$ bootstrap

$$= \left[\frac{1}{2}\right]\left[\frac{5}{6}\right]\left[\frac{1}{6} + \frac{1}{\lambda}\right]\left[\frac{1}{\lambda} - \frac{1}{6}\right]. \quad (4.7)$$

Similarly, through consideration of the direct channel bound state at $t = \frac{1}{6} - \frac{1}{2\lambda}$ in $\mathcal{S}_{B_1 K_1}$ (see figure 4.7), it can be shown that the scattering amplitudes $\mathcal{S}_{K_2 K_1}^a$ take the form

$$\begin{aligned} \mathcal{S}_{K_1 K_2}^a(\theta) &= \mathcal{S}_{B_1 K_1}\left(\theta - \frac{i\pi}{6}\right)\mathcal{S}_a\left(\theta + i\pi\left(\frac{1}{2} - \kappa\right)\right) \\ &= t\left(\frac{1}{3} + \frac{1}{2\lambda}\right)t\left(\frac{1}{3} - \frac{1}{2\lambda}\right)t\left(\frac{1}{2\lambda}\right)t\left(\frac{2}{3} - \frac{1}{2\lambda}\right)\mathcal{S}_a\left(\theta + i\pi\left(\frac{1}{2\lambda}\right)\right) \end{aligned} \quad (4.8)$$

where $t(a) = \tanh\left(\frac{\theta}{2} + \frac{i\pi a}{2}\right)$. Once again there are four possible amplitudes corresponding to the four different vacuum structures. Using these two results and the bootstrap equation corresponding to figure 4.8 it follows that

$$\mathcal{S}_{K_2 K_2}^a(\theta) = \mathcal{S}_{B_1 K_2}\left(\theta + \frac{i\pi}{6}\right)\mathcal{S}_{K_2 K_1}^a\left(\theta - \frac{i\pi}{2\lambda}\right)$$

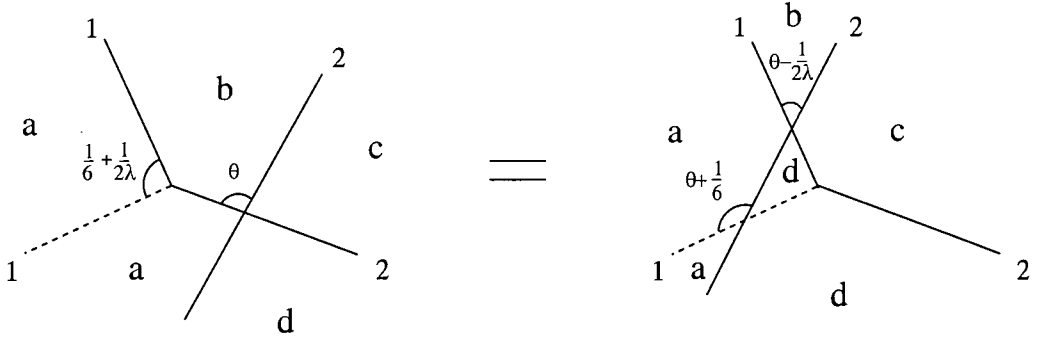


Figure 4.8: $\mathcal{S}_{K_2 K_2}$ bootstrap

$$= \mathcal{S}_{B_1 K_2}(\theta + \frac{i\pi}{6}) \mathcal{S}_{B_1 K_1}(\theta - \frac{i\pi}{6} - \frac{i\pi}{2\lambda}) \mathcal{S}_a(\theta) \quad (4.9)$$

$$= -[\frac{2}{3}]^2 [\frac{1}{3} + \frac{1}{\lambda}] [\frac{1}{\lambda}] \mathcal{S}_a(\theta). \quad (4.10)$$

The bootstrap procedure used above can be systematically applied to other bound states in order to determine the remaining scattering amplitudes $\mathcal{S}_{B_3 K_1}$, $\mathcal{S}_{B_3 K_2}$, $\mathcal{S}_{B_3 B_3}$ and $\mathcal{S}_{B_3 B_1}$:

$$\mathcal{S}_{B_3 K_1}(\theta) = [\frac{1}{3}]^2 [\frac{1}{\lambda}] [\frac{1}{\lambda} + \frac{1}{3}] \quad (4.11)$$

$$\mathcal{S}_{B_3 K_2}(\theta) = [1 - \frac{1}{2\lambda}]^2 [\frac{1}{3} + \frac{1}{2\lambda}]^3 [\frac{2}{3} + \frac{1}{2\lambda}] [\frac{3}{2\lambda} - \frac{1}{3}] [\frac{3}{2\lambda}] \quad (4.12)$$

$$\mathcal{S}_{B_3 B_3}(\theta) = [\frac{2}{3}]^3 [\frac{1}{\lambda}]^3 [\frac{4}{3} - \frac{1}{\lambda}]^2 [\frac{1}{3} + \frac{1}{\lambda}] [\frac{2}{\lambda} - \frac{2}{3}] [\frac{2}{\lambda} - \frac{1}{3}] \quad (4.13)$$

$$\mathcal{S}_{B_3 B_1}(\theta) = [\frac{1}{6} + \frac{1}{2\lambda}]^2 [\frac{1}{2} + \frac{1}{2\lambda}] [\frac{7}{6} - \frac{1}{2\lambda}] [\frac{3}{2\lambda} - \frac{1}{2}] [\frac{3}{2\lambda} - \frac{1}{6}] \quad (4.14)$$

As a given amplitude may be calculated several different ways, the bootstrap equations also provide an extensive set of consistency conditions which must be satisfied. Whilst most of these are fairly straightforward to verify, those involving kink-kink scattering prove to be more time consuming. In these cases a comparison of pole structures was deemed to be sufficient.

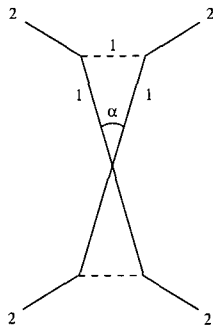


Figure 4.9: K_2K_2 scattering: $t = (\frac{2}{3})$ second order poles

4.3.2 Pole structure of K_2, B_3 amplitudes

The amplitudes (4.7)-(4.14) may now be examined in an identical fashion to those in section (4.2). Once again it is found that a number of poles inhabit the physical strip whereas all zeroes are located outside of this region. The interpretation of the resulting pole structure will now be given, starting with $\mathcal{S}_{K_2K_2}^a(\theta)$.

Bound states in $\mathcal{S}_{K_2K_2}^a(\theta)$

Looking at Table (4.5) it is immediately obvious that there must be non-trivial scattering processes taking place due to the occurrence of second and third order poles. The poles at $t = \frac{2}{3}$ can be associated with the scattering process shown in figure 4.9. Here we have a second order pole, and a factor of $\mathcal{S}_a(\frac{2}{3} - \frac{1}{\lambda})$ associated to the scattering amplitude $\mathcal{S}_{K_2K_2}^a$. Referring to Table (4.4) we see that K_2 appears as a direct channel bound state in \mathcal{S}_0 and \mathcal{S}_1 at this angle, providing a satisfactory explanation for the third order poles in $\mathcal{S}_{K_2K_2}^0$ and $\mathcal{S}_{K_2K_2}^1$ as shown in figure 4.10.

The next set of poles prove to be slightly more complicated to explain.

$t = \theta/i\pi$	Poles: $t =$			Poles: $t =$	
$\mathcal{S}_{K_2K_2}^0(\theta) :$	$(\frac{2}{3})^3$	$(\frac{1}{3})^3$	$\mathcal{S}_{K_2K_2}^1(\theta) :$	$(\frac{2}{3})^3$	$(\frac{1}{3})^2$
	$(\frac{2}{3} - \frac{1}{\lambda})^2$	$(\frac{1}{3} + \frac{1}{\lambda})^2$		$(\frac{2}{3} - \frac{1}{\lambda})^2$	$\frac{1}{3} + \frac{1}{\lambda}$
	$1 - \frac{1}{\lambda}$	$\frac{1}{\lambda}$		$1 - \frac{1}{\lambda}$	$(\frac{1}{\lambda})^2$
					$\frac{2}{\lambda}$
$\mathcal{S}_{K_2K_2}^2(\theta) :$	$(\frac{2}{3})^2$	$(\frac{1}{3})^3$	$\mathcal{S}_{K_2K_2}^3(\theta) :$	$(\frac{2}{3})^2$	$(\frac{1}{3})^2$
	$\frac{2}{3} - \frac{1}{\lambda}$	$(\frac{1}{3} + \frac{1}{\lambda})^2$		$\frac{2}{3} - \frac{1}{\lambda}$	$\frac{1}{3} + \frac{1}{\lambda}$
	$(1 - \frac{1}{\lambda})^2$	$\frac{1}{\lambda}$		$(1 - \frac{1}{\lambda})^2$	$(\frac{1}{\lambda})^2$
		$1 - \frac{2}{\lambda}$		$1 - \frac{2}{\lambda}$	$\frac{2}{\lambda}$

Table 4.5: Pole structure for $K_2K_2 \rightarrow K_2K_2$ scattering

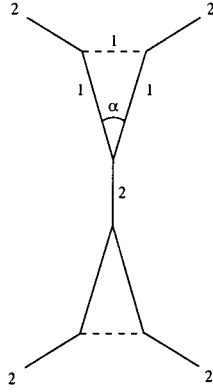


Figure 4.10: K_2K_2 scattering: $t = (\frac{2}{3})$ third order poles

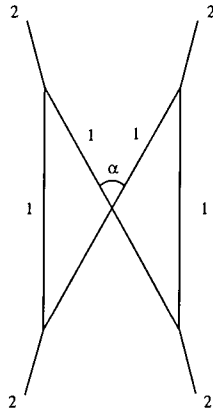


Figure 4.11: K_2K_2 scattering: $t = (\frac{2}{3} - \frac{1}{\lambda})$

The distribution of simple poles at $t = \frac{2}{3} - \frac{1}{\lambda}$ seem to suggest that they correspond to a direct channel breather, the appearance of which is prevented by the scattering process shown in figure 4.11. The S-matrix amplitudes associated with this graph are

$$\mathcal{A}_{K_2K_2}^0(\alpha) = (q-3)\mathcal{S}_0(\alpha) + (q-4)[\mathcal{S}_2(\alpha) + (q-4)\mathcal{S}_0(\alpha)] \quad (4.15)$$

$$\mathcal{A}_{K_2K_2}^1(\alpha) = (q-2)\mathcal{S}_1(\alpha) + (q-3)[\mathcal{S}_3(\alpha) + (q-3)\mathcal{S}_1(\alpha)] \quad (4.16)$$

$$\mathcal{A}_{K_2K_2}^2(\alpha) = (q-3)[\mathcal{S}_2(\alpha) + (q-4)\mathcal{S}_0(\alpha)] \quad (4.17)$$

$$\mathcal{A}_{K_2K_2}^3(\alpha) = (q-2)[\mathcal{S}_3(\alpha) + (q-3)\mathcal{S}_1(\alpha)] \quad (4.18)$$

where $\alpha = \frac{4}{3} - \frac{2}{\lambda}$. It is a simple matter to show that

$$\mathcal{S}_2(\alpha) + (q-4)\mathcal{S}_0(\alpha) = 0$$

$$\mathcal{S}_3(\alpha) + (q-3)\mathcal{S}_1(\alpha) = 0$$

thus reproducing the simple poles found in $\mathcal{S}_{K_2K_2}^2$ and $\mathcal{S}_{K_2K_2}^3$. Figure 4.11 can be drawn for $\frac{3}{2} < \lambda < 6$ and thus prevents the appearance of any bound state for $\lambda < 3$ with the exception of two special points. At $\lambda = 2$, $q = 3$ it seems that amplitude (4.15) develops a zero, and amplitude (4.17) a double zero. On closer inspection we see that for $\lambda = 2$ the scattering angle $\alpha = \frac{1}{3}$, at which point K_1 appears as a *cross* channel pole in both \mathcal{S}_0 and \mathcal{S}_2 . This leads to the modified scattering process shown in figure 4.12. The appropriate direct channel processes are simply obtained by rotating graphs 4.11 and 4.12 by 90° as shown in figure 4.13. There is one final detail to be taken care of concerning $\mathcal{S}_{K_2K_2}^3$. Looking at the form of $\mathcal{S}_3(\theta)$ in equation (4.4) we see that a factor of $(q-3)$ may be extracted from amplitude (4.18) this means that the corresponding scattering process is regular at $q = 3$. This causes no

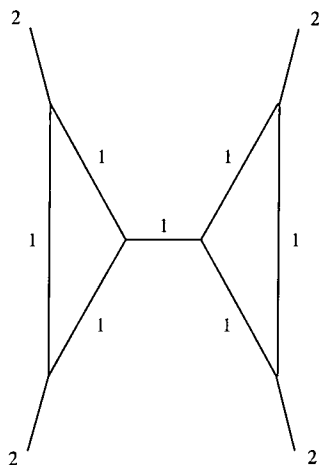


Figure 4.12: K_2K_2 scattering: $t = (\frac{2}{3} - \frac{1}{\lambda})$, $\lambda = 2$

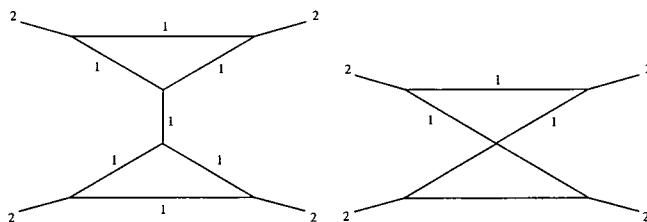


Figure 4.13: K_2K_2 scattering (direct channel): $t = (\frac{2}{3} - \frac{1}{\lambda})$, $\lambda = 2$

problems as $\mathcal{S}_{K_2K_2}^3$ has the self same $\sin(\lambda\pi)$ factor which gives the $(q - 3)$ term in $\mathcal{S}_3(\theta)$, so all of its poles are reduced in order by one at $q = 3$.

The other point at which care must be taken is when $\lambda = \frac{9}{4}$, $q = 2$. Here it is amplitude (4.16) which develops a zero, and amplitude (4.18) a double zero. This time the internal scattering angle $\alpha = \frac{4}{9}$ which, for $\lambda = \frac{9}{4}$, corresponds to the cross channel B_1 bound state in both \mathcal{S}_1 and \mathcal{S}_3 (see figure 4.14). Once again we find that the direct channel pole is located at $t = \frac{1}{3} + \frac{1}{\lambda}$. This seems

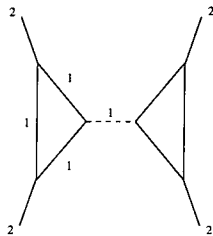


Figure 4.14: K_2K_2 scattering: $t = (\frac{2}{3} - \frac{1}{\lambda})$, $\lambda = \frac{9}{4}$

quite curious in itself as it is generally assumed that a bound state may only arise from a pole whose order is odd, whereas $\mathcal{S}_{K_2K_2}^2$ has a second order pole at this point. In actual fact there is no real contradiction here, as for $q = 2$ there are not enough vacua for this scattering process to take place. Indeed, there are not enough vacua to allow for $\mathcal{S}_{K_2K_2}^2$. The point to be drawn from this is that the bootstrap can be treated formally for general q , without reference to the physical pictures available at special values (ie. q integer), and it will remain internally consistent. At the moment it is this general perspective that is being taken, leaving the extra information available for those special cases to be considered in a later section.

Turning to the next pair of poles at $t = \frac{1}{\lambda}, 1 - \frac{1}{\lambda}$ it is found that figure 4.15 may be drawn for $t = \frac{1}{\lambda}$. This is the same sort of process as that encountered in $\mathcal{S}_{B_1B_1}$ for $t = \frac{1}{\lambda} - \frac{1}{3}$ (see figure 4.5). The simplest S-matrix amplitude to calculate is that for $\mathcal{S}_{K_2K_2}^3$, for which we get

$$\begin{aligned} \mathcal{A}_{K_2K_2}^3 &= (q-2)(q-3) [\mathcal{S}_1(2\alpha) + (q-4)\mathcal{S}_0(2\alpha)] [\mathcal{S}_1(\alpha)(q-4)\mathcal{S}_0(\alpha)]^2 \\ &+ (q-2)(q-3)^2 \mathcal{S}_0^2(\alpha) [\mathcal{S}_1(2\alpha) + (q-3)\mathcal{S}_0(2\alpha)]. \end{aligned} \quad (4.19)$$

where $\alpha = \frac{1}{\lambda} - \frac{1}{3}$. It is then a simple matter to show that

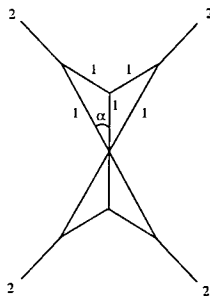


Figure 4.15: K_2K_2 scattering: $t = (\frac{1}{\lambda})$

$$\begin{aligned}\mathcal{S}_1(2\alpha) + (q - 3)\mathcal{S}_0(2\alpha) &= 0 \\ \mathcal{S}_1(\alpha) + (q - 4)\mathcal{S}_0(\alpha) &= 0.\end{aligned}$$

The amplitude $\mathcal{A}_{K_2K_2}^3$ will thus contribute a single zero for $\frac{3}{2} < \lambda < 3$ with the possible exception of $q = 3$ and $q = 2$.

The calculation of $\mathcal{A}_{K_2K_2}^2$ proves to be rather more involved, but in the end we find

$$\begin{aligned}\mathcal{A}_{K_2K_2}^2 &= 2(q - 3)^2\mathcal{S}_0(\alpha) [\mathcal{S}_1(\alpha) + (q - 4)\mathcal{S}_0(\alpha)] [(\mathcal{S}_1(2\alpha) + (q - 3)\mathcal{S}_0(2\alpha))] \\ &+ (q - 3)(q - 4) [\mathcal{S}_1(\alpha) + (q - 4)\mathcal{S}_0(\alpha)]^2 [\mathcal{S}_1(2\alpha) + (q - 3)\mathcal{S}_0(2\alpha)] \\ &+ (q - 3)\mathcal{S}_0(2\alpha) [\mathcal{S}_1(\alpha) + (q - 4)\mathcal{S}_0(\alpha)]^2\end{aligned}\quad (4.20)$$

This amplitude contributes a double zero, with $q = 3$ again being singled out for further investigation. The amplitudes $\mathcal{A}_{K_2K_2}^1$ and $\mathcal{A}_{K_2K_2}^0$ may also be calculated. Unsurprisingly, the calculation of $\mathcal{A}_{K_2K_2}^1$ is much the same as that for $\mathcal{A}_{K_2K_2}^2$ but leading to a single pole. On reaching $\mathcal{A}_{K_2K_2}^0$ the combinatorics

become quite involved to say the least (see appendix (A)), but in the end it is found to have a double zero for $q \neq 3$ and, like the rest, $q = 3$ requires closer attention. All in all, the pole structure found at $t = \frac{1}{\lambda}$ is reproduced with the exception of $q = 3$, $\lambda = 2$. At this point, $\alpha = \frac{1}{6} = \frac{2}{3} - \frac{1}{\lambda}$ where K_2 appears as a direct channel bound state in both \mathcal{S}_0 and \mathcal{S}_1 , and $2\alpha = \frac{1}{3}$ corresponding to a cross channel K_1 bound state in \mathcal{S}_0 . Figure 4.15 is therefore modified, and the relevant scattering processes are those found in figures 4.16 and 4.17. The direct channel B_3 bound state in figure (4.16) for $\mathcal{S}_{K_2K_2}^2$ and $\mathcal{S}_{K_2K_2}^3$ will be shown to appear in $\mathcal{S}_{K_2K_1}$ at $t = 1 - \frac{3}{2\lambda}$. This is equal to $\alpha = \frac{3}{2\lambda} - \frac{1}{2}$ for $\lambda = 2$ alone, typical of the intricate balancing act performed by the S-matrix in order to satisfy the bootstrap equations. The amplitudes associated with these diagrams may be calculated as before. To use $\mathcal{S}_{K_2K_2}^3$ as an example, we get

$$\mathcal{A}_{K_2K_2}^3 = (q - 2)^2(q - 3)^2,$$

so figure 4.16 is reduced from a fifth to a third order pole. It must be remembered that $\mathcal{S}_{K_2K_2}^3$ has an extra zero at $q = 3$ arising from the $\sin(\lambda\pi)$ factor. Once again it should be noted that, although this overall zero means that $\mathcal{S}_{K_2K_2}^3$ does not actually appear for $q = 3$, its pole structure is still explicable at this point.

For $q = 2$, $\lambda = \frac{9}{4}$ and $2\alpha = \frac{2}{9} = \frac{2}{3} - \frac{1}{\lambda}$. Once again a modified scattering process occurs as seen in figure 4.18 and the amplitudes recalculated once more, for example

$$\mathcal{A}_{K_2K_2}^3 = (q - 2)(q - 3)^2 [\mathcal{S}_1(\alpha) + (q - 4)\mathcal{S}_0(\alpha)]^2 (q - 2)^2(q - 3)^2\mathcal{S}_0(\alpha)^2.$$

$\mathcal{S}_1(\alpha) + (q - 4)\mathcal{S}_0(\alpha) = 0$, so the fourth order pole is reduced to the double pole required.

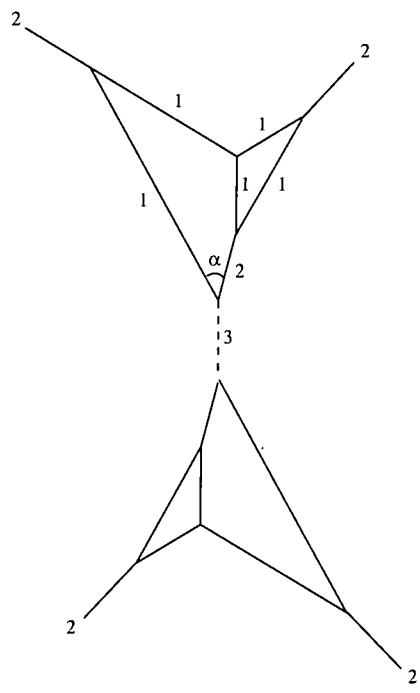


Figure 4.16: K_2K_2 scattering: $t = (\frac{1}{\lambda})$, $\lambda = 2$ third order poles

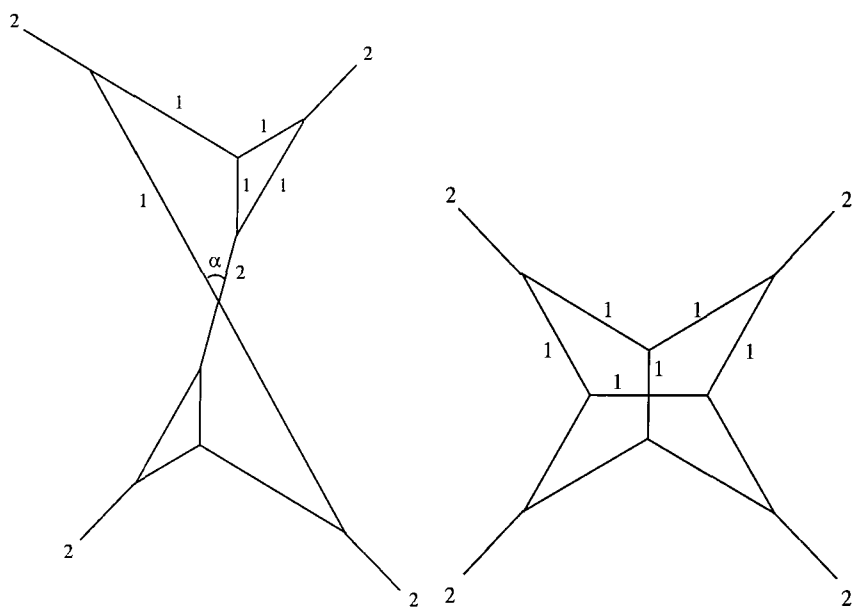


Figure 4.17: K_2K_2 scattering: $t = (\frac{1}{\lambda})$, $\lambda = 2$ second order poles

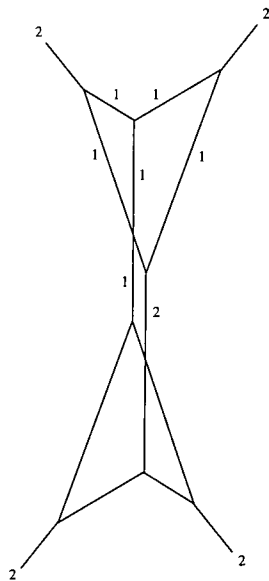


Figure 4.18: K_2K_2 scattering: $t = (\frac{1}{\lambda})$, $\lambda = \frac{9}{4}$

It is with great relief that, on examination of the poles at $t = \frac{2}{\lambda}$ and $1 - \frac{2}{\lambda}$, no higher order diagrams have to be considered. The bound state can simply be identified as the breather B_5 with mass $4m \cos(\frac{\pi}{3} - \frac{\pi}{2\lambda}) \sin(\frac{\pi}{\lambda})$ which appears for $\lambda > 2$. This completes the examination of K_2K_2 scattering, the results of which are summarised in Table (4.6).

Bound states in $\mathcal{S}_{K_2K_1}^a(\theta)$

Turning now to $K_2K_1 \rightarrow K_1K_2$ scattering, we find the pole structure given in Table (4.7). The direct channel pole at $t = \frac{2}{3} + \frac{1}{2\lambda}$ can be identified as a K_1 bound state, the fusion angle fitting with that found for the $K_1K_1 \rightarrow K_2$ vertex earlier. The next pole, at $t = \frac{2}{3} - \frac{1}{2\lambda}$, also poses few problems as it can be explained using figure (4.19). This is practically identical to the scattering

Pole: $t =$	$\left(\frac{2}{3}\right)^3$	$\left(\frac{1}{3} + \frac{1}{\lambda}\right)^2$	$\frac{1}{\lambda}$	$1 - \frac{2}{\lambda}$
Bound state particle	$\lambda > \frac{3}{2}$	$\lambda = 2$ $\lambda = 3$	$\lambda = 2$	$\lambda > 2$
Particle:	K_2	K at $\lambda = 2$ B_1 at $\lambda = \frac{9}{4}$	B_3 at $\lambda = 2$	B_5
Mass:	m_{K_2}	m at $\lambda = 2$ m_{B_1} at $\lambda = \frac{9}{4}$	m_{B_3} at $\lambda = 2$	$4m \sin\left(\frac{\pi}{\lambda}\right) \cos\left(\frac{\pi}{3} - \frac{\pi}{2\lambda}\right)$ $= m_{B_5}$

Table 4.6: Bound state poles for $\mathcal{S}_{K_2K_2}^0, \mathcal{S}_{K_2K_2}^1, \mathcal{S}_{K_2K_2}^2$ and $\mathcal{S}_{K_2K_2}^3$

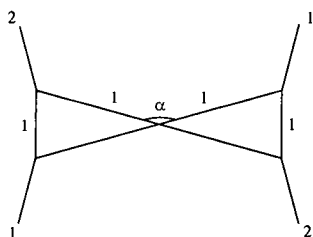


Figure 4.19: K_2K_1 scattering: $t = \left(\frac{2}{3} - \frac{1}{2\lambda}\right)$



$t = \theta/i\pi$	Poles: $t =$					
$\mathcal{S}_{K_2K_1}^0(\theta) :$	$\frac{2}{3} + \frac{1}{2\lambda}$	$(\frac{1}{3} + \frac{1}{2\lambda})^2$	$\frac{2}{3} - \frac{3}{2\lambda}$			
	$\frac{1}{3} - \frac{1}{2\lambda}$	$(\frac{2}{3} - \frac{1}{2\lambda})^2$	$\frac{1}{3} + \frac{3}{2\lambda}$			
$\mathcal{S}_{K_2K_1}^1(\theta) :$	$\frac{2}{3} + \frac{1}{2\lambda}$	$\frac{1}{3} + \frac{1}{2\lambda}$	$\frac{2}{3} - \frac{3}{2\lambda}$			
		$(\frac{2}{3} - \frac{1}{2\lambda})^2$		$\frac{1}{2\lambda}$	$\frac{3}{2\lambda}$	$\frac{5}{2\lambda}$
$\mathcal{S}_{K_2K_1}^2(\theta) :$		$(\frac{1}{3} + \frac{1}{2\lambda})^2$		$1 - \frac{1}{2\lambda}$	$1 - \frac{3}{2\lambda}$	$1 - \frac{5}{2\lambda}$
	$\frac{1}{3} - \frac{1}{2\lambda}$	$\frac{2}{3} - \frac{1}{2\lambda}$	$\frac{1}{3} + \frac{3}{2\lambda}$			
$\mathcal{S}_{K_2K_1}^3(\theta) :$		$\frac{1}{3} + \frac{1}{2\lambda}$		$1 - \frac{1}{2\lambda}$	$1 - \frac{3}{2\lambda}$	$1 - \frac{5}{2\lambda}$
		$\frac{2}{3} - \frac{1}{2\lambda}$		$\frac{1}{2\lambda}$	$\frac{3}{2\lambda}$	$\frac{5}{2\lambda}$

Table 4.7: Pole structure for $K_2K_1 \rightarrow K_1K_2$ scattering

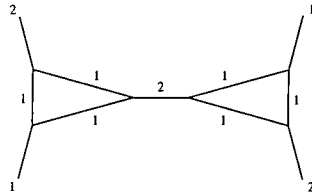


Figure 4.20: K_2K_1 scattering: $t = (\frac{2}{3} - \frac{1}{2\lambda})$ at $\lambda = 2$

process found for $t = \frac{2}{3} - \frac{1}{\lambda}$ in $\mathcal{S}_{K_2K_2}^a$ but with $\alpha = \frac{4}{3} - \frac{1}{\lambda}$, a difference of $\frac{1}{\lambda}$. The only difference this makes is that at $\lambda = 2$, K_2 appears as a bound state instead of K_1 , and at $\lambda = \frac{9}{4}$ it is B_2 as opposed to B_1 . These are shown in figures 4.20 and 4.21.

Just when it looks as if things are proceeding smoothly, we reach the pole at $t = \frac{2}{3} - \frac{3}{2\lambda}$. This enters the physical strip for $\lambda > \frac{9}{4}$ and on the surface looks like a new excited kink state. Once again we must determine whether the generalized bootstrap is in operation or not, and it is at this point that serious problems arise. Treating this as a new bound state we may calculate the associated conserved charges which turn out to be complex. It is also found that neither the particles mass nor the fusing angles of the associated three particle vertex are the simple functions in $\frac{1}{\lambda}$ that we have come to expect. We must therefore search for some other explanation of the pole, and the only other possibility we have come across is the generalized bootstrap. In order to construct a higher order scattering process to account for this first order pole using the particles already encountered, we may only use kinks as internal particle states. Otherwise, we will not get the required summations over S matrix elements which provide the necessary zeroes. It can easily be checked that there are no such second order diagrams, either for $t = \frac{2}{3} - \frac{3}{2\lambda}$, or $t = \frac{1}{3} + \frac{3}{2\lambda}$. Despite all efforts no higher order diagram

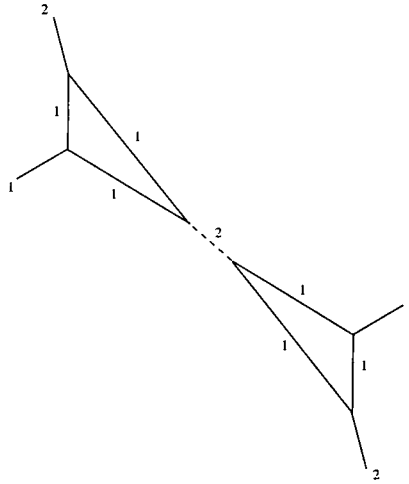


Figure 4.21: K_2K_1 scattering: $t = (\frac{2}{3} - \frac{1}{2\lambda})$ at $\lambda = \frac{9}{4}$

has yet been found to account for this pole. This problem will be dealt with (although not resolved) in a later section.

The distribution of the remaining poles suggests that they should be interpreted as breather bound states. Indeed, the $(1 - \frac{1}{2\lambda})$ and $(1 - \frac{3}{2\lambda})$ poles are found to be B_1 , and B_3 direct channel bound states respectively. This only leaves the $(1 - \frac{5}{2\lambda})$ pole to be interpreted. This enters the physical strip at $\lambda = \frac{5}{2}$ ($q = 1$) and, like the $(\frac{2}{3} - \frac{3}{2\lambda})$ pole, no satisfactory explanation has yet been found for it.

$\mathcal{S}_{B_1K_2}, \mathcal{S}_{B_3K_1}, \text{etc.} \dots$

Having dealt with the slightly more tricky S-matrix elements, illustrating the operation of the generalized bootstrap in these cases, I shall confine myself to giving a brief summary for each of the remaining elements.

Pole: $t =$	$\left(\frac{2}{3} - \frac{1}{2\lambda}\right)$	$\left(\frac{1}{3} + \frac{1}{2\lambda}\right)$	$\left(\frac{2}{3} - \frac{3}{2\lambda}\right)$	$1 - \frac{1}{2\lambda}$	$1 - \frac{3}{2\lambda}$	$1 - \frac{5}{2\lambda}$
Bound state particle	$\lambda > \frac{3}{2}$	$\lambda = 2$ $\lambda = \frac{9}{4}$		$\lambda > \frac{3}{2}$	$\lambda > \frac{3}{2}$	
Particle:	K_1	K_2 at $\lambda = 2$ B_2 at $\lambda = \frac{9}{4}$		B_1	B_3	
Mass:	m_{K_1}	m_{K_2} at $\lambda = 2$ m_{B_2} at $\lambda = \frac{9}{4}$		m_{B_1}	m_{B_3}	

Table 4.8: Bound state poles for $\mathcal{S}_{K_2K_1}^0, \mathcal{S}_{K_2K_1}^1, \mathcal{S}_{K_2K_1}^2$ and $\mathcal{S}_{K_2K_1}^3$

Pole:	$\left[\frac{1}{2}\right]$	$\left[\frac{5}{6}\right]$	$\left[\frac{1}{6} + \frac{1}{\lambda}\right]$	$\left[\frac{1}{\lambda} - \frac{1}{6}\right]$
Bound state:		K_1	K_2 at $\lambda = \frac{9}{4}$	K_3 at $\lambda = \frac{9}{4}$

Table 4.9: Pole structure of $\mathcal{S}_{B_1K_2}$

Starting with $\mathcal{S}_{B_1K_2}$ we find that most of its poles can be explained satisfactorily. The appearance of bound states is summarized in table (4.9). Where poles are not interpreted as particles, appropriate diagrams may be found for all but one case — the $\left[\frac{1}{\lambda} - \frac{1}{6}\right]$ poles for $\lambda > \frac{9}{4}$. At $\lambda = \frac{9}{4}$ these poles are explicable as bound states of a new kink-type particle K_3 , but away from this point the conserved charges associated with such a bound state become complex.

For $\mathcal{S}_{B_3B_1}$ (table (4.10)), everything works well up until $\lambda = \frac{5}{2}$, after which the same problems occur for the poles of $\left[\frac{3}{2\lambda} - \frac{1}{6}\right]$. Also worth noting is the appearance of B_5 and B_2 . These breathers are both delayed from entering the particle spectrum until $\lambda = 2$ at which point B_5 also appears in $\mathcal{S}_{K_2K_2}$, and B_2 in $\mathcal{S}_{K_1K_1}$ and $\mathcal{S}_{B_1B_1}$. These are the only new particles that appear before $\lambda = \frac{9}{4}$.

The interpretation of $\mathcal{S}_{B_3B_3}$ is fairly straight forward (see table (4.11) for bound states), and here we find more new particles. These can be identified as B_6 and B_7 , both of which appear for $\lambda > \frac{9}{4}$. Their masses are given by

$$m_{B_6} = 4m \cos\left(\frac{\pi}{2} - \frac{\pi}{\lambda}\right) \cos\left(\frac{\pi}{2\lambda} - \frac{\pi}{6}\right)$$

Pole:	$\left[\frac{7}{6} - \frac{1}{2\lambda}\right]$	$\left[\frac{1}{2} + \frac{1}{2\lambda}\right]$	$\left[\frac{3}{2\lambda} - \frac{1}{2}\right]$	$\left[\frac{3}{2\lambda} - \frac{1}{6}\right]$	$\left[\frac{1}{6} + \frac{1}{2\lambda}\right]^2$
Bound state:	B_1			B_3 at $\lambda = 2$	
		B_2 $\lambda > 2$	B_5 $\lambda > 2$	B_4 at $\lambda = \frac{5}{2}$	

Table 4.10: Pole structure of $\mathcal{S}_{B_3B_1}$

$$m_{B_7} = 8m \cos\left(\frac{\pi}{2} - \frac{\pi}{2\lambda}\right) \cos\left(\frac{\pi}{2\lambda} - \frac{\pi}{6}\right) \cos\left(\frac{\pi}{\lambda} - \frac{\pi}{3}\right).$$

The two remaining S-matrix elements both pose problems : in $\mathcal{S}_{B_3K_1}$ for $\left[\frac{1}{\lambda}\right]$; and for $\left[\frac{1}{3} + \frac{1}{2\lambda}\right]$ and $\left[\frac{3}{2\lambda} - \frac{1}{3}\right]$ in $\mathcal{S}_{B_3K_2}$. Once more, no explanation can be found for these poles when $\lambda > \frac{9}{4}$. The bound states of $\mathcal{S}_{B_3K_1}$ and $\mathcal{S}_{B_3K_2}$ are summarized in tables (4.12) and (4.13) respectively.

4.4 $2 < \lambda < \frac{9}{4}$

At $\lambda = 2$, B_2 and B_5 enter the particle spectrum. This introduces 11 additional S-matrix elements which must be calculated and interpreted. As much of the behaviour of these scattering amplitudes has been seen in those treated above, the following discussion will be kept quite brief. New behaviour will be pointed out, as will the increasing number of unexplained poles. The scattering processes of the generalized bootstrap, which become ever more complexity and numerous, have been relegated to appendix (B).

Pole:	$\left[\frac{4}{3} - \frac{1}{\lambda}\right]^2$	$\left[\frac{1}{3} + \frac{1}{\lambda}\right]$	$\left[\frac{2}{3}\right]^3$	$\left[\frac{2}{\lambda} - \frac{1}{3}\right]$	$\left[\frac{2}{\lambda} - \frac{2}{3}\right]$	$\left[\frac{1}{\lambda}\right]^3$
Bound state:			$B_3 \lambda < 2$			
	B_1 at $\lambda = 2$		B_3 at $\lambda = 2$			
		B_2 at $\lambda = \frac{5}{2}$	$B_3 \lambda > 2$	B_5 at $\lambda = \frac{5}{2}$	$B_7 \lambda > \frac{9}{4}$	$B_6 \lambda > \frac{9}{4}$

Table 4.11: Pole structure of $\mathcal{S}_{B_3 B_3}$

Pole:	$\left[\frac{1}{3}\right]^2$	$\left[\frac{1}{3} + \frac{1}{\lambda}\right]$	$\left[\frac{1}{\lambda}\right]$
Bound state:		K_2	K_3 at $\lambda = \frac{9}{4}$

Table 4.12: Pole structure of $\mathcal{S}_{B_3 K_1}$

Pole:	$[\frac{2}{3} + \frac{1}{2\lambda}]$	$[1 - \frac{1}{2\lambda}]^2$	$[\frac{3}{2\lambda}]$	$[\frac{1}{3} + \frac{1}{2\lambda}]^3$	$[\frac{3}{2\lambda} - \frac{1}{3}]$
Bound state:	K_1	K_2 at $\lambda = 2$	K_3 at $\lambda = \frac{9}{4}$		

Table 4.13: Pole structure of $\mathcal{S}_{B_3K_2}$

4.4.1 S-matrix elements of B_2

Using the bootstrap, it is a simple matter to calculate the scattering amplitudes of B_2 :

$$\begin{aligned}
\mathcal{S}_{B_2B_1}(\theta) &= [1 - \frac{1}{2\lambda}][\frac{2}{3} - \frac{1}{2\lambda}][\frac{3}{2\lambda}][\frac{3}{2\lambda} - \frac{1}{3}] \\
\mathcal{S}_{B_2B_2}(\theta) &= [\frac{2}{3}][\frac{2}{3} - \frac{1}{\lambda}][\frac{1}{\lambda} - \frac{1}{3}][\frac{2}{\lambda}][\frac{2}{\lambda} - \frac{1}{3}][1 - \frac{1}{\lambda}]^2 \\
\mathcal{S}_{B_2B_3}(\theta) &= [\frac{1}{2}][\frac{5}{6}][\frac{2}{\lambda} - \frac{1}{6}][\frac{7}{6} - \frac{1}{\lambda}]^2[\frac{2}{\lambda} - \frac{1}{2}][\frac{5}{6} - \frac{1}{\lambda}]^2 \\
\mathcal{S}_{B_2K_1}(\theta) &= [\frac{1}{2}][\frac{1}{6}][\frac{1}{2} + \frac{1}{\lambda}][\frac{1}{6} + \frac{1}{\lambda}] \\
\mathcal{S}_{B_2K_2}(\theta) &= [\frac{1}{2} - \frac{1}{2\lambda}]^2[\frac{1}{6} + \frac{1}{2\lambda}]^2[\frac{1}{6} + \frac{3}{2\lambda}][\frac{3}{2\lambda} - \frac{1}{6}]
\end{aligned}$$

$\mathcal{S}_{B_2B_1}$ has B_1 and B_3 as bound states (see table (4.14)) as would be expected from the analysis of $\mathcal{S}_{B_1B_1}$ and $\mathcal{S}_{B_3B_1}$ respectively. The only place in $\mathcal{S}_{B_2B_1}$ where no explanation can be found for $[\frac{3}{2\lambda} - \frac{1}{3}]$ when $\lambda > \frac{5}{2}$.

There are no such difficulties in interpreting the pole structure of $\mathcal{S}_{B_2B_2}$. The location of bound state particles is summarized in table (4.15). For $\mathcal{S}_{B_2B_3}$, the poles of $[\frac{2}{\lambda} - \frac{1}{2}]$ remain unexplained for $\lambda > \frac{9}{4}$, as do the $[\frac{1}{6}]$ poles of $\mathcal{S}_{B_2K_1}$. The bound states for these amplitudes are given in tables (4.16)

Pole:	$[1 - \frac{1}{2\lambda}]$	$[\frac{2}{3} - \frac{1}{2\lambda}]$	$[\frac{3}{2\lambda}]$	$[\frac{3}{2\lambda} - \frac{1}{3}]$
Bound state:	B_1	B_3	B_2 at $\lambda = \frac{5}{2}$	B_4 at $\lambda = \frac{5}{2}$

Table 4.14: Pole structure of $\mathcal{S}_{B_2 B_1}$

Pole:	$[\frac{2}{3}]$	$[\frac{2}{3} - \frac{1}{\lambda}]$	$[\frac{1}{\lambda} - \frac{1}{3}]$	$[\frac{2}{\lambda}]$	$[\frac{2}{\lambda} - \frac{1}{3}]$	$[1 - \frac{1}{\lambda}]^2$
Bound state:	B_2	B_5			B_3 at $\lambda = \frac{9}{4}$	
			B_6 $\lambda > \frac{9}{4}$	B_1 at $\lambda = \frac{5}{2}$	B_4 at $\lambda = \frac{5}{2}$	

Table 4.15: Pole structure of $\mathcal{S}_{B_2 B_2}$

Pole:	$[\frac{1}{2}]$	$[\frac{5}{6}]$	$[\frac{2}{\lambda} - \frac{1}{6}]$	$[\frac{7}{6} - \frac{1}{\lambda}]^2$	$[\frac{2}{\lambda} - \frac{1}{2}]$	$[\frac{5}{6} - \frac{1}{\lambda}]^2$
Bound state:		B_1	B_2 at $\lambda = \frac{9}{4}$		B_5 at $\lambda = \frac{9}{4}$	
			B_3 at $\lambda = \frac{5}{2}$		B_6 at $\lambda = \frac{5}{2}$	

Table 4.16: Pole structure of $\mathcal{S}_{B_2 B_3}$

Pole:	$[\frac{1}{2}]$	$[\frac{1}{6}]$	$[\frac{1}{2} + \frac{1}{\lambda}]$	$[\frac{1}{6} + \frac{1}{\lambda}]$
Bound state:		K_3 at $\lambda = \frac{9}{4}$	K_1	K_2 at $\lambda = \frac{9}{4}$

Table 4.17: Pole structure of $\mathcal{S}_{B_2 K_1}$

Pole:	$[\frac{1}{2} - \frac{1}{2\lambda}]^2$	$[\frac{1}{6} + \frac{1}{2\lambda}]^2$	$[\frac{1}{6} + \frac{3}{2\lambda}]$	$[\frac{3}{2\lambda} - \frac{1}{6}]$
Bound state:			K_1 at $\lambda = \frac{9}{4}$	

Table 4.18: Pole structure of $\mathcal{S}_{B_2K_2}$

and (4.17) respectively. All the poles of $\mathcal{S}_{B_2K_2}$ can be accounted for, and it is found to possess but a single bound state for $\lambda = \frac{9}{4}$ alone (see table (4.18)).

4.4.2 S-matrix elements of B_5

The scattering amplitudes involving B_5 are as follows:

$$\begin{aligned}
\mathcal{S}_{B_5B_1} &= [\frac{1}{3}]^2[\frac{4}{3} - \frac{1}{\lambda}][\frac{1}{3} + \frac{1}{\lambda}][\frac{2}{\lambda} - \frac{2}{3}][\frac{2}{\lambda} - \frac{1}{3}][1 - \frac{1}{\lambda}]^2 \\
\mathcal{S}_{B_5B_2} &= [\frac{4}{3} - \frac{3}{2\lambda}]^2[1 - \frac{3}{2\lambda}]^2[\frac{2}{3} + \frac{1}{2\lambda}][\frac{1}{3} + \frac{1}{2\lambda}]^3[1 - \frac{1}{2\lambda}]^2[\frac{5}{2\lambda} - \frac{1}{3}][\frac{5}{2\lambda} - \frac{2}{3}] \\
\mathcal{S}_{B_5B_3} &= [\frac{7}{6} - \frac{1}{2\lambda}][\frac{1}{6} + \frac{3}{2\lambda}][\frac{3}{2} - \frac{3}{2\lambda}]^2[\frac{5}{2\lambda} - \frac{5}{6}][\frac{1}{2} + \frac{1}{2\lambda}]^3[\frac{3}{2\lambda} - \frac{1}{6}]^3[\frac{5}{2\lambda} - \frac{1}{2}][\frac{5}{6} - \frac{1}{2\lambda}]^4 \\
\mathcal{S}_{B_5B_5} &= [\frac{5}{3} - \frac{2}{\lambda}]^2[\frac{2}{3}]^5[\frac{3}{\lambda} - 1][\frac{3}{\lambda} - \frac{2}{3}][\frac{1}{\lambda}]^5[\frac{1}{3} + \frac{1}{\lambda}]^3[\frac{4}{3} - \frac{2}{\lambda}]^3[\frac{2}{\lambda}][\frac{4}{3} - \frac{1}{\lambda}]^2 \\
\mathcal{S}_{B_5K_1} &= [\frac{1}{2} - \frac{1}{2\lambda}]^2[\frac{5}{6} - \frac{1}{2\lambda}]^2[\frac{1}{6} + \frac{3}{2\lambda}][\frac{3}{2\lambda} - \frac{1}{6}] \\
\mathcal{S}_{B_5K_2} &= [\frac{5}{6}]^2[\frac{1}{2}]^2[\frac{7}{6} - \frac{1}{\lambda}]^2[\frac{5}{6} - \frac{1}{\lambda}]^3[\frac{1}{2} + \frac{1}{\lambda}][\frac{2}{\lambda} - \frac{1}{6}][\frac{2}{\lambda} - \frac{1}{2}]
\end{aligned}$$

The occurrence of bound states for these amplitudes is summarised in tables (4.19)—(4.27) below. Aswell as having its fair share of unexplained poles for $\lambda > \frac{9}{4}$ or $\lambda > \frac{5}{2}$, the $[\frac{5}{6}]^2$ poles of $\mathcal{S}_{B_5K_2}$ cannot be accounted for $2 < \lambda \leq \frac{15}{7}$. Again, a conclusive proof that non-trivial scattering processes

Pole:	$[\frac{1}{3}]^2$	$[\frac{4}{3} - \frac{1}{\lambda}]$	$[\frac{1}{3} + \frac{1}{\lambda}]$	$[\frac{2}{\lambda} - \frac{2}{3}]$	$[\frac{2}{\lambda} - \frac{1}{3}]$	$[1 - \frac{1}{\lambda}]^2$
Bound state:		B_3			B_5 at $\lambda = \frac{9}{4}$	
			B_4 at $\lambda = \frac{5}{2}$	B_7 $\lambda > \frac{9}{4}$	B_6 at $\lambda = \frac{5}{2}$	

Table 4.19: Pole structure of $\mathcal{S}_{B_5 B_1}$

cannot account for these poles proves to be elusive. It is therefore not possible to say for certain whether this instance is a prelude to the general breakdown that appears to happen for $\lambda > \frac{9}{4}$ or not. A further example of curious behaviour arises from consideration of the $[\frac{3}{\lambda} - 1]$ and $[\frac{3}{\lambda} - \frac{2}{3}]$ poles in $\mathcal{S}_{B_5 B_5}$. They seem to imply the appearance of two new particles for $\lambda > \frac{9}{4}$ which disappear for $\lambda = \frac{5}{2}$ only to reappear immediately after this point.

Pole:	$[\frac{4}{3} - \frac{3}{2\lambda}]^2$	$[1 - \frac{3}{2\lambda}]^2$	$[\frac{2}{3} + \frac{1}{2\lambda}]$	$[\frac{1}{3} + \frac{1}{2\lambda}]^3$
Bound state:			B_2	B_6 $\lambda > \frac{9}{4}$

Table 4.20: Pole structure of $\mathcal{S}_{B_5 B_2}$

Pole:	$[1 - \frac{1}{2\lambda}]^2$	$[\frac{5}{2\lambda} - \frac{1}{3}]$	$[\frac{5}{2\lambda} - \frac{2}{3}]$
Bound state:	B_3 at $\lambda = \frac{9}{4}$		

Table 4.21: Pole structure of $\mathcal{S}_{B_5 B_2}$ continued

Pole:	$[\frac{7}{6} - \frac{1}{2\lambda}]$	$[\frac{1}{6} + \frac{3}{2\lambda}]$	$[\frac{3}{2} - \frac{3}{2\lambda}]^2$	$[\frac{5}{2\lambda} - \frac{5}{6}]$
Bound state:	B_1	B_2 at $\lambda = \frac{9}{4}$		
		B_3 at $\lambda = \frac{5}{2}$		B_8 at $\lambda = \frac{5}{2}$

Table 4.22: Pole structure of $\mathcal{S}_{B_5 B_3}$

Pole:	$[\frac{1}{2} + \frac{1}{2\lambda}]^3$	$[\frac{3}{2\lambda} - \frac{1}{6}]^3$	$[\frac{5}{2\lambda} - \frac{1}{2}]$	$[\frac{5}{6} - \frac{1}{2\lambda}]^4$
Bound state:			B_5 at $\lambda = \frac{9}{4}$	
	B_4 at $\lambda = \frac{5}{2}$	B_7 at $\lambda = \frac{5}{2}$		

Table 4.23: Pole structure of $\mathcal{S}_{B_5 B_3}$ continued

Pole:	$[\frac{5}{3} - \frac{2}{\lambda}]^2$	$[\frac{2}{3}]^5$	$[\frac{3}{\lambda} - 1]$	$[\frac{3}{\lambda} - \frac{2}{3}]$	$[\frac{1}{\lambda}]^5$
Bound state:	B_5 $\lambda < \frac{9}{4}$				
	B_5 at $\lambda = \frac{9}{4}$				
	B_5 $\lambda > \frac{9}{4}$				B_8 $\lambda > \frac{9}{4}$

Table 4.24: Pole structure of $\mathcal{S}_{B_5 B_5}$

Pole:	$[\frac{1}{3} + \frac{1}{\lambda}]^3$	$[\frac{4}{3} - \frac{2}{\lambda}]^3$	$[\frac{2}{\lambda}]$	$[\frac{4}{3} - \frac{1}{\lambda}]^2$
Bound state:	B_3 at $\lambda = \frac{9}{4}$		B_1 at $\lambda = \frac{9}{4}$	
	B_4 at $\lambda = \frac{5}{2}$			

Table 4.25: Pole structure of $\mathcal{S}_{B_5 B_5}$ continued

Pole:	$[\frac{1}{2} - \frac{1}{2\lambda}]^2$	$[\frac{5}{6} - \frac{1}{2\lambda}]^2$	$[\frac{1}{6} + \frac{3}{2\lambda}]$	$[\frac{3}{2\lambda} - \frac{1}{6}]$
Bound state:			K_3 at $\lambda = \frac{9}{4}$	

Table 4.26: Pole structure of $\mathcal{S}_{B_5 K_1}$

Pole:	$[\frac{5}{6}]^2$	$[\frac{1}{2}]^2$	$[\frac{7}{6} - \frac{1}{\lambda}]^2$	$[\frac{5}{6} - \frac{1}{\lambda}]^3$	$[\frac{1}{2} + \frac{1}{\lambda}]$	$[\frac{2}{\lambda} - \frac{1}{6}]$	$[\frac{2}{\lambda} - \frac{1}{2}]$
Bound state:					K_2	K_3 at $\lambda = \frac{9}{4}$	

Table 4.27: Pole structure of $\mathcal{S}_{B_5 K_2}$

4.5 $\lambda = 2, \frac{9}{4}$ and $\frac{5}{2}$

In this section I will examine the special points at which q takes an integer value. For $\lambda = 2, \frac{9}{4}$ and $\frac{5}{2}$ the S-matrix reduces to the E_6, E_7 and E_8 S-matrices respectively. The bootstrap for these models has been discussed extensively elsewhere (see [29] for a full treatment of all three cases, and [30], [31], and [16] for E_6, E_7 and E_8 respectively), so most attention will be devoted to the manner in which these S-matrices are reproduced rather than trying to account for every single pole. Having said that, scattering processes were constructed to account for the pole structure of each of these models, but these have not been included. The analysis of the pole structure proves to be quite straight forward due to the fact that all poles that may produce particles (ie. odd order poles) actually do. The generalized bootstrap therefore plays no part in this discussion.

4.5.1 $\lambda = 2, q = 3$

At this point, we only have K_1, K_2, B_1 and B_3 to worry about. For the E_6 model, there are two neutral particles, and two particle-antiparticle pairs.

The neutral particles may be straightforwardly associated with the breathers, but a slight reformulation is necessary to move between the kink and the particle-antiparticle pictures. For $q = 3$ it is possible to define a particle as a kink which interpolates between vacua in a 'clockwise' sense (see figure 4.22), ie. viewing the kink from say, left to right, a particle is a kink that separates vacuum 1 from 2, 2 from 3, or 3 from 1. An anti-kink thus interpolates from $1 \rightarrow 3 \rightarrow 2 \rightarrow 1$.

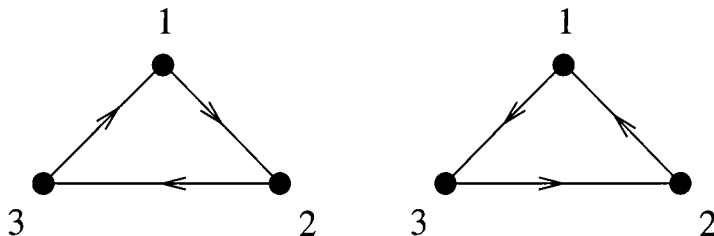


Figure 4.22: Interpolation of (a)Kink and (b)Anti-kink between vacua

Looked at in this way it can be seen that only 2 out of the 4 amplitudes are relevant for each scattering process. Taking $K_1 K_1 \rightarrow K_1 K_1$ as an example, there are not enough vacua to allow \mathcal{S}_0 for a start, and \mathcal{S}_3 is identically zero for $q = 3$. This leaves us with just \mathcal{S}_1 and \mathcal{S}_2 to consider. Denoting the corresponding particle-antiparticle pair by K_1 and \bar{K}_1 respectively, \mathcal{S}_1 thus gives the amplitude for $K_1 K_1 \rightarrow K_1 K_1$ and $\bar{K}_1 \bar{K}_1 \rightarrow \bar{K}_1 \bar{K}_1$ scattering, whereas \mathcal{S}_2 will correspond to $K_1 \bar{K}_1 \rightarrow \bar{K}_1 K_1$ and $\bar{K}_1 K_1 \rightarrow K_1 \bar{K}_1$ scattering (see figures 4.23 and 4.24). This obviously holds for the other kink-kink scattering processes as well.

Using this change of picture, the conserved charges for the E_6 model may be reproduced. From table (4.4), we see that \mathcal{S}_1 has bound states at

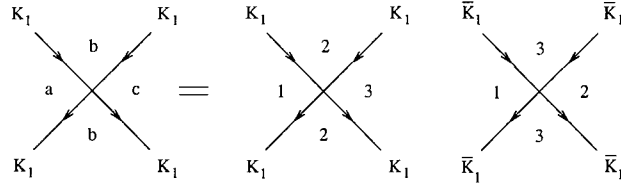


Figure 4.23: $\mathcal{S}_1(\theta)$: Particle/Antiparticle scattering for $\lambda = 2$

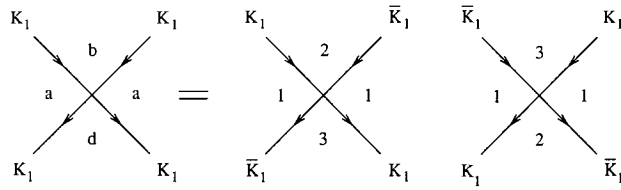


Figure 4.24: $\mathcal{S}_2(\theta)$: Particle/Antiparticle scattering for $\lambda = 2$

$t = \frac{2}{3}$ and $\frac{1}{6}$ corresponding to K_1 and K_2 respectively. In the E_6 , particle-antiparticle picture these correspond to $K_1 K_1 \rightarrow \bar{K}_1$, $K_1 K_1 \rightarrow \bar{K}_2$ and their counterparts under charge conjugation. From this we see that, unlike the kink picture, the ϕ^3 property no longer holds in the E_6 model. From the K_1 and \bar{K}_1 bound states comes the condition

$$\left(e^{\frac{i\pi s}{3}} + e^{-\frac{i\pi s}{3}}\right)^2 = 1 \Rightarrow s \bmod 3 \neq 0: \quad s = 1, 2, 4, 5 + 6n.$$

In the kink picture, where the ϕ^3 property does hold, we have

$$\left(e^{\frac{i\pi s}{3}} + e^{-\frac{i\pi s}{3}}\right) = 1 \Rightarrow s \bmod 3 \neq 0, s \bmod 2 \neq 0: \quad s = 1, 5 + 6n.$$

Looking at table (4.6) we see that K_1 appears as a bound state in $\mathcal{S}_{K_2 K_2}^1$ at $t = \frac{5}{6}$. In conjunction with the K_2 bound state of \mathcal{S}_1 , this allows us to derive the further condition

$$\left(e^{\frac{i\pi s}{2}} + e^{-\frac{i\pi s}{2}}\right) + \left(e^{\frac{i\pi s}{3}} + e^{-\frac{i\pi s}{3}}\right) = 1.$$

In the kink picture this just implies that $s \bmod 2 \neq 0$ which we already knew, but for the E_6 model it imposes a greater restriction on s which may now only take the values $s = 1, 4, 5, 7, 8, 11 + 12n$. This is the expected set of conserved charges for the E_6 model, and on inspection no further restrictions are found in either picture.

In reproducing the pole structure of the E_6 model, it is found that various poles overlap. This has already been noted in the discussion of $\mathcal{S}_{K_2K_2}$ regarding the poles of $[\frac{1}{\lambda}]$. These combine to give a third order pole that may be interpreted as either a direct or cross channel scattering process. In other instances it is a case of different pairs of poles overlapping, for example $[\frac{1}{6} + \frac{1}{2\lambda}]^2$ and $[\frac{3}{2\lambda} - \frac{1}{6}]$ in $\mathcal{S}_{B_3B_1}$, or $[\frac{1}{6} + \frac{1}{\lambda}]$ and $[\frac{1}{\lambda} - \frac{1}{6}]$ in $\mathcal{S}_{B_1K_2}$. When a pair of poles cross over care must be taken. Using analytic continuation around such points, it is found that the sign of their residues will change. If a pole involved in such a crossover is being interpreted as a particle, then it will change from a direct to a cross channel bound state or vice versa depending on the initial sign of its residue. The only case where this threatens to happen at $\lambda = 2$ occurs in $\mathcal{S}_{B_3B_3}$. Here, the poles of $[\frac{2}{3}]^3$, $[\frac{2}{\lambda} - \frac{1}{3}]$, and $[\frac{2}{\lambda} - \frac{2}{3}]$ overlap (see table (4.11)). Away from $\lambda = 2$ the $[\frac{2}{3}]^3$ poles corresponds to a B_3 bound state, whereas the other two pairs are covered by the generalized bootstrap. Since the third order poles at $t = \frac{1}{3}$ and $\frac{2}{3}$ will each cross two other poles, the signs of their residues will remain unaltered. This neatly avoids the contradictions inherent in interpreting $(\frac{1}{3})$ as the direct channel bound state. Other instances where poles overlap either do not produce bound states both before and after the crossover, or produce them only at the point of intersection.

4.5.2 $\lambda = \frac{9}{4}, q = 2$

At $\lambda = \frac{9}{4}$ we see much of the same behaviour as at $\lambda = 2$. This time there is only one relevant amplitude for each kink-kink scattering amplitude, namely those of \mathcal{S}_3 type, due to the presence of only 2 distinct vacuum states. Once again several sets of poles overlap resulting in some intricate scattering processes, but the swapping over of direct and cross channel poles is avoided as before.

On passing $\lambda = 2$, B_2 and B_5 enter the particle spectrum bringing the number of known particles to 6. Previously, the particles appearing for an integer value of q have been present since the last point at which q was integer, if not longer, but for $\lambda = \frac{9}{4}$ a new kink K_3 appears out of nowhere. There is no great problem with this — the action of the generalized bootstrap means that it does not enter at threshold and so has non-zero rapidity — but it is curious nonetheless. What is more surprising is that this is the only point at which K_3 appears. For $\lambda < \frac{9}{4}$ the poles in question are covered by the generalized bootstrap, and for $\lambda > \frac{9}{4}$ none may be interpreted as particles without reducing to zero the number of conserved charges. At $\lambda = \frac{9}{4}$ we reach the end of the last region where a satisfactory explanation can be found for all amplitudes, and the bootstrap closed for a continuous range of λ .

4.5.3 $\lambda = \frac{5}{2}, q = 1$

The only other point at which the situation simplifies occurs at $\lambda = \frac{5}{2}$. There are not enough vacua for any kink type particles here, so we are left with the breather-breather amplitudes alone. Aswell as the 7 breathers which are present for $\lambda > \frac{9}{4}$, there appears a B_4 for $\lambda = \frac{5}{2}$ alone — much the same as K_3 at $\lambda = \frac{9}{4}$.

In calculating the various amplitudes involving B_6 , B_7 , and B_8 which appear for $\lambda > \frac{9}{4}$, it is found that some contain zeroes in the physical strip. Although physical strip zeroes are not as pathological as unexplained poles, their appearance seems to be another sign heralding the breakdown of the bootstrap. For $\lambda = \frac{5}{2}$ these zeroes coincide with other higher order poles, reducing them by an appropriate order for the E_8 model. When examining the pole structure of $\mathcal{S}_{B_5 B_5}$ in an earlier section, it was mentioned that the poles at $[\frac{3}{\lambda} - 1]$ and $[\frac{3}{\lambda} - \frac{2}{3}]$ could be interpreted as particles without destroying the set of conserved charges. The problem with such an interpretation was that they not only produced amplitudes with physical strip zeroes, but that they disappeared at $\lambda = \frac{5}{2}$. In light of the recent discussion concerning overlapping poles it becomes evident that not only would these particles disappear at this point, but their direct and cross channel poles would swap as well.

As λ increases past $\frac{5}{2}$ the number of unexplicable poles increases and no attempt at closing the bootstrap has yet been successful.

4.6 Summary

In conclusion, we may give the particle spectrum for $\lambda \leq \frac{9}{4}$ with some certainty. For $q \leq 3$ ($\lambda \leq 1$) there is only the kink state K_1 , but as λ becomes greater than 1, B_1 also appears. No further particles enter the spectrum until $\lambda = \frac{3}{2}$, at which point both K_2 and B_3 appear. These form the full complement of particles for $\lambda < 2$, beyond which B_2 and B_5 appear. Beyond $\lambda = \frac{9}{4}$, B_6 , B_7 , and B_8 are the only new particles we can be sure of. It has also been possible to give a complete account for the S-matrix amplitudes up until $\lambda = \frac{9}{4}$ (bar one pole for $2 < \lambda < \frac{15}{7}$), after which point we can reproduce

the E_8 S-matrix for $\lambda = \frac{5}{2}$.

The question arises as to whether the poles causing the trouble are actually present, or if there is some ambiguity in the amplitudes that allows for a more minimal solution to the bootstrap equations. This does not appear to be likely, given the accurate reproduction of known amplitudes for the E_6 , E_7 , E_8 , 3-state Potts and Ising models. At these points, all amplitudes can be given in terms of ratios of sinh functions, thus all poles and zeroes both in and out of the physical strip must fit together precisely, and any extraneous factors must cancel each other out. In $\mathcal{S}_{K_1 K_2}$ for example, it can be checked that the poles of $[\frac{2}{3} - \frac{3}{2\lambda}]$ and $[1 - \frac{5}{2\lambda}]$ overlap with zeroes of $\Pi(\frac{\lambda\theta}{i\pi})$ at these points. In searching for an explanation via the generalized bootstrap, it was found that there were no appropriate diagrams of either second or third order before cancellations. This rules out any more complex scattering processes involving these as subdiagrams. This leaves diagrams without the obvious symmetry of those found for most other cases, and consequently much harder to either find or rule out.

Looking at the manner in which particles enter the spectrum suggests another possibility. All the particles which appear before $\lambda = \frac{9}{4}$ do so as a bound state at threshold in at least one scattering amplitude. This means that when they appear, their mass is the sum of two existing particle's masses. This does not happen for particles appearing after $\lambda = \frac{9}{4}$, suggesting that there may possibly be one or more additional particles present that are not generated by application of the bootstrap to $K_1 K_1 \rightarrow K_1 K_1$ scattering amplitudes. This is also quite difficult to rule out, involving as it does the application of the bootstrap in reverse.

Overall, it seems quite possible that genuinely new behaviour is behind

the difficulties experienced in closing the bootstrap. A complete account of $\Phi_{(1,2)}$ and $\Phi_{(2,1)}$ perturbed conformal field theories has yet to be given, and they are still capable of producing the unexpected [32], [33]. This makes investigation of the problems brought to light in this thesis all the more relevant.

Chapter 5

Statistical Mechanics & Field Theory with Boundaries

Up to now we have considered theories living in an infinite, two-dimensional space. When looking at bounded domains, we must also consider the possible boundary conditions that may be imposed. In this chapter I shall review the behaviour which arises from imposition of boundary conditions on bulk theories. Starting with statistical mechanical models, the discussion will quickly move on to boundary conformal field theory and then boundary S-matrices. This prepares the way for a treatment of various boundary conditions on the q -state Potts model.

5.1 Boundary conditions and duality relations in statistical mechanics

In this section, the partition functions of a given model with different boundary conditions will be considered.

5.1.1 Fixed & free boundary conditions in the 2-d Ising model

The simplest system to consider is the Ising model, which is equivalent to the 2-state Potts model. Using a square lattice of spins as in Chapter 1, the interaction energy between adjacent spins in the bulk is defined to be $-J\sigma_i\sigma_j$ where σ can take either of the values ± 1 . Boundary conditions enter through restrictions placed on the allowed values of spins at the boundary, and also (in some cases) as an explicit boundary term in the action. This latter possibility will not be needed in the present discussion. The partition function for an $m \times n$ lattice is therefore given by

$$\mathcal{Z}_{m,n} = \sum_{\sigma} e^{\frac{J}{k_B T} \sum_{\langle i,j \rangle} \sigma_i \sigma_j}. \quad (5.1)$$

where the sum is over allowed spin configurations. Making use of the identity $\delta(\sigma_i, \sigma_j) = \frac{1}{2}(1 + \sigma_i\sigma_j)$ we see that this indeed gives the partition function for the 2-state Potts model with coupling $\tilde{J} = J/2$, up to an overall factor.

Let us consider an $m \times n$ lattice of spins $\sigma(x, y)$ ($x = 1, 2, \dots, m; y = 1, 2, \dots, n$) which is periodic in the x direction ie. $\sigma(1, y) = \sigma(m + 1, y)$, effectively making the lattice into a cylinder. The spins may alternatively be labelled as σ_i $i = 1, 2, \dots, mn$ when it is more convenient to do so. The spins on the two remaining boundaries will either be fixed to one value (+1 or -1) or left free to take on either value. These possibilities will be denoted as $+, -$ and f respectively.

‘High temperature’ expansion & fixed boundary conditions

Imposing fixed boundary conditions on both sides ($\sigma(x, 1) = \sigma_a$ and $\sigma(x, n) = \sigma_b$), we may write the partition function as

$$\mathcal{Z}_{m,n} = e^{2mK} \sum_{\sigma} e^{K \sum_{(i,j)} \sigma_i \sigma_j}$$

where $K = \frac{J}{k_B T}$. The sum is over nearest neighbour spin pairs, excluding those pairs with both spins on the boundary. These are accounted for by the factor of e^{2mK} . We may rewrite this as

$$\begin{aligned} \mathcal{Z}_{m,n}^P &= e^{2mK} \sum_{\sigma} \prod_{(i,j)} (\cosh(K) + \sinh(K) \sigma_i \sigma_j) \\ &= e^{2mK} \cosh(K)^{(2n-3)m} \sum_{\sigma} \prod_{(i,j)} (1 + \nu \sigma_i \sigma_j) \quad \nu = \tanh(K). \end{aligned}$$

Expanding the product, we obtain a sum of $2^{(2n-3)m}$ terms, each term containing either a 1 or a $\nu \sigma_i \sigma_j$ from each nearest neighbour pair (i, j) . As in chapter 1 we may associate a unique graph with each term by placing a bond on the edge (i, j) between the i^{th} and j^{th} spins if a factor of $\nu \sigma_i \sigma_j$ is present, but leaving (i, j) empty if the factor 1 appears instead. The sum over σ for a given term will be non-zero only if each spin σ_i that is not on the boundary appears an even number of times. We are thus left with a sum over all graphs on the lattice where lines of bonds must either form closed loops, or end on the boundaries. Denoting the number of bonds by l and the number of lines from one boundary to the other by p , each allowed graph will have a factor of $\nu^l (\sigma_a \sigma_b)^p$ associated with it, and a weight of $2^{(n-2)m}$ from the sum over spins. As a result, the partition function now takes the form

$$\mathcal{Z}_{m,n}^P = e^{2mK} \cosh(K)^{(2n-3)m} 2^{(n-2)m} \sum_{\mathcal{G}} \nu^l (\sigma_a \sigma_b)^p. \quad (5.2)$$

This form of the partition function is often referred to as a ‘high temperature’ representation of \mathcal{Z}_N since for large T , ν becomes small and the

leading term comes from the $l = 0$ graph. This can be slightly misleading, as equation (5.2) is exact for all temperatures — for a finite sized lattice this sum is obviously finite, whereas in the infinite volume limit the sum will only converge for $T > T_c$. There are two different cases covered by this partition function: we may fix both sides to the same value ($++$ or $--$), both of which give the same partition function; or fix each side to a different value ($+ -$). The only difference between $\mathcal{Z}_{m,n}^{P++}$ and $\mathcal{Z}_{m,n}^{P+-}$ is the sign of configurations with an odd number of lines joining opposite boundaries:

$$\mathcal{Z}_{m,n}^{P++} = e^{2mK} \cosh(K)^{(2n-3)m} 2^{(n-2)m} \sum_{\mathcal{G}} \nu^l \quad (5.3)$$

$$\mathcal{Z}_{m,n}^{P+-} = e^{2mK} \cosh(K)^{(2n-3)m} 2^{(n-2)m} \sum_{\mathcal{G}} \nu^l (-1)^p. \quad (5.4)$$

‘Low temperature’ expansion & free boundary conditions

For a given spin configuration on an $m \times n$ lattice \mathcal{L} , there will be l unlike, and $(2n - 1)m - l$ like spin pairs. Equation (5.1) can thus be written as

$$\mathcal{Z}_{m,n} = \sum_{\sigma} e^{K[(2n-1)m-2l]}.$$

Noting that the contribution of a given configuration depends solely on the number of unlike pairs, we may once again reformulate $\mathcal{Z}_{m,n}$ in a more convenient form. A dual lattice $\mathcal{L}_{\mathcal{D}}$ can be constructed with its sites at the center of the faces of \mathcal{L} , and edges joining neighbouring sites. As we can see from figure 5.1, $\mathcal{L}_{\mathcal{D}}$ is another square lattice, and the spins of \mathcal{L} are located on its faces. Using this perspective, we can represent the configurations of $\mathcal{Z}_{m,n}$ graphically by placing a line on each edge of $\mathcal{L}_{\mathcal{D}}$ that lies between two unlike spins. Away from the boundary, these lines will form closed loops as there must be an even number of changes of spin around — and hence

an even number of lines connected to — each site. Allowing free boundary conditions on both boundaries means that lines are allowed to start and end on them. The only restriction placed on such lines is that the number going from one boundary to the other must be even in order to preserve periodicity in the x direction. The partition function thus becomes a sum over graphs on \mathcal{L}_D composed of closed loops and lines between boundaries. Each such graph corresponds to 2 spin configurations which can be obtained one from the other by swapping the sign of all spins. Denoting the number of lines joining opposite boundaries as p , $\mathcal{Z}_{m,n}$ can be written

$$\mathcal{Z}_{m,n}^{P\ ff} = 2e^{K(2n-1)m} \sum_{\mathcal{G}} e^{-2Kl} \quad p = 0 \pmod{2}. \quad (5.5)$$

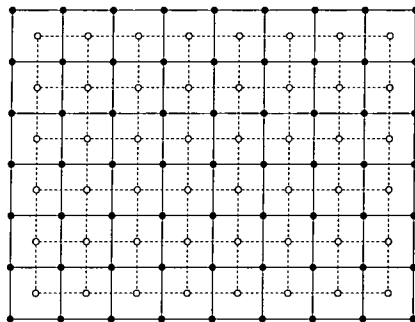


Figure 5.1: Construction of dual lattice \mathcal{L}_D (dashed lines, empty circles) for lattice \mathcal{L} (solid lines, full circles)

5.1.2 Fixed & free boundary conditions in 3-state Potts model

The approach used in the previous section may be generalized to cover this more complicated case. As we know from chapter 1, the partition function

is defined as

$$\mathcal{Z}_{m,n} = \sum_{\sigma} e^{\left(\frac{J}{k_B T} \sum_{(i,j)} \delta(\sigma_i, \sigma_j)\right)} = \sum_{\sigma} \prod_{(i,j)} e^{K \delta(\sigma_i, \sigma_j)}$$

Setting the allowed values of σ_i to be 1, $e^{\frac{2\pi i}{3}}$ and $e^{-\frac{2\pi i}{3}}$, we may use the identity $\delta(\sigma_i \sigma_j) = \frac{1}{3} (1 + \sigma_i \bar{\sigma}_j + \bar{\sigma}_i \sigma_j)$ to rewrite $\mathcal{Z}_{m,n}$ as

$$\begin{aligned} \mathcal{Z}_{m,n} &= \sum_{\sigma} \prod_{(i,j)} \left[1 + (e^K - 1) \delta(\sigma_i \sigma_j) \right] \\ &= \sum_{\sigma} \prod_{(i,j)} \left[g + \nu \sigma_i \bar{\sigma}_j + \nu \bar{\sigma}_i \sigma_j \right] \end{aligned}$$

where $\bar{\sigma} = \sigma^*$, $\nu = \frac{1}{3}(e^K - 1)$ and $g = 1 + \nu$. On expanding the product, we may associate each term with a unique graph on the lattice. If the factor g appears for a given edge (i, j) , it is left empty, but if either of the other two factors appears a line is drawn along the edge. These two factors may be distinguished by placing an arrow on the line pointing from the σ to the $\bar{\sigma}$. When taking the sum over spin values, only terms with powers of $|\sigma_i|$ for each σ_i will give a non-zero contribution. The partition function may consequently be expressed as a sum over all sets of closed, directed loops on \mathcal{L} . Making the lattice periodic in the x direction, and imposing fixed boundary conditions at either end of the resulting cylinder means that lines ending on boundaries must also be taken into account. After taking all these factors into consideration, we end up with the expression

$$\begin{aligned} \mathcal{Z}_{m,n}^{xy} &= e^{2mK} \sum_{\sigma} \sum_{d.g.} g^{(2n-3)m-l} \nu^l (\sigma_x \bar{\sigma}_y)^{p_1} (\bar{\sigma}_x \sigma_y)^{p_2} \\ &= 3^{(n-2)m} e^{2mK} g^{(2n-3)m} \sum_{d.g.} \left(\frac{\nu}{g}\right)^l (\sigma_x \bar{\sigma}_y)^{p_1} (\bar{\sigma}_x \sigma_y)^{p_2} \end{aligned}$$

The remaining sum is over all allowed directed graphs, and the contribution for a given directed graph is completely determined by its total number of links l , the number of lines from the $y = 1$ to the $y = n$ boundary (p_1), and the number of lines from $y = n$ to $y = 1$ (p_2). The boundary conditions are given by $\sigma(x, 1) = \sigma_x$ and $\sigma(x, n) = \sigma_y$.

There are three distinct combinations of boundary conditions that are covered by this. Denoting $\sigma = 1, e^{\frac{2\pi i}{3}}, e^{-\frac{2\pi i}{3}}$ as a, b and c respectively, we have

$$\begin{aligned} \mathcal{Z}_{m,n}^{aa} &= 3^{(n-2)m} e^{2mK} g^{(2n-3)m} \sum_{d.g.} \left(\frac{\nu}{g}\right)^l \\ \mathcal{Z}_{m,n}^{ab} &= 3^{(n-2)m} e^{2mK} g^{(2n-3)m} \sum_{d.g.} \left(\frac{\nu}{g}\right)^l e^{\frac{2\pi i}{3}P} \\ \mathcal{Z}_{m,n}^{ac} &= 3^{(n-2)m} e^{2mK} g^{(2n-3)m} \sum_{d.g.} \left(\frac{\nu}{g}\right)^l e^{-\frac{2\pi i}{3}P} \quad \text{where } P = p_2 - p_1. \end{aligned}$$

All other fixed boundary conditions are related to these by the \mathcal{Z}_3 symmetry of the model.

The directed graphs contributing to these partition functions may be viewed in an alternative manner. The lines of a given graph on an $m \times n$ lattice may be seen as separating regions of differing spin for an $m \times (n - 1)$ lattice, and being located on the edges of the dual lattice. This is much the same as the Ising model duality, but we now have three spin states to allocate consistently to different regions of the lattice. Imagining that we are standing on a line, facing the direction in which its arrow is pointing, we may enforce the rule that the spin on the right hand side of the line is $e^{\frac{2\pi i}{3}}$ times that on the left. This means that on crossing from left to right $a \rightarrow b$, $b \rightarrow c$, and $c \rightarrow a$. All that is needed is to specify the value of the spins

in one region, and the rest will follow. If we wish to make the $m \times (n - 1)$ lattice periodic, then only graphs with $p = 0 \pmod{3}$ are allowable. The set of graphs remaining for a periodic lattice will be that which generates the partition function for free boundary conditions:

$$Z_{m,n-1}^{ff} = 3e^{(2n-3)mK} \sum_{d.g.} e^{-lK} \quad p = 0 \pmod{3}.$$

5.2 Boundary conformal field theory

In a series of papers ([34], [35], [36] and [37]), Cardy explored the consequences of limiting a conformal field theory to the half plane. The results, although of great importance, are not directly relevant to the work presented in this chapter and must be passed over briefly. In this series of papers it was shown that in order to preserve the boundary under conformal transformations, the condition

$$T_{xy} = [T(z) - \bar{T}(\bar{z})] = 0$$

must be satisfied at the boundary. If we are dealing for example with a conformal field theory defined on the upper half plane $Im(z) > 0$, then $\bar{T}(\bar{z})$ may be taken as the analytic continuation of $T(z)$ in the lower half plane. The theory can thus be seen to possess a structure similar to that of the bulk theory developed in Chapter 2 — the difference being that there is now only one copy of the Virasoro algebra.

Boundary conditions are changed by insertion of boundary operators at the boundary, and in [37] the operator content of a theory on an annulus was related to its boundary conditions through the fusion rules of the algebra. This deserves a short explanation. The upper half plane may be mapped into

an infinitely long strip, and boundary conditions α and β imposed on either side. On mapping back to the upper half plane, there is now a discontinuity at $z = 0$ — with boundary conditions $(\alpha\alpha)$, the lowest energy boundary state is invariant under translations (ie. action of L_{-1}), but for boundary conditions $(\alpha\beta)$ this is not the case. Juxtaposition of different conformally invariant boundary conditions $(\alpha\beta)$ is thus seen to be equivalent to the insertion of a (primary) boundary operator $\phi_{\alpha\beta}(0)$.

On making the strip periodic, the type of boundary states allowed by modular invariance were then related to representations of the Virasoro algebra of highest weight h . For boundary conditions of type j and k , the partition function was shown to take the form

$$\mathcal{Z}_{jk} = \sum_i N_{jk}^i \chi_i(q) \quad (5.6)$$

where $\chi_i(q)$ is the character of the representation with highest weight i , and N_{jk}^i are the fusion coefficients — the number of distinct ways that representation i appears in the fusion of two fields belonging to representations j and k respectively.

Taking for example the three state Potts model, Cardy [37] constructed boundary states $|\tilde{0}\rangle$, $|\frac{2}{3}\rangle$ and $|\frac{2^v}{3}\rangle$ related by Z_3 rotations. Identifying $|\tilde{0}\rangle$ with $|a\rangle$ — all sites on the boundary being in state a — the other two states may be identified with $|b\rangle$ and $|c\rangle$ respectively. From equation (5.6) we see that

$$\mathcal{Z}_{aa} = \chi_0 \quad ; \quad \mathcal{Z}_{ab} = \chi_{\frac{2}{3}} \quad ; \quad \mathcal{Z}_{ac} = \chi_{\frac{2^v}{3}}.$$

Using the fusion rules

$$\left[\frac{2^v}{3}\right] \times \left[\frac{2}{3}\right] = [0] \quad \text{and} \quad \left[\frac{2^v}{3}\right] \times \left[\frac{2^v}{3}\right] = \left[\frac{2}{3}\right]$$

it can be seen that $\mathcal{Z}_{aa} = \mathcal{Z}_{bb} = \mathcal{Z}_{cc}$ and $\mathcal{Z}_{ab} = \mathcal{Z}_{bc} = \mathcal{Z}_{ca}$ as expected by the Z_3 symmetry of the model. The partition function \mathcal{Z}_{ff} takes the form ([36], [37] and [38])

$$\begin{aligned}\mathcal{Z}_{ff} &= \chi_0 + \chi_{\frac{2}{3}} + \chi_{\frac{2}{3}^v} \\ &= \mathcal{Z}_{aa} + \mathcal{Z}_{ab} + \mathcal{Z}_{ac}\end{aligned}$$

5.3 Boundary S-matrices

In this section, we will be concerned with adapting the S-matrix approach of chapter 3 to the semi-infinite plane. This was first treated in papers by Goshal and Zamolodchikov [39], and Fring and Koberle [40]. Starting with a conformal field theory on the half-plane with a particular conformal boundary condition (CBC), we may now add a perturbation at the boundary as well as in the bulk. If $\Phi_B(y)$ is the (relevant) perturbing operator acting on the boundary at $x = 0$, this may be written as

$$\mathcal{A} = \mathcal{A}_{CFT+CBC} + \int_{-\infty}^{\infty} dy \int_{-\infty}^0 dx \Phi(x, y) + \int_{-\infty}^{\infty} dy \Phi_B(y)$$

In general, such boundary conditions will not allow the integrals of motion required for integrability. It will be assumed that the boundary conditions under consideration are those ‘integrable’ boundary conditions [39] for which non-trivial integrals of motion may be found. Even with this assumption, the boundary interactions may still not give rise to a well defined quantum field theory [41].

In-states will consist of n particles moving towards the boundary at $x = 0$, and are once again generated by particle creation operators $A_a(\theta)$ satisfying

the same commutation relations as before. Asymptotic in-states can thus be written as

$$|A_{a_1}(\theta_1)A_{a_2}(\theta_2)\dots A_{a_n}(\theta_n)\rangle_{B,in} = A_{a_1}(\theta_1)A_{a_2}(\theta_2)\dots A_{a_n}(\theta_n)|0\rangle_B$$

with $\theta_1 > \theta_2 > \dots > \theta_n > 0$. The ground state $|0\rangle_B$ may be thought of as a stationary, impenetrable particle sitting at $x = 0$ with creation operator B such that

$$|0\rangle_B = B|0\rangle.$$

We may therefore consider asymptotic in-states to be created by products of operators

$$A_{a_1}(\theta_1)A_{a_2}(\theta_2)\dots A_{a_n}(\theta_n)B \tag{5.7}$$

acting on the vacuum state $|0\rangle$. Asymptotic out-states can be similarly defined as consisting of some number of particles moving away from the boundary with rapidities $\theta'_1, \theta'_2, \dots, \theta'_m < 0$. The presence of integrals of the motion again implies that scattering is elastic, and particle trajectories may be shifted relative to one another so that collisions take place at well separated locations. Out-states are thus constrained to take the form:

$$A_{b_1}(-\theta_1)A_{b_2}(-\theta_2)\dots A_{b_n}(-\theta_n)B.$$

The n-particle S-matrix elements $R_{a_1 a_2 \dots a_n}^{b_1 b_2 \dots b_n}$ relate the in and out states by

$$A_{a_1}(\theta_1)A_{a_2}(\theta_2)\dots A_{a_n}(\theta_n)B = R_{a_1 a_2 \dots a_n}^{b_1 b_2 \dots b_n}(\theta_1, \theta_2, \dots, \theta_n)A_{b_1}(-\theta_1)A_{b_2}(-\theta_2)\dots A_{b_n}(-\theta_n)B.$$

Factorisability of the S-matrix ensures that these may all be expressed in terms of the bulk scattering amplitudes $\mathcal{S}_{a_1 a_2}^{b_1 b_2}(\theta)$, and the one particle boundary scattering amplitudes $R_a^b(\theta)$ (figure 5.2) given by

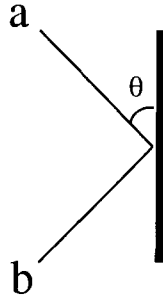


Figure 5.2: Boundary scattering amplitude $R_a^b(\theta)$

$$A_a(\theta)B = R_a^b(\theta)A_b(\theta)B. \quad (5.8)$$

The amplitudes $R_a^b(\theta)$ must satisfy a set of conditions analogous to those required of $\mathcal{S}_{a_1 a_2}^{b_1 b_2}(\theta)$:

1. Boundary Yang-Baxter equation: This arises in the same manner as the bulk Yang-Baxter relation, and takes the form

$$R_{a_2}^{c_2}(\theta_2)\mathcal{S}_{a_1 c_2}^{c_1 d_2}(\theta_1 + \theta_2)R_{c_1}^{d_1}(\theta_1)\mathcal{S}_{d_2 d_1}^{b_2 b_1}(\theta_1 - \theta_2) = \mathcal{S}_{a_1 a_2}^{c_1 c_2}(\theta_1 - \theta_2)R_{c_1}^{d_1}(\theta_1)\mathcal{S}_{c_2 d_1}^{d_2 b_1}(\theta_1 + \theta_2)R_{d_2}^{b_2}(\theta_2)$$

and may be represented pictorially as in figure 5.3.

2. Unitarity: By applying (5.8) twice, the condition

$$R_a^c(\theta)R_c^b(-\theta) = \delta_a^b$$

is obtained. This is shown in figure 5.4.

3. Crossing Symmetry: It was shown in [39] that the amplitude $K^{ab}(\theta)$ defined by

$$K^{ab}(\theta) = R_a^b\left(\frac{i\pi}{2} - \theta\right)$$

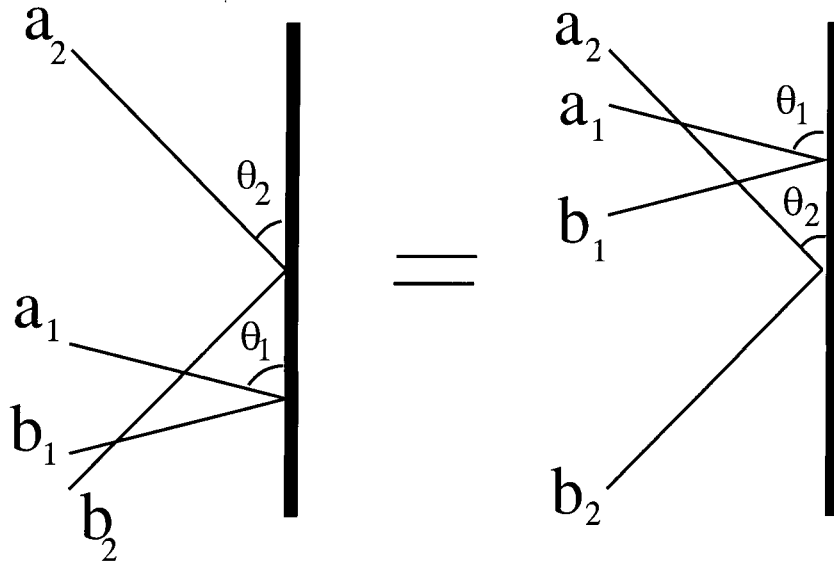


Figure 5.3: Boundary Yang-Baxter

must satisfy the boundary ‘cross-unitarity’ condition (see figure 5.5)

$$K^{ab}(\theta) = \mathcal{S}_{cd}^{ab}(2\theta)K^{cd}(-\theta).$$

Any ambiguity $\Phi_B(\theta)$ left in $R_a^b(\theta)$ such that

$$R_a^b(\theta) \rightarrow R_a^b(\theta)\Phi_B(\theta)$$

also yields a valid solution, must satisfy the conditions

$$\Phi_B(\theta) = \Phi_B(i\pi - \theta)$$

and

$$\Phi_B(\theta)\Phi_B(-\theta) = 1.$$

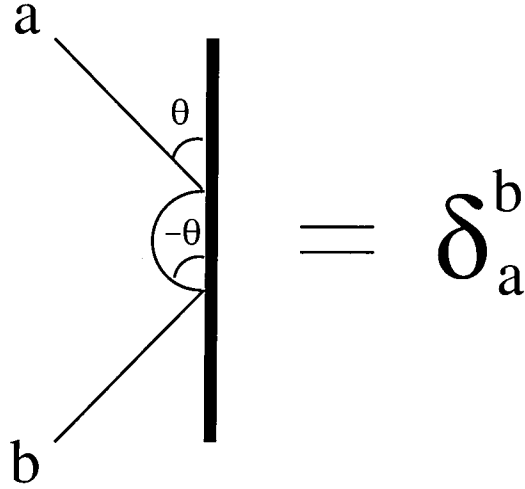


Figure 5.4: Boundary unitarity

4. Boundary Bootstrap: Additional constraints must be satisfied if the bulk S-matrix possesses any bound state poles. If particle A_c appears as a bound state in $A_a A_b$ scattering at $\theta = iu_{ab}^c$, then $R_a^b(\theta)$ must satisfy

$$f_{ab}^d R_d^c(\theta) = R_b^{b_2}(\theta - i\bar{u}_{bd}^a) \mathcal{S}_{ab_2}^{a_2 b_1}(2\theta + i\bar{u}_{ad}^b - i\bar{u}_{bd}^a) R_{a_2}^{a_1}(\theta + i\bar{u}_{ad}^b) f_{b_1 a_1}^c$$

shown in figure 5.6. If A_a and A_b have the same mass, then it is to be expected that $R_a^b(\theta)$ will possess a pole at $\theta = \frac{i\pi}{2} - \frac{iu_{ab}^c}{2}$ (see figure 5.7), and $K^{ab}(\theta)$ takes the form

$$K^{ab}(\theta) \simeq \frac{i}{2} \frac{f_c^{ab} g^c}{\theta - \frac{iu_{ab}^c}{2}}$$

where g^c is the coupling amplitude of A_c to the boundary. If $g^a, g^b \neq 0$ then $K^{ab}(\theta)$ will have a pole at $\theta = 0$ as shown in figure 5.8, and may be written as

$$K^{ab}(\theta) \simeq -\frac{i}{2} \frac{g^a g^b}{\theta}.$$

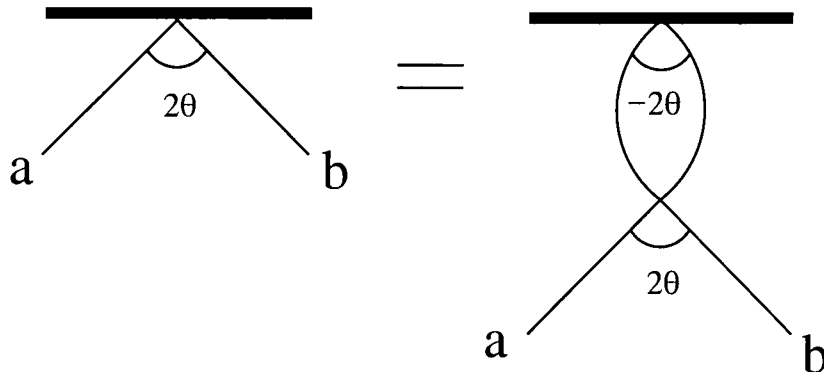


Figure 5.5: Boundary ‘cross-unitarity’

5.4 Boundary S-matrix for q -state Potts model

In order to illustrate how the technology developed in the previous section may be applied in practice, we turn our attention back to the Potts model. In [2], Chim calculated the boundary S-matrix elements associated with fixed and free boundary conditions for the q -state Potts model with $0 < q \leq 3$. What now follows will be a summary of this work, followed by a discussion of one further possible boundary condition.

It will be recalled that the bulk q -state Potts model has q distinct vacua so, before any restrictions are imposed at the boundary, there are q different possible boundary states B_a , ($a = 1, 2, \dots, q$). It should be remembered that q is not necessarily an integer. The n -particle asymptotic in-state (5.7) thus becomes an n -kink in-state of the form

$$A_{a_1 a_2}(\theta_1) A_{a_2 a_3}(\theta_2) \dots A_{a_n a}(\theta_n) B_a$$

where $a_i \neq a_{i+1}$, $a_n \neq a$ and $\theta_1 > \theta_2 > \dots > \theta_n > 0$. One-particle reflection amplitudes $R_{ba}^c(\theta)$, shown in figure 5.9, are defined by

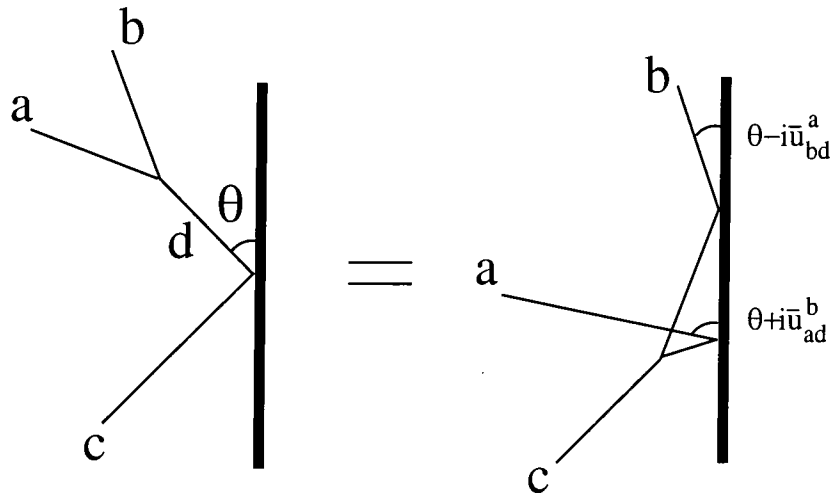


Figure 5.6: Boundary bootstrap

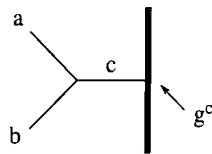


Figure 5.7: Boundary coupling of bulk bound state

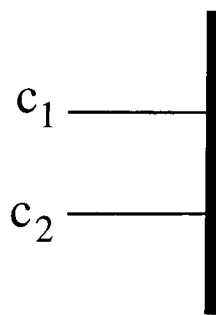


Figure 5.8: Two particle coupling to boundary

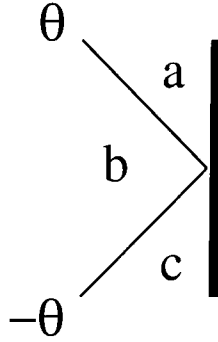


Figure 5.9: Kink reflection amplitude $R_{ba}^c(\theta)$

$$A_{ba}(\theta)B_a = \sum_c R_{ba}^c(\theta)A_{bc}(-\theta)B_c.$$

The various constraints mentioned in the last section must now be rewritten in terms of this kink picture.

1. The boundary Yang-Baxter equation becomes

$$\begin{aligned} & \sum_g \sum_f R_{ba}^f(\theta_1) \mathcal{S}_{cf}^{bg}(\theta_1 + \theta_2) R_{gf}^e(\theta_2) \mathcal{S}_{ce}^{gd}(\theta_2 - \theta_1) \\ &= \sum_{g'} \sum_{f'} \mathcal{S}_{ca}^{bg'}(\theta_2 - \theta_1) R_{g'a}^{f'}(\theta_2) \mathcal{S}_{cf'}^{g'd}(\theta_1 + \theta_2) R_{df'}^e(\theta_1) \end{aligned}$$

and may be represented pictorially as in figure 5.10. The bulk amplitudes $\mathcal{S}_{ac}^{bd}(\theta)$, treated in chapter 3, are shown in figures 5.11 and 5.12.

2. Unitarity of the boundary S-matrix (figure 5.13) takes the form

$$\sum_{c \neq b} R_{ba}^c(\theta) R_{bc}^d(-\theta) = \delta_a^d$$

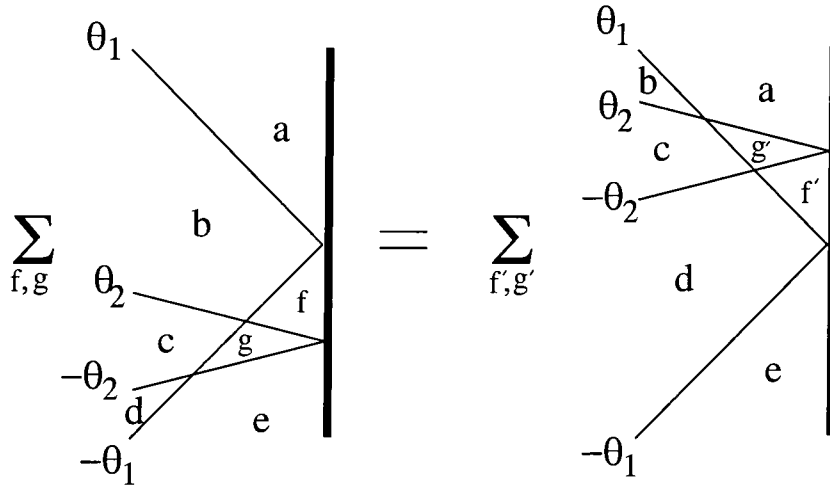


Figure 5.10: Kink boundary Yang-Baxter equations

3. The cross-channel amplitude is now defined as

$$K^{abc}(\theta) = R_{ba}^c\left(\frac{i\pi}{2} - \theta\right)$$

in terms of which the ‘cross-unitarity’ condition (figure 5.14) now looks like

$$K^{abc}(\theta) = \sum_{d \neq a, c} S_{ca}^{bd}(2\theta) K^{adc}(-\theta).$$

4. As discussed in previous chapters, for $q \leq 3$ there is only the K_1 type of kink state to worry about, and only one bound state $K_1 K_1 \rightarrow K_1$ which appears at $\theta = \frac{2\pi i}{3}$. The boundary bootstrap equation (figure 5.15) for this pole is given by

$$R_{ab}^d(\theta) = \sum_{j \neq c} \sum_{e \neq a, d} R_{cb}^j\left(\theta - \frac{i\pi}{3}\right) S_{af}^{ce}(2\theta) R_{ef}^d\left(\theta + \frac{i\pi}{3}\right). \quad (5.9)$$

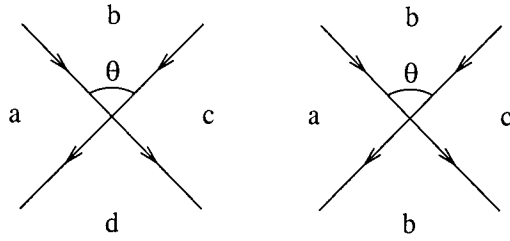


Figure 5.11: Kink amplitudes $\mathcal{S}_0(\theta)$ and $\mathcal{S}_1(\theta)$

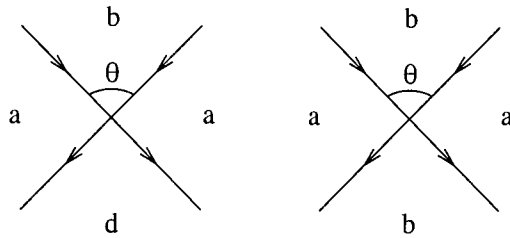


Figure 5.12: Kink amplitudes $\mathcal{S}_2(\theta)$, and $\mathcal{S}_3(\theta)$

If a boundary condition respects the S_q symmetry of the bulk model, then $R_{ab}^c(\theta)$ will be expected to possess a pole at $\theta = \frac{i\pi}{6}$ (figure 5.16) with residue

$$R_{ba}^c(\theta) \simeq \frac{i}{2} \frac{f g_b^c}{\theta - \frac{i\pi}{6}}.$$

If the boundary couplings g_a^c and G_b^a are non-zero, then $R_{ab}^c(\theta)$ must have an additional pole at $\theta = \frac{i\pi}{2}$ (figure 5.17). This will have residue

$$R_{ba}^c(\theta) \simeq \frac{i}{2} \frac{g_a^c g_b^a}{\theta - \frac{i\pi}{2}}.$$

5.4.1 Fixed boundary condition

This is the simplest boundary condition to consider, as the S_q symmetry of the bulk is broken completely at the boundary where there is only one

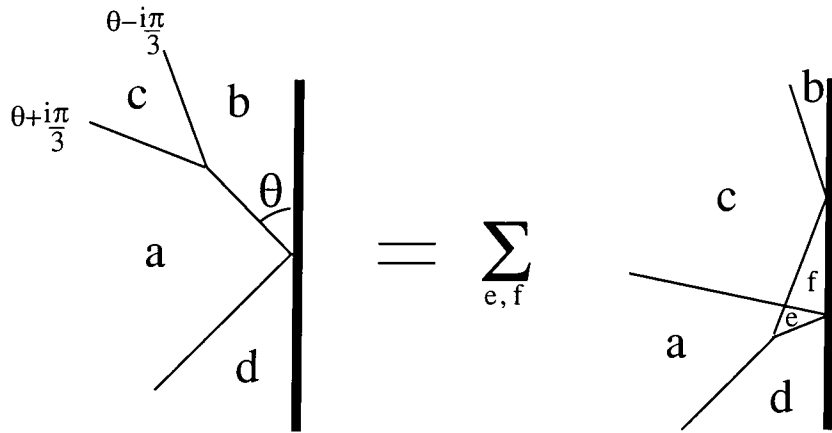


Figure 5.15: Kink boundary bootstrap condition

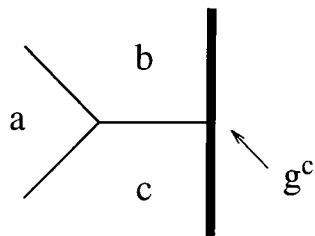


Figure 5.16: Boundary coupling of bulk bound state at $\theta = \frac{i\pi}{6}$

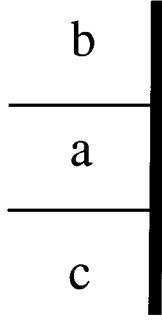


Figure 5.17: Boundary coupling of bulk bound state at $\theta = \frac{i\pi}{2}$

allowed spin value and thus only one boundary scattering amplitude

$$R_{ba}^a(\theta) = R_f(\theta).$$

The boundary Yang-Baxter equation is automatically satisfied, so we must look to unitarity, cross-unitarity and the boundary bootstrap conditions in order to determine the structure of $R_f(\theta)$. These take the respective forms

$$1 = R_f(\theta)R_f(-\theta) \quad (5.10)$$

$$K_f(\theta) = [(q-2)\mathcal{S}_2(2\theta) + \mathcal{S}_3(2\theta)]K_f(-\theta) \quad (5.11)$$

$$R_f(\theta) = [\mathcal{S}_1(2\theta) + (q-3)\mathcal{S}_0(2\theta)]R_f(\theta - \frac{i\pi}{3})R_f(\theta + \frac{i\pi}{3}) \quad (5.12)$$

where the cross amplitude is defined by

$$K_f(\theta) = R_f(\frac{i\pi}{2} - \theta).$$

There is no reason to expect $R_f(\theta)$ to possess any poles in the physical strip $0 \leq \theta \leq \frac{i\pi}{2}$, so for the sake of simplicity none will be assumed. Looking at conditions (5.11)–(5.12) we see that $R_f(\theta)$ may be factorized as

$$R_f(\theta) = F_0(\theta)F_1\left(\frac{\lambda\theta}{i\pi}\right).$$

Equation (5.12) then forces $F_0(\theta)$ to satisfy

$$F_0(\theta) = -\tan\left(\frac{\pi}{4} + \frac{i\theta}{2}\right) \cot\left(\frac{\pi}{12} + \frac{i\theta}{2}\right) \cot\left(\frac{5\pi}{12} + \frac{i\theta}{2}\right) F_0\left(\theta - \frac{i\pi}{3}\right) F_0\left(\theta + \frac{i\pi}{3}\right).$$

This has the solution

$$F_0(\theta) = -\tan\left(\frac{\pi}{4} + \frac{i\theta}{2}\right).$$

The factor of $F_1(X)$ must solve

$$F_1(X) = \Pi(\lambda - 2X) \frac{\sin[2\pi(\lambda - X)]}{\sin[2\pi(\frac{\lambda}{3} - X)]} F_1(\lambda - X)$$

and

$$F_1(X)F_1(-X) = 1.$$

The minimal solution to these conditions is given by

$$F_1(X) = \prod_{k=1}^{\infty} \frac{\Sigma_k(X)}{\Sigma_k(-X)}$$

where

$$\Sigma_k(X) = \frac{\Gamma[(4k-1)\lambda+2X]\Gamma[(4k-3)\lambda+2X+1]\Gamma[(4k-\frac{8}{3})\lambda+2X]\Gamma[(4k-\frac{5}{3})\lambda-2X]}{\Gamma[4k\lambda+2X]\Gamma[(4k-4)\lambda+2X+1]\Gamma[(4k-\frac{7}{3})\lambda+2X+1]\Gamma[(4k-\frac{4}{3})\lambda-2X+1]}.$$

For integer values of q , the boundary amplitude takes on more simple forms. For $\lambda = \frac{3}{4}$ ($q = 2$) Chim shows that

$$R_f(\theta) = i \tanh\left(\frac{i\pi}{4} - \frac{\theta}{2}\right),$$

in agreement with [39], and for $\lambda = 1$ ($q = 3$) it becomes

$$R_f(\theta) = -\frac{\sin\left(\frac{\pi}{3} + \frac{i\theta}{2}\right)}{\sin\left(\frac{\pi}{3} - \frac{i\theta}{2}\right)}.$$

5.4.2 Free boundary condition

When we allow boundary spins to freely take any of the q values, the S_q symmetry remains unbroken. The only independent amplitudes are therefore $R_1(\theta)$ and $R_2(\theta)$ result as shown in figures 5.18 and 5.19 respectively. The boundary Yang-Baxter equations are no longer trivial, and provide the three conditions shown in figures 5.20–5.22:

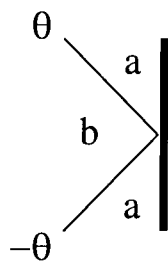


Figure 5.18: $R_{ba}^a(\theta) = R_1(\theta)$

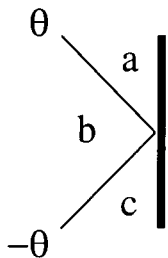


Figure 5.19: $R_{ba}^c(\theta) = R_2(\theta)$

1.

$$R_1 S_3 R_2 S_1 + R_2 S_1 R_1 S_1 + (q - 3) R_2 S_1 R_2 S_1 + (q - 3) R_1 S_2 R_2 S_0 \\ + (q - 3) R_2 S_0 R_1 S_0 + (q - 3)(q - 4) R_2 S_0 R_2 S_0$$

$$\begin{aligned}
&= (q-2)R_2S_2R_1S_2 + (q-3)R_1S_0R_2S_2 + (q-3)^2R_2S_0R_2S_2 + R_1S_1R_2S_3 \\
&\quad + R_2S_3R_1S_3 + (q-3)R_2S_1R_2S_3;
\end{aligned}$$

2.

$$\begin{aligned}
&R_1S_1R_2S_2 + (q-3)R_2S_1R_2S_2 + R_2S_2R_1S_3 + (q-3)R_2S_0R_2S_3 \\
&+ (q-3)R_2S_2R_1S_2 + R_2S_3R_1S_2 + (q-3)R_1S_0R_2S_2 + (q-3)(q-4)R_2S_0R_2S_2 \\
&= R_1S_2R_2S_1 + (q-3)R_1S_2R_2S_0 + (q-3)R_2S_0R_2S_1 + (q-3)^2R_2S_0R_2S_0;
\end{aligned}$$

3.

$$\begin{aligned}
&R_1S_3R_2S_0 + R_1S_2R_2S_1 + (q-4)R_1S_2R_2S_0 + R_2S_1R_1S_0 + R_2S_0R_1S_1 \\
&+ (q-4)R_2S_0R_1S_0 + (q-3)R_2S_1R_2S_0 + (q-4)R_2S_0R_2S_1 + (q-4)^2R_2S_0R_2S_0 \\
&= R_1S_1R_2S_2 + R_1S_0R_2S_3 + (q-4)R_1S_0R_2S_2 + R_2S_3R_1S_2 + R_2S_2R_1S_3 \\
&\quad + (q-3)R_2S_2R_1S_2 + (q-3)R_2S_1R_2S_2 + (q-4)R_2S_0R_2S_3 \\
&\quad + [(q-3) + (q-4)^2]R_2S_0R_2S_2;
\end{aligned}$$

where each term has the form

$$R_iS_jR_kS_l = R_i(\theta_1)S_j(\theta_1 + \theta_2)R_k(\theta_2)S_l(\theta_2 - \theta_1).$$

Making use of the fact that both $R_1(\theta)$ and $R_2(\theta)$ have a simple pole at $\theta = \frac{i\pi}{2}$ with the same residue, we may solve these three equations for $R_1(\theta)/R_1(\theta)$ by taking the limit $\theta_2 \rightarrow \frac{i\pi}{2}$. This ratio may then be disentangled, noting that

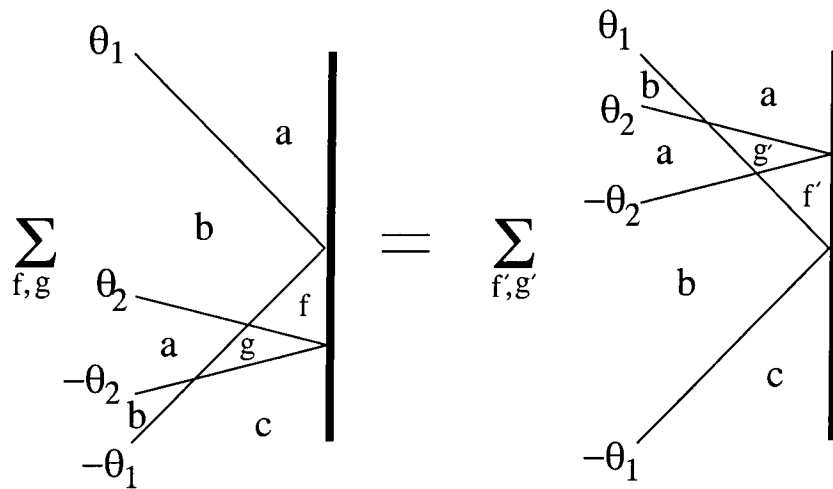


Figure 5.20: Free boundary condition: Yang-Baxter equation 1.

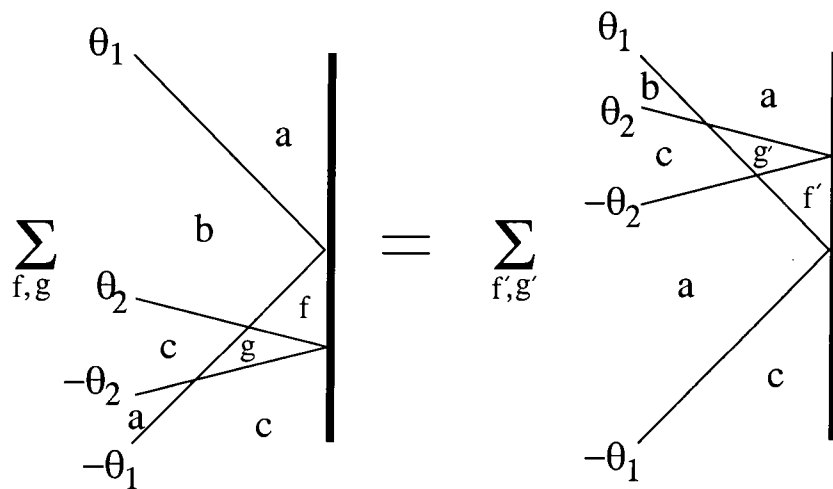


Figure 5.21: Free boundary condition: Yang-Baxter equation 2.

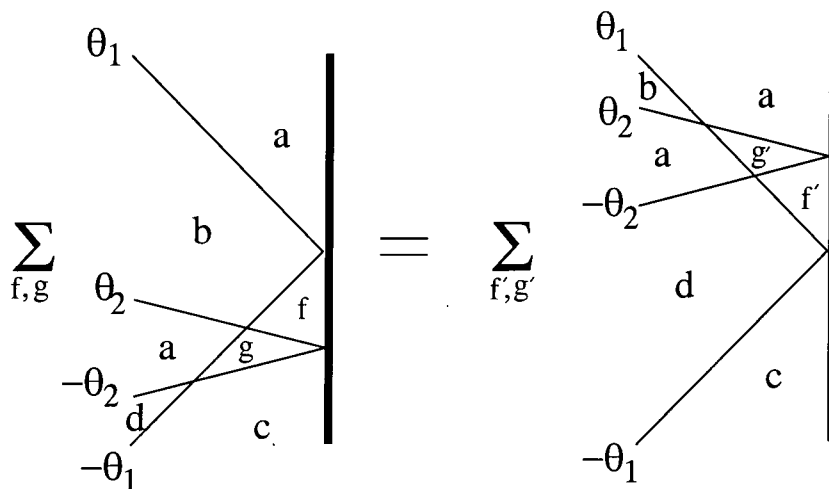


Figure 5.22: Free boundary condition: Yang-Baxter equation 3.

on physical grounds $R_2(\theta)$ should have a simple pole at $\theta = \frac{i\pi}{6}$ while $R_1(\theta)$ should not, and that no further poles are expected in the physical strip. This leads to the solution

$$R_1(\theta) = (q-3) \frac{\sinh[\lambda(\frac{i\pi}{3} + 2\theta)]}{\sinh[\lambda(i\pi - 2\theta)]} P\left(\frac{\lambda\theta}{i\pi}\right) \quad (5.13)$$

$$R_2(\theta) = \frac{\sin(\frac{2\pi\lambda}{3}) \sinh(2\lambda\theta)}{\sin(\frac{\pi\lambda}{3}) \sinh[\lambda(i\pi - 2\theta)]} \frac{\sinh[\lambda(\frac{i\pi}{3} + 2\theta)]}{\sinh[\lambda(\frac{i\pi}{3} - 2\theta)]} P\left(\frac{\lambda\theta}{i\pi}\right) \quad (5.14)$$

The factor $P(\frac{\lambda\theta}{i\pi})$ is constrained by unitarity and crossing unitarity through the respective equations

$$P(\theta)P(-\theta) = 1$$

and

$$P\left(\frac{i\pi}{2} - \frac{\theta}{2}\right) = -\Pi\left(\frac{\lambda\theta}{i\pi}\right) \frac{\sinh[\lambda(i\pi + \theta)] \sinh[\lambda(\frac{4\pi i}{3} + \theta)]}{\sinh[\lambda(\frac{i\pi}{3} - \theta)] \sinh[\lambda(\frac{4\pi i}{3} - \theta)]} P\left(\frac{i\pi}{2} + \frac{\theta}{2}\right).$$

t :	$\frac{1}{2\lambda} - \frac{1}{6}$	$\frac{1}{\lambda} - \frac{1}{6}$	$\frac{3}{2\lambda} - \frac{1}{6}$	$\frac{1}{2\lambda}$	$\frac{1}{\lambda}$
-----	------------------------------------	-----------------------------------	------------------------------------	----------------------	---------------------

Table 5.1: Pole structure of $P(\frac{\lambda\theta}{i\pi})$

These have the minimal solution

$$P(X) = \prod_{k=1}^{\infty} \frac{\Omega_k(X)}{\Omega_k(-X)}, \quad (5.15)$$

where

$$\Omega_k(X) = \frac{\Gamma[(4k-1)\lambda+2X]\Gamma[(4k-3)\lambda+2X+1]\Gamma[(4k+\frac{1}{3})\lambda-2X]\Gamma[(4k-\frac{13}{3})\lambda-2X+1]}{\Gamma[4k\lambda+2X]\Gamma[(4k-4)\lambda+2X+1]\Gamma[(4k-\frac{8}{3})\lambda-2X]\Gamma[(4k-\frac{4}{3})\lambda-2X+1]}. \quad (5.16)$$

The pole structure of these amplitudes is rather more complicated than that of the fixed boundary condition. In [2] Chim only identifies the poles located at $\frac{i\pi}{6}$ and $\frac{i\pi}{2}$, but here I shall attempt to explain all the additional poles which appear for $\frac{3}{2} < \lambda < 3$.

Looking first at the normalization factor $P(\frac{\lambda\theta}{i\pi})$, we find the array of poles as reproduced in table (5.1). In addition to this, both $R_1(\theta)$ and $R_2(\theta)$ possess a factor

$$\frac{\sinh[\lambda(\frac{i\pi}{3} + 2\theta)]}{\sinh[\lambda(i\pi - 2\theta)]}$$

which has poles at $t = \frac{1}{2} - \frac{n}{2\lambda}$, and zeroes at $t = \frac{n}{2\lambda} - \frac{1}{6}$ where $n = 0, 1, \dots$. Finally, $R_2(\theta)$ has poles at $t = \frac{1}{6} + \frac{n}{2\lambda}$ and zeroes at $t = \frac{n}{2\lambda}$. These combine to produce the overall pole structures shown in tables (5.2) and (5.3).

Several of these poles can readily be identified as corresponding to the boundary scattering of bulk bound states by comparison with the bulk S-

Pole: $t =$	$\frac{1}{2}$	$\frac{1}{2\lambda}$	$\frac{1}{2} - \frac{1}{2\lambda}$	$\frac{1}{\lambda}$	$\frac{1}{2} - \frac{1}{\lambda}$
Bound state:	$\forall \lambda$	$\lambda > 1$		$\lambda > 2$	
Particle:	2-particle bound state	B_1		B_2	

Table 5.2: Pole structure of $R_1(\theta)$, free boundary conditions

Pole: $t =$	$\frac{1}{6}$	$\frac{1}{2}$	$\frac{1}{2} - \frac{1}{2\lambda}$	$\frac{1}{6} + \frac{1}{2\lambda}$	$\frac{1}{2} - \frac{1}{\lambda}$
Bound state:	$\forall \lambda$		$\lambda > 1$	$\lambda > \frac{3}{2}$	$\lambda > 2$
Particle:	K_1	2-particle bound state		K_2	

Table 5.3: Pole structure of $R_2(\theta)$, free boundary conditions

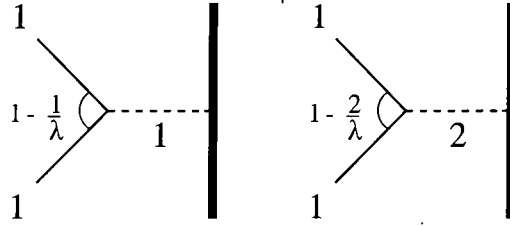


Figure 5.23: Boundary scattering of breather bound states in $R_1(\theta)$

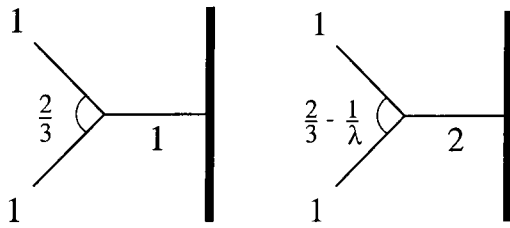


Figure 5.24: Boundary scattering of kink bound states in $R_2(\theta)$

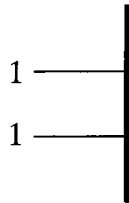


Figure 5.25: Coupling of two kinks to boundary

matrix described in the previous chapter (see table (4.4) and figure 4.1). These match precisely with breathers appearing in $R_1(\theta)$ and single kink bound states in $R_2(\theta)$ as shown in figures 5.23 and 5.24. The $\frac{1}{2}$ may be interpreted as two kinks coupling to the boundary, as shown figure 5.25. compatible with R_1 or R_2 . This leaves the poles at $t = \frac{1}{2} - \frac{1}{2\lambda}$ and $t = \frac{1}{2} - \frac{1}{\lambda}$ to be accounted for. These appear at $\lambda = 1$ and $\lambda = 2$ respectively, where the breathers B_1 and B_2 enter the particle spectrum, and are present in both R_1 and R_2 . It is suggested that they correspond to excited boundary states. If such states exist for this model, it is to be expected that they will be related to excitations over a single vacuum. The energy e_α of an excited boundary state $|\alpha\rangle$ is given by

$$e_\alpha = e_0 + m_\alpha \cos(\pi v_\alpha)$$

where $R_a^b(\theta)$ has a pole at $t = v_\alpha$, e_0 is the ground state energy, and m_α is the mass of the incoming particle (see figure 5.26). For the poles under consideration, the respective energies are such that

$$e_1 - e_0 = m \cos\left(\frac{\pi}{2} - \frac{\pi}{2\lambda}\right) = \frac{1}{2}m_{B_1} \quad ; \quad e_2 - e_0 = m \cos\left(\frac{\pi}{2} - \frac{\pi}{\lambda}\right) = \frac{1}{2}m_{B_2}.$$

In [2], Chim gives the form of the boundary S-matrix at the points $\lambda = \frac{3}{4}$ and $\lambda = 1$, which correspond to the Ising, and the 3-state Potts model respectively. For $\lambda = \frac{3}{4}$, R_1 is given by

$$R_1(\theta) = -\cot\left(\frac{\pi}{4} + \frac{i\theta}{2}\right).$$

R_2 is not considered as there are not enough vacua present, even though it is non-zero at this point. For $\lambda = 1$, both types of scattering are potentially present, and the boundary S-matrix takes the form

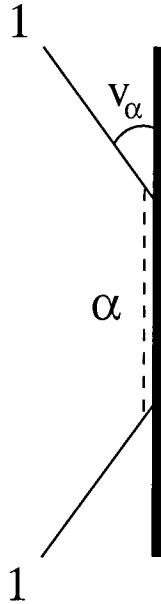


Figure 5.26: Excited boundary state

$$\begin{aligned}
 R_1(\theta) &= 0 \\
 R_2(\theta) &= \frac{\sin(\frac{\pi}{12} - \frac{i\theta}{2}) \sin(\frac{\pi}{4} - \frac{i\theta}{2})}{\sin(\frac{\pi}{12} + \frac{i\theta}{2}) \sin(\frac{\pi}{4} + \frac{i\theta}{2})}.
 \end{aligned}$$

These agree with scattering amplitudes given in [39].

5.4.3 ‘Excluded’ boundary condition

One possibility not considered in [2] is where the boundary is allowed to take all but one of the q possible values. This amounts to a partial breaking of the S_q symmetry down to an S_{q-1} symmetry at the boundary. For $q = 2$ this is the same as imposing fixed boundary conditions, and for $q = 3$ equates with the mixed boundary conditions of [36], [37]. Denoting the excluded vacuum

state by A , the resulting four boundary reflection amplitudes R_1 , R_1^A , R_2 and R_2^A are shown in figures 5.27 and 5.28.

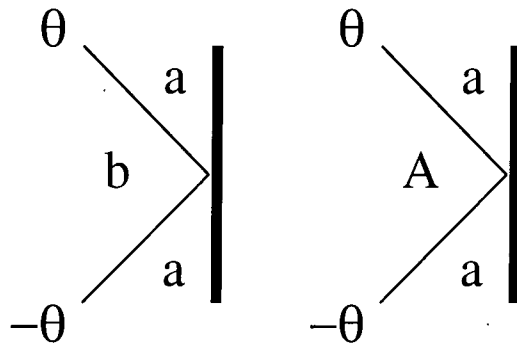


Figure 5.27: Boundary scattering amplitudes $R_1(\theta)$ and $R_1^A(\theta)$

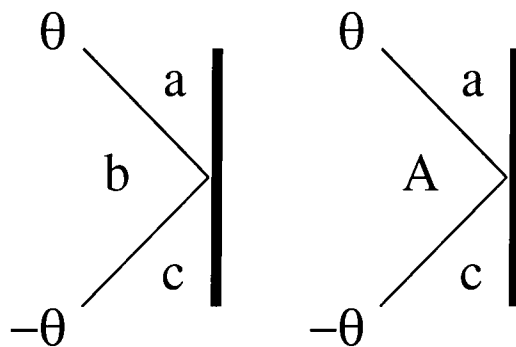


Figure 5.28: Boundary scattering amplitudes $R_2(\theta)$ and $R_2^A(\theta)$

There are now 13 distinct permutations of vacua for which boundary Yang-Baxter equations must be solved. These equations are given in appendix (C). It is to be expected that R_1 and R_2 will both possess simple poles at $\theta = \frac{i\pi}{2}$ with the same residue, just like their free boundary condition

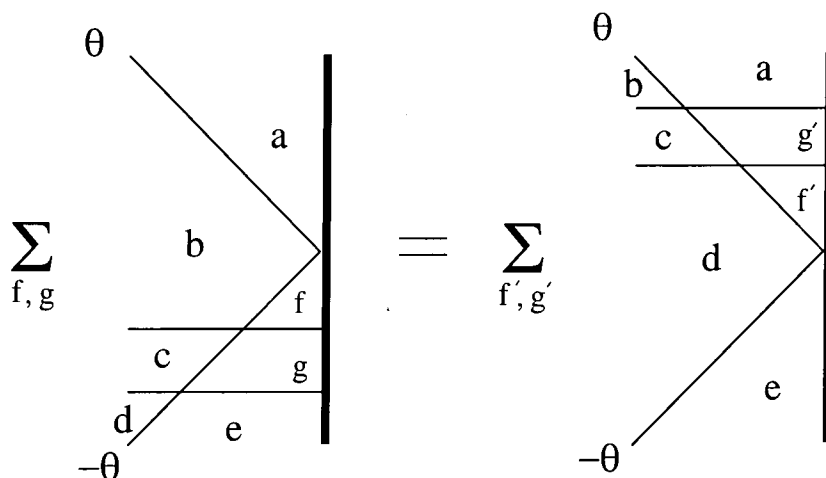


Figure 5.29: Boundary Yang-Baxter conditions arising from $\frac{\pi}{2}$ pole in $R(\theta)$

counterparts. Making use of this the following set of equations can be obtained, corresponding to scattering processes of the type shown in figure 5.29.

1.

$$R_1[S_3S_2 - S_1S_3 + (q-4)(S_2S_0 - S_0S_1)] =$$

$$R_2[S_3S_3 + (q-4)S_1S_3 + (q-4)^2(S_0S_1 - S_0S_0)]$$

2.

$$R_1[S_2S_2 - S_1S_1 + (q-4)(S_2S_0 - S_0S_1)] = R_2[S_2S_3 + S_3S_1]$$

$$+(q-4)R_2[(S_2S_1 + S_1S_1 + S_0S_3 - S_2S_0 - S_1S_0) + (q-4)(S_0S_1 - S_0S_0)]$$

3.

$$R_1[S_2S_2 - S_1S_1 + (q-5)(S_2S_0 - S_0S_1)] = R_2[S_2S_3 + S_3S_1 - S_1S_0]$$

$$+R_2[(q-4)(S_2S_1 + S_1S_1 - S_0S_2) + (q-5)(S_0S_3 - S_0S_0) + (q-5)^2(S_0S_1 - S_0S_0)]$$

4.

$$R_1[S_1S_0 - S_0S_2] = R_2[(q-4)(S_0S_0 - S_1S_0) - S_3S_0]$$

5.

$$\begin{aligned} R_1^A[S_2S_3 + (q-3)S_2S_1] + (q-3)R_2^A[S_0S_3 + (q-3)S_0S_1] = \\ R_1[S_3S_1 + (q-3)S_2S_1] + (q-3)R_2[S_1S_1 + (q-4)S_0S_1] \end{aligned}$$

6.

$$\begin{aligned} R_1^A[S_2S_2 + (q-4)S_2S_0] + (q-3)R_2^A[S_0S_2 + (q-4)S_0S_0] = \\ R_1[S_1S_1 + (q-4)S_0S_1] + R_2[S_3S_1 + (q-3)S_2S_1 + (q-4)S_1S_1 + (q-4)^2S_0S_1] \end{aligned}$$

7.

$$\begin{aligned} R_1^A(q-3)S_0S_1 + R_2^A[S_2S_3 + (q-3)(S_2S_1 + S_0S_3 - S_0S_1) + (q-3)^2S_0S_1] \\ = (q-3)[R_1S_2S_0 + R_2(q-4)S_0S_0] \end{aligned}$$

8.

$$\begin{aligned} R_1^A(q-4)S_0S_0 + R_2^A[S_2S_2 + (2q-7)S_2S_0 + (q-4)^2S_0S_0] \\ = R_1(q-4)S_0S_0 + R_2[(q-3)S_2S_0 + (q-4)^2S_0S_0] \end{aligned}$$

9.

$$\begin{aligned} R_1^A[S_0S_2 + (q-4)S_0S_0] + R_2^A[S_2S_2 + (2q-8)S_2S_0 + (q-4)^2S_0S_0] \\ = R_1[S_1S_0 + (q-4)S_0S_0] + R_2[(q-3)S_3S_0 + (q-4)^2S_0S_0] \end{aligned}$$

10.

$$\begin{aligned} R_1^A[S_0S_3 + (q-4)S_0S_1] + R_2^A[S_2S_3 + (q-3)(S_2S_1 + S_0S_1) + (q-4)(S_0S_3 + (q-4)S_0S_1)] \\ = R_1[S_3S_0 + (q-4)S_2S_0] + R_2[(q-3)S_1S_0 + (q-4)^2S_0S_0] \end{aligned}$$

11.

$$R_1^A[S_0S_2+(q-5)S_0S_0]+R_2^A[(2q-8)(S_2S_0+S_0S_0)+S_2S_2+(q-5)^2S_0S_0] =$$

$$R_1[S_1S_0+(q-5)S_0S_0]+R_2[(S_3S_0+(q-4)(S_1S_0+S_2S_0+S_0S_0)+(q-5)^2S_0S_0]$$

12.

$$R_1[S_0S_2 - S_1S_0] = R_2[(q-3)(S_1S_0 - S_0S_0) + S_2S_0]$$

13.

$$R_1^A(q-3)[S_0S_1 - S_2S_0] = R_2^A[(q-3)^2(S_0S_0 - S_0S_1) - (q-2)S_2S_1]$$

where $R = R(\theta)$ and $S = S(\theta + \frac{i\pi}{2})/\Pi(X + \frac{\lambda}{2})$. These may be reduced to the conditions

$$R_1(\theta) = \frac{S_3 + (q-4)(S_1 - S_0)}{S_2 - S_1} R_2(\theta)$$

$$R_2^A(\theta) = \frac{(q-3)S_0}{S_2 + (q-3)S_0} R_2(\theta)$$

$$R_1^A(\theta) - R_2^A(\theta) = R_1(\theta) - R_2(\theta)$$

Using these to express all scattering amplitudes in terms of R_2 we find that

$$\frac{R_1(\theta)}{R_2(\theta)} = \frac{\sinh[\lambda(\theta - \frac{i\pi}{6})] \left(\sinh[\lambda(\theta + \frac{i5\pi}{6})] - 2 \sinh[\lambda(\theta - \frac{i5\pi}{6})] \cos(\frac{\lambda\pi}{3}) \right)}{i \sin(\frac{\lambda 2\pi}{3}) \sinh(2\lambda\theta)} \quad (5.17)$$

$$\frac{R_1^A(\theta)}{R_2(\theta)} = \frac{\sin(\lambda\pi) \sinh[\lambda(\theta - \frac{i\pi}{2})]}{\sin(\frac{\lambda\pi}{3}) \sinh[\lambda(\theta - \frac{i\pi}{6})]} - \frac{\sinh[\lambda(\theta - \frac{i5\pi}{6})] \sinh[\lambda(\theta - \frac{i\pi}{2})]}{i \sin(\frac{\lambda 2\pi}{3}) \sinh(2\lambda\theta)} \quad (5.18)$$

$$\frac{R_2^A(\theta)}{R_2(\theta)} = -(q-3) \frac{\sinh[\lambda(\frac{i\pi}{2} - \theta)]}{\sinh[\lambda(\frac{i\pi}{6} - \theta)]} \quad (5.19)$$

It is very non-trivial to show that these ratios satisfy the full Yang-Baxter relations, but extensive checks (many performed numerically, using Maple) confirmed that this was so.

In order to determine $R_2(\theta)$, we must make use of the unitarity and cross-unitarity conditions. These take the form of equations

$$R_1(\theta)R_1(-\theta) + (q - 3)R_2(\theta)R_2(-\theta) = 1 \quad (5.20)$$

$$R_1^A(\theta)R_1^A(-\theta) + (q - 2)R_2^A(\theta)R_2^A(-\theta) = 1 \quad (5.21)$$

$$R_1(\theta)R_2(-\theta) + R_2(\theta)R_1(-\theta) + (q - 4)R_2(\theta)R_2(-\theta) = 0 \quad (5.22)$$

$$R_1^A(\theta)R_2^A(-\theta) + R_2^A(\theta)R_1^A(-\theta) + (q - 3)R_2^A(\theta)R_2^A(-\theta) = 0 \quad (5.23)$$

and

$$R_1\left(\frac{i\pi}{2} - \frac{\theta}{2}\right) = [\mathcal{S}_3(\theta) + (q - 3)\mathcal{S}_2(\theta)] R_1\left(\frac{i\pi}{2} + \frac{\theta}{2}\right) + \mathcal{S}_2(\theta)R_1^A\left(\frac{i\pi}{2} + \frac{\theta}{2}\right) \quad (5.24)$$

$$R_1^A\left(\frac{i\pi}{2} - \frac{\theta}{2}\right) = (q - 2)\mathcal{S}_2(\theta)R_1\left(\frac{i\pi}{2} + \frac{\theta}{2}\right) + \mathcal{S}_3(\theta)R_1^A\left(\frac{i\pi}{2} + \frac{\theta}{2}\right) \quad (5.25)$$

$$R_2\left(\frac{i\pi}{2} - \frac{\theta}{2}\right) = [\mathcal{S}_1(\theta) + (q - 4)\mathcal{S}_0(\theta)] R_2\left(\frac{i\pi}{2} + \frac{\theta}{2}\right) + \mathcal{S}_0(\theta)R_2^A\left(\frac{i\pi}{2} + \frac{\theta}{2}\right) \quad (5.26)$$

$$R_2^A\left(\frac{i\pi}{2} - \frac{\theta}{2}\right) = (q - 3)\mathcal{S}_0(\theta)R_2\left(\frac{i\pi}{2} + \frac{\theta}{2}\right) + \mathcal{S}_1(\theta)R_2^A\left(\frac{i\pi}{2} + \frac{\theta}{2}\right) \quad (5.27)$$

respectively. From equation (5.20) we obtain the expression

$$R_2(\theta)R_2(-\theta) = \frac{\sin(\frac{\lambda 2\pi}{3})^2 \sinh(2\lambda\theta)^2}{\sinh[\lambda(\frac{i5\pi}{6} + \theta)] \sinh[\lambda(\frac{i5\pi}{6} - \theta)] \sinh[\lambda(\frac{i\pi}{2} + \theta)] \sinh[\lambda(\frac{i\pi}{2} - \theta)]}$$

from which we may identify the form of R_2 as

$$R_2(\theta) = \frac{i \sin(\frac{\lambda 2\pi}{3}) \sinh(2\lambda\theta)}{\sinh[\lambda(\frac{i\pi}{2} - \theta)] \sinh[\lambda(\frac{i5\pi}{6} - \theta)]} P(\theta) \quad ; \quad P(\theta)P(-\theta) = 1$$

The factor $P(\theta)$ is also constrained by cross-unitarity, giving rise to the equation

$$P(\frac{i\pi}{2} - \frac{\theta}{2}) = \frac{\sinh[\lambda(i\pi + \theta)] \sinh[\lambda(\frac{i\pi}{3} + \frac{\theta}{2})]^2 \sinh[\lambda(\frac{2\pi i}{3} + \frac{\theta}{2})]}{\sinh[\lambda(\frac{i\pi}{3} - \theta)] \sinh[\lambda(\frac{i\pi}{3} - \frac{\theta}{2})]^2 \sinh[\lambda(\frac{2\pi i}{3} - \frac{\theta}{2})]} \Pi(\frac{\lambda\theta}{i\pi}) P(\frac{i\pi}{2} + \frac{\theta}{2}) \quad (5.28)$$

We are free to multiply R_2 by any factor $f(\theta)$ satisfying $f(\theta)f(-\theta) = 1$ as long as equation (5.28) is altered accordingly. Choosing

$$f(\theta) = \frac{\sinh[\lambda(\frac{i\pi}{3} + 2\theta)]}{\sinh[\lambda(\frac{i\pi}{3} - 2\theta)]},$$

the cross-unitarity condition becomes

$$P(\frac{i\pi}{2} - \frac{\theta}{2}) = \frac{\sinh[\lambda(i\pi + \theta)] \sinh[\lambda(\frac{4\pi i}{3} + \theta)] \cosh[\lambda(\frac{i\pi}{3} - \frac{\theta}{2})] \sinh[\lambda(\frac{i\pi}{3} + \frac{\theta}{2})] \sinh[\lambda(\frac{2\pi i}{3} + \frac{\theta}{2})]}{\sinh[\lambda(\frac{i\pi}{3} - \theta)] \sinh[\lambda(\frac{4\pi i}{3} - \theta)] \cosh[\lambda(\frac{i\pi}{3} + \frac{\theta}{2})] \sinh[\lambda(\frac{i\pi}{3} - \frac{\theta}{2})] \sinh[\lambda(\frac{2\pi i}{3} - \frac{\theta}{2})]} \Pi(\frac{\lambda\theta}{i\pi}) P(\frac{i\pi}{2} + \frac{\theta}{2}).$$

It is possible to factorise $P(\theta)$ into two parts:

$$P(\theta) = P_1(\theta)P_2(\theta),$$

satisfying

$$P_1(\frac{i\pi}{2} - \frac{\theta}{2}) = \frac{\sinh[\lambda(i\pi + \theta)] \sinh[\lambda(\frac{4\pi i}{3} + \theta)]}{\sinh[\lambda(\frac{i\pi}{3} - \theta)] \sinh[\lambda(\frac{4\pi i}{3} - \theta)]} \Pi(\frac{\lambda\theta}{i\pi}) P_1(\frac{i\pi}{2} + \frac{\theta}{2})$$

$$P_2(\frac{i\pi}{2} - \frac{\theta}{2}) = \frac{\cosh[\lambda(\frac{i\pi}{3} - \frac{\theta}{2})] \sinh[\lambda(\frac{i\pi}{3} + \frac{\theta}{2})] \sinh[\lambda(\frac{2\pi i}{3} + \frac{\theta}{2})]}{\cosh[\lambda(\frac{i\pi}{3} + \frac{\theta}{2})] \sinh[\lambda(\frac{i\pi}{3} - \frac{\theta}{2})] \sinh[\lambda(\frac{2\pi i}{3} - \frac{\theta}{2})]} P_2(\frac{i\pi}{2} + \frac{\theta}{2}).$$

P_1 is thus identical with the normalization factor for free boundary conditions, given in equations (5.15) and (5.16), and P_2 takes the form (see appendix (D))

$$P_2(\theta) = \prod_{k=1}^{\infty} \frac{\Phi_k(X)}{\Phi_k(-X)}$$

where

$$\begin{aligned} \Phi_k(X) &= \frac{\Gamma[(4k-1)\frac{\lambda}{2} + \frac{1}{2} - \frac{\lambda}{3} - X] \Gamma[(4k-1)\frac{\lambda}{2} + \frac{\lambda}{3} - X] \Gamma[(4k-1)\frac{\lambda}{2} + \frac{2\lambda}{3} - X]}{\Gamma[(4k-3)\frac{\lambda}{2} + \frac{1}{2} - \frac{\lambda}{3} - X] \Gamma[(4k-3)\frac{\lambda}{2} + \frac{\lambda}{3} - X] \Gamma[(4k-3)\frac{\lambda}{2} + \frac{2\lambda}{3} - X]} \\ &\times \frac{\Gamma[(4k-3)\frac{\lambda}{2} + 1 - \frac{\lambda}{3} - X] \Gamma[(4k-3)\frac{\lambda}{2} + \frac{1}{2} + \frac{\lambda}{3} - X] \Gamma[(4k-3)\frac{\lambda}{2} - \frac{2\lambda}{3} + 1 - X]}{\Gamma[(4k-1)\frac{\lambda}{2} + 1 - \frac{\lambda}{3} - X] \Gamma[(4k-1)\frac{\lambda}{2} + \frac{1}{2} + \frac{\lambda}{3} - X] \Gamma[(4k-1)\frac{\lambda}{2} - \frac{2\lambda}{3} + 1 - X]} \end{aligned}$$

with $t = \frac{\theta}{i\pi}$, and $X = \frac{\lambda\theta}{i\pi}$ as before. P_2 has a physical strip poles located at $t = \frac{1}{\lambda} - \frac{1}{6}$, and a zero at $\frac{1}{6} + \frac{1}{2\lambda}$.

It remains to fix the sign of $P(\theta)$, and this can be done by looking at the special point $q = 3$, $\lambda = 1$. At this point R_2^A disappears, and there are not enough vacua for R_2 type boundary scattering to take place. This just leaves R_1 and R_1^A which take the simplified forms

$$\begin{aligned} R_1(\theta) &= \frac{\sin(\frac{\pi}{4} - \frac{i\theta}{2}) \sin(\frac{\pi}{3} + \frac{i\theta}{2}) \sin(\frac{5\pi}{12} - \frac{i\theta}{2})}{\sin(\frac{\pi}{4} + \frac{i\theta}{2}) \sin(\frac{\pi}{3} - \frac{i\theta}{2}) \sin(\frac{5\pi}{12} + \frac{i\theta}{2})} \\ R_1^A(\theta) &= \frac{\sin(\frac{\pi}{4} - \frac{i\theta}{2}) \sin(\frac{\pi}{3} + \frac{i\theta}{2}) \sin(\frac{\pi}{12} - \frac{i\theta}{2})}{\sin(\frac{\pi}{4} + \frac{i\theta}{2}) \sin(\frac{\pi}{3} - \frac{i\theta}{2}) \sin(\frac{\pi}{12} + \frac{i\theta}{2})}. \end{aligned}$$

These may be shown to satisfy the boundary bootstrap equations (5.9), fixing the sign of $P(\theta)$. As an additional consistency check, it can also be seen that they satisfy the cross-unitarity equations (5.24) and (5.25) (previously only (5.26) and (5.27) had been used in the derivation of the reflection factors).

However, examination of these amplitudes also reveals a feature which has so far resisted explanation: at $q = 3$, R_1^A has poles at $\theta = \frac{i\pi}{6}$ and $\frac{i\pi}{2}$. As we saw in the treatment of Chim's work, these are usually associated with the coupling of bulk bound states to the boundary (see figures 5.16 and 5.17). Neither of these processes may occur in R_1^A , due to its vacuum structure and the particular boundary condition under consideration. As with the bulk model described in the last chapter, we seem to have encountered some poles for which the usual explanations break down. Until this has been resolved, the physical interpretation of this new solution to the boundary Yang-Baxter equations must remain unclear.

Conclusions

A general theme of this thesis has been the interpretation of poles in $1 + 1$ dimensional field theories both with and without boundaries.

In chapter 4 it has been shown that the particle spectrum of the q -state Potts model as described in [1] must be revised due to the previously unsuspected operation of the generalized bootstrap principle. This has already been of use in the calculation of universal amplitude ratios by Cardy and Delfino [3]. As mentioned before, it does seem that genuinely new and unexpected behaviour has been brought to light in the efforts to close the bootstrap for the Potts model. It remains to be seen how widespread such problems are. In recent work [42] on the minimal model $M(3, 5)$ perturbed by $\phi_{(1,2)}$, Acerbi, Mussardo and Takacs were also unable to close the bootstrap. Their work was based on an alternative approach to $\phi_{(1,2)}$ perturbations of minimal models proposed by Smirnov [43]. One avenue for future research will be to see how the alternative approaches of Smirnov and of Chim and Zamolodchikov compare, and whether they both break down in the same situations.

In chapter 5, attention turned to boundary scattering amplitudes. The pole structure of the ‘free’ boundary scattering amplitudes was found to be consistent with physical expectations, but that for the ‘excluded’ boundary condition, at the point $q = 3$, still remains to be interpreted satisfactorily. The fact that such a solution to the boundary Yang-Baxter and other consistency conditions should exist is nevertheless highly non-trivial, although more work will be needed before the implications of its existence can be clarified.

Appendix A

Calculation of $\mathcal{A}_{K_2 K_2}^0$ for $t = \frac{1}{\lambda}$ pole

The scattering process under consideration is reproduced in figure A.1, and figure A.2 shows the factorization in terms of two-particle scattering processes. The internal vacua e, f, g, h and i are constrained as follows:

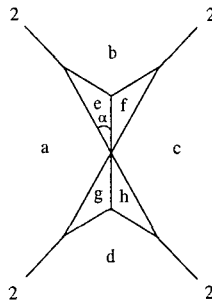


Figure A.1: $\mathcal{S}_{K_2 K_2}^0: t = (\frac{1}{\lambda})$

- $e \neq a, b$

$$\sum_{e,f,g,h} \begin{array}{c} 1 \quad 1 \quad 1 \\ \diagdown \quad | \quad / \\ e \quad f \\ a \quad c \\ / \quad | \quad \diagdown \\ g \quad h \end{array} = \sum_{e,f,g,h,i} \begin{array}{c} 1 \quad 1 \quad 1 \\ \diagdown \quad | \quad / \\ e \quad f \\ a \quad i \quad c \\ / \quad | \quad \diagdown \\ g \quad h \end{array}$$

Figure A.2: Factorised scattering in Figure (A.1)

- $f \neq b, c, e$
- $h \neq c, d$
- $i \neq a, f, h$
- $g \neq a, d, h.$

The sum over internal vacua is thus composed of the terms given below, with o denoting any vacua other than those given above.

- $e = c, f = a:$

$$h = a:$$

$$\begin{aligned} & \mathcal{S}_3(2\alpha)\mathcal{S}_3(\alpha)[\mathcal{S}_3(\alpha) + (q-3)\mathcal{S}_2(\alpha)] \\ & + \mathcal{S}_1(2\alpha)\mathcal{S}_2(\alpha)[(q-2)\mathcal{S}_2(\alpha) + (q-3)[\mathcal{S}_3(\alpha) + (q-3)\mathcal{S}_2(\alpha)]] \end{aligned}$$

$$h = b, o:$$

$$\begin{aligned} & (q-3)[\mathcal{S}_3(\alpha)\mathcal{S}_2(2\alpha)[\mathcal{S}_1(\alpha) + (q-4)\mathcal{S}_0(\alpha)]] \\ & + \mathcal{S}_2(\alpha)\mathcal{S}_0(2\alpha)[(q-3)\mathcal{S}_0(\alpha) + (q-4)[\mathcal{S}_1(\alpha) + (q-4)\mathcal{S}_0(\alpha)]] \end{aligned}$$

- $e = c, f = d$

$h = a:$

$$\begin{aligned} & \mathcal{S}_1(\alpha)\mathcal{S}_2(2\alpha)[\mathcal{S}_3(\alpha) + (q-3)\mathcal{S}_2(\alpha)] \\ & + \mathcal{S}_0(\alpha)\mathcal{S}_0(2\alpha)(q-3)[\mathcal{S}_3(\alpha) + (q-3)\mathcal{S}_2(\alpha)] \end{aligned}$$

$h = b, o:$

$$\begin{aligned} & (q-3)[\mathcal{S}_1(\alpha)\mathcal{S}_2(2\alpha)[\mathcal{S}_1(\alpha) + (q-4)\mathcal{S}_0(\alpha)] \\ & + \mathcal{S}_0(\alpha)\mathcal{S}_0(2\alpha)(q-4)[\mathcal{S}_1(\alpha) + (q-4)\mathcal{S}_0(\alpha)] \end{aligned}$$

- $e = c, f = o$

$h = a:$

$$\begin{aligned} & (q-4)[\mathcal{S}_1(\alpha)\mathcal{S}_2(2\alpha)[\mathcal{S}_3(\alpha) + (q-3)\mathcal{S}_2(\alpha)] \\ & + \mathcal{S}_0(\alpha)\mathcal{S}_0(2\alpha)[(q-2)\mathcal{S}_2(\alpha) + (q-4)[\mathcal{S}_3(\alpha) + (q-3)\mathcal{S}_2(\alpha)]] \end{aligned}$$

$h = f:$

$$\begin{aligned} & (q-4)[\mathcal{S}_1(\alpha)\mathcal{S}_3(2\alpha)[\mathcal{S}_1(\alpha) + (q-4)\mathcal{S}_0(\alpha)] \\ & + \mathcal{S}_0(\alpha)\mathcal{S}_1(2\alpha)[(q-3)\mathcal{S}_0(\alpha) + (q-4)[\mathcal{S}_1(\alpha) + (q-4)\mathcal{S}_0(\alpha)]] \end{aligned}$$

$h = 0:$

$$\begin{aligned} & (q-4)(q-4)[\mathcal{S}_1(\alpha)\mathcal{S}_2(2\alpha)[\mathcal{S}_1(\alpha) + (q-4)\mathcal{S}_0(\alpha)] \\ & + \mathcal{S}_0(\alpha)\mathcal{S}_0(2\alpha)[(q-3)\mathcal{S}_0(\alpha) + (q-5)[\mathcal{S}_1(\alpha) + (q-4)\mathcal{S}_0(\alpha)]] \end{aligned}$$

- $e = d, f = a$

$h = a:$

$$\begin{aligned} & \mathcal{S}_2(\alpha)\mathcal{S}_3(2\alpha)[\mathcal{S}_3(\alpha) + (q-3)\mathcal{S}_2(\alpha)] \\ & + \mathcal{S}_3(\alpha)\mathcal{S}_1(2\alpha)(q-2)\mathcal{S}_2(\alpha) + (q-3)\mathcal{S}_2(\alpha)\mathcal{S}_1(2\alpha)[\mathcal{S}_3(\alpha) + (q-3)\mathcal{S}_2(\alpha)] \end{aligned}$$

$h = b, o:$

$$(q-3)[\mathcal{S}_2(\alpha)\mathcal{S}_2(2\alpha)[\mathcal{S}_1(\alpha) + (q-4)\mathcal{S}_0(\alpha)] \\ + \mathcal{S}_3(\alpha)\mathcal{S}_0(2\alpha)(q-3)\mathcal{S}_0(\alpha) + (q-4)\mathcal{S}_2(\alpha)\mathcal{S}_0(2\alpha)[\mathcal{S}_1(\alpha) + (q-4)\mathcal{S}_0(\alpha)]]$$

• $e = d, f = o$

$h = a:$

$$(q-4)[\mathcal{S}_0(\alpha)\mathcal{S}_2(2\alpha)[\mathcal{S}_3(\alpha) + (q-3)\mathcal{S}_2(\alpha)] \\ + \mathcal{S}_1(\alpha)\mathcal{S}_0(2\alpha)(q-2)\mathcal{S}_2(\alpha) + (q-4)\mathcal{S}_0(\alpha)\mathcal{S}_0(2\alpha)[\mathcal{S}_3(\alpha) + (q-3)\mathcal{S}_2(\alpha)]]$$

$h = f:$

$$(q-4)[\mathcal{S}_0(\alpha)\mathcal{S}_3(2\alpha)[\mathcal{S}_1(\alpha) + (q-4)\mathcal{S}_0(\alpha)] \\ + \mathcal{S}_1(\alpha)\mathcal{S}_1(2\alpha)(q-3)\mathcal{S}_0(\alpha) + (q-4)\mathcal{S}_0(\alpha)\mathcal{S}_1(2\alpha)[\mathcal{S}_1(\alpha) + (q-4)\mathcal{S}_0(\alpha)]]$$

$h = 0:$

$$(q-4)^2[\mathcal{S}_0(\alpha)\mathcal{S}_2(2\alpha)[\mathcal{S}_1(\alpha) + (q-4)\mathcal{S}_0(\alpha)] \\ + \mathcal{S}_1(\alpha)\mathcal{S}_0(2\alpha)(q-3)\mathcal{S}_0(\alpha) + (q-5)\mathcal{S}_0(\alpha)\mathcal{S}_0(2\alpha)[\mathcal{S}_1(\alpha) + (q-4)\mathcal{S}_0(\alpha)]]$$

• $e = o, f = a$

$h = a:$

$$(q-4)[\mathcal{S}_2(\alpha)\mathcal{S}_3(2\alpha)[\mathcal{S}_3(\alpha) + (q-3)\mathcal{S}_2(\alpha)] \\ + \mathcal{S}_2(\alpha)\mathcal{S}_1(2\alpha)(q-2)\mathcal{S}_2(\alpha) + \mathcal{S}_3(\alpha)\mathcal{S}_1(2\alpha)[\mathcal{S}_3(\alpha) + (q-3)\mathcal{S}_2(\alpha)] \\ + (q-4)[\mathcal{S}_2(\alpha)\mathcal{S}_1(2\alpha)[\mathcal{S}_3(\alpha) + (q-3)\mathcal{S}_2(\alpha)]]$$

$h = e:$

$$(q-4)[[\mathcal{S}_2(\alpha)\mathcal{S}_2(2\alpha) + (q-4)\mathcal{S}_2(\alpha)\mathcal{S}_0(2\alpha)] \\ [\mathcal{S}_1(\alpha) + (q-4)\mathcal{S}_0(\alpha)] + \mathcal{S}_2(\alpha)\mathcal{S}_0(2\alpha)(q-3)\mathcal{S}_0(\alpha)]$$

$h = o$:

$$(q-4)^2 [[\mathcal{S}_2(\alpha)\mathcal{S}_2(2\alpha) + \mathcal{S}_3(\alpha)\mathcal{S}_0(2\alpha) + (q-5)\mathcal{S}_2(\alpha)\mathcal{S}_0(2\alpha)] \\ \times [\mathcal{S}_1(\alpha) + (q-4)\mathcal{S}_0(\alpha)] + \mathcal{S}_2(\alpha)\mathcal{S}_0(2\alpha)(q-3)\mathcal{S}_0(\alpha)]$$

- $e = 0, f = d$

$h = a$:

$$(q-4) [[\mathcal{S}_0(\alpha)\mathcal{S}_2(2\alpha) + \mathcal{S}_1(\alpha)\mathcal{S}_0(2\alpha) + (q-4)\mathcal{S}_0(\alpha)\mathcal{S}_0(2\alpha)] \\ \times [\mathcal{S}_3(\alpha) + (q-3)\mathcal{S}_2(\alpha)]$$

$h = e$:

$$(q-4) [[\mathcal{S}_0(\alpha)\mathcal{S}_2(2\alpha) + (q-4)\mathcal{S}_0(\alpha)\mathcal{S}_0(2\alpha)] \\ \times [\mathcal{S}_1(\alpha) + (q-4)\mathcal{S}_0(\alpha)]$$

$h = 0$:

$$(q-4)^2 [[\mathcal{S}_0(\alpha)\mathcal{S}_2(2\alpha) + \mathcal{S}_1(\alpha)\mathcal{S}_0(2\alpha) + (q-5)\mathcal{S}_0(\alpha)\mathcal{S}_0(2\alpha)] \\ \times [\mathcal{S}_1(\alpha) + (q-4)\mathcal{S}_0(\alpha)]$$

- $e = 0, f = o'$

$h = a$:

$$(q-4)(q-5) [[\mathcal{S}_0(\alpha)\mathcal{S}_2(2\alpha) + \mathcal{S}_1(\alpha)\mathcal{S}_0(2\alpha) + (q-5)\mathcal{S}_0(\alpha)\mathcal{S}_0(2\alpha)] \\ \times [\mathcal{S}_3(\alpha) + (q-3)\mathcal{S}_2(\alpha)] + \mathcal{S}_0(\alpha)\mathcal{S}_0(2\alpha)(q-2)\mathcal{S}_2(\alpha)]$$

$h = e$:

$$(q-4)(q-5) [[\mathcal{S}_0(\alpha)\mathcal{S}_2(2\alpha) + (q-5)\mathcal{S}_0(\alpha)\mathcal{S}_0(2\alpha)] \\ \times [\mathcal{S}_1(\alpha) + (q-4)\mathcal{S}_0(\alpha)] + \mathcal{S}_0(\alpha)\mathcal{S}_0(2\alpha)(q-3)\mathcal{S}_0(\alpha)]$$

$h = f$:

$$(q-4)(q-5)[[\mathcal{S}_0(\alpha)\mathcal{S}_3(2\alpha) + \mathcal{S}_1(\alpha)\mathcal{S}_1(2\alpha) + (q-5)\mathcal{S}_0(\alpha)\mathcal{S}_1(2\alpha)] \\ \times [\mathcal{S}_1(\alpha) + (q-4)\mathcal{S}_0(\alpha)] + \mathcal{S}_0(\alpha)\mathcal{S}_1(2\alpha)(q-3)\mathcal{S}_0(\alpha)]$$

$h = o''$:

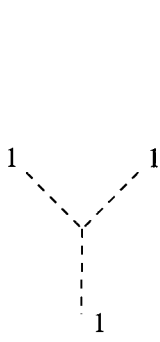
$$(q-4)(q-5)^2[[\mathcal{S}_0(\alpha)\mathcal{S}_2(2\alpha) + \mathcal{S}_1(\alpha)\mathcal{S}_0(2\alpha) + (q-6)\mathcal{S}_0(\alpha)\mathcal{S}_0(2\alpha)] \\ \times [\mathcal{S}_1(\alpha) + (q-4)\mathcal{S}_0(\alpha)] + \mathcal{S}_0(\alpha)\mathcal{S}_0(2\alpha)(q-3)\mathcal{S}_0(\alpha)]$$

Appendix B

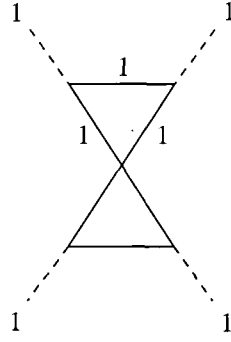
Bootstrap and generalised bootstrap scattering processes for $\lambda < \frac{9}{4}$

The pole structures of all scattering amplitudes appearing for $\lambda < \frac{9}{4}$ are accounted for, apart from the kink-kink scattering amplitudes as they are treated in great detail in the main body of the text. The simplest scattering processes are not accurately portrayed, due to the excessive number of them.

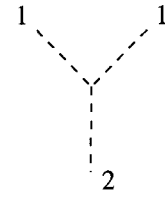
$$\mathcal{S}_{B_1 B_1}(\theta) : \left[\frac{2}{3}\right] \left[\frac{1}{\lambda}\right] \left[\frac{1}{\lambda} - \frac{1}{3}\right]$$



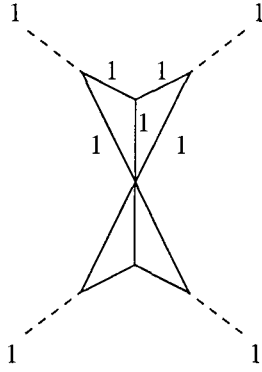
$$\left[\frac{2}{3}\right] : \lambda > 1$$



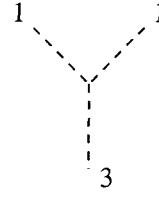
$$\left[\frac{1}{\lambda}\right] : 1 < \lambda < 2$$



$$\left[\frac{1}{\lambda}\right] : \lambda > 2$$

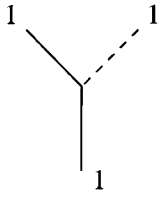


$$\left[\frac{1}{\lambda} - \frac{1}{3}\right] : 1 < \lambda < \frac{3}{2}$$

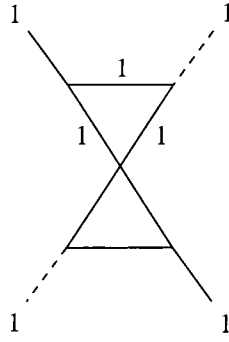


$$\left[\frac{1}{\lambda} - \frac{1}{3}\right] : \lambda > \frac{3}{2}$$

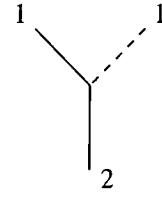
$$\mathcal{S}_{B_1 K_1}(\theta) : \left[\frac{1}{2} + \frac{1}{2\lambda}\right] \left[\frac{1}{6} + \frac{1}{2\lambda}\right]$$



$$\left[\frac{1}{2} + \frac{1}{2\lambda}\right] : \lambda > 1$$

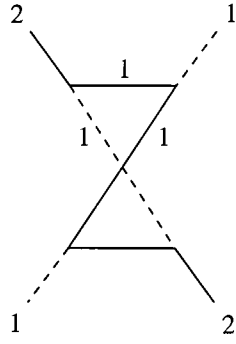


$$\left[\frac{1}{6} + \frac{1}{2\lambda}\right] : 1 < \lambda < \frac{3}{2}$$

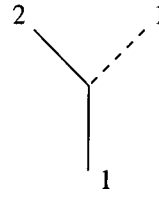


$$\left[\frac{1}{6} + \frac{1}{2\lambda}\right] : \lambda > \frac{3}{2}$$

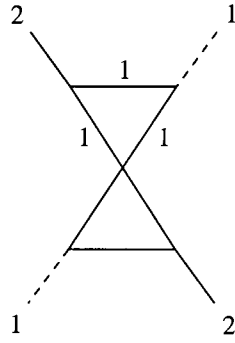
$$\mathcal{S}_{K_2B_1}(\theta) : \left[\frac{1}{2}\right]\left[\frac{5}{6}\right]\left[\frac{1}{6} + \frac{1}{\lambda}\right]\left[\frac{1}{\lambda} - \frac{1}{6}\right]$$



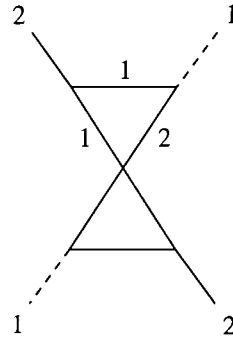
$$\left[\frac{1}{2}\right] : \frac{3}{2} < \lambda < 3$$



$$\left[\frac{5}{6}\right] : \lambda > \frac{3}{2}$$

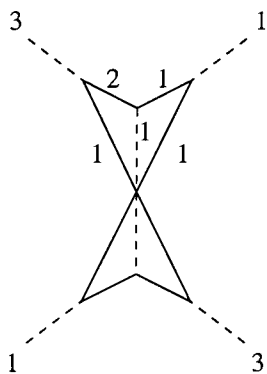


$$\left[\frac{1}{6} + \frac{1}{\lambda}\right] : \frac{3}{2} < \lambda < 3$$

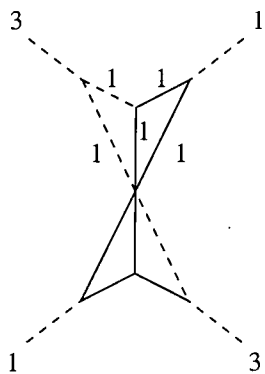


$$\left[\frac{1}{\lambda} - \frac{1}{6}\right] : \frac{3}{2} < \lambda < \frac{9}{4}$$

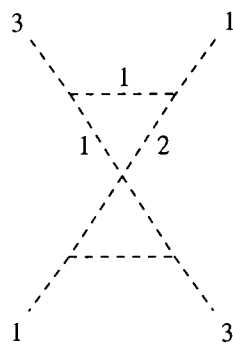
$$\mathcal{S}_{B_3 B_1}(\theta) : \left[\frac{7}{6} - \frac{1}{2\lambda}\right] \left[\frac{1}{2} + \frac{1}{2\lambda}\right] \left[\frac{3}{2\lambda} - \frac{1}{2}\right] \left[\frac{3}{2\lambda} - \frac{1}{6}\right] \left[\frac{1}{6} + \frac{1}{2\lambda}\right]^2$$



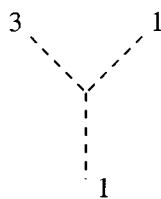
$$\left[\frac{1}{6} + \frac{1}{2\lambda}\right]^2 : \frac{3}{2} < \lambda < \frac{9}{5}$$



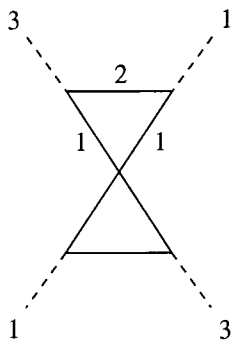
$$\left[\frac{1}{6} + \frac{1}{2\lambda}\right]^2 : \frac{9}{5} < \lambda < 2$$



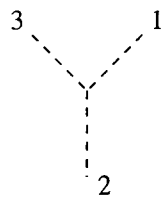
$$\left[\frac{1}{6} + \frac{1}{2\lambda}\right]^2 : \lambda > 2$$



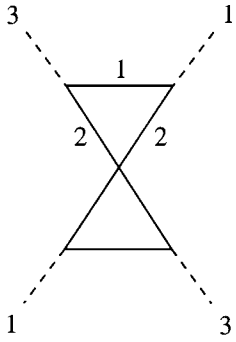
$$\left[\frac{7}{6} - \frac{1}{2\lambda}\right] : \lambda > \frac{3}{2}$$



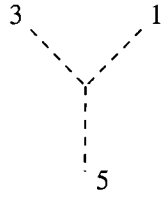
$$\left[\frac{1}{2} + \frac{1}{2\lambda}\right] : \frac{3}{2} < \lambda < 2$$



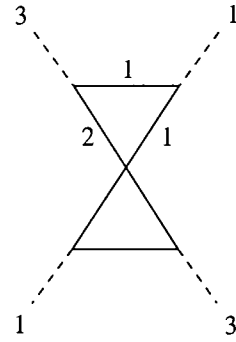
$$\left[\frac{1}{2} + \frac{1}{2\lambda}\right] : \lambda > 2$$



$$\left[\frac{3}{2\lambda} - \frac{1}{2}\right] : \frac{3}{2} < \lambda < 2$$

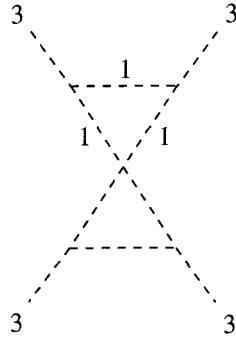


$$\left[\frac{3}{2\lambda} - \frac{1}{2}\right] : \lambda > 2$$

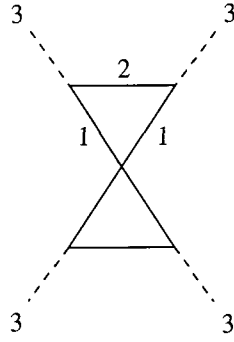


$$\left[\frac{3}{2\lambda} - \frac{1}{6}\right] : \frac{3}{2} < \lambda < \frac{5}{2}$$

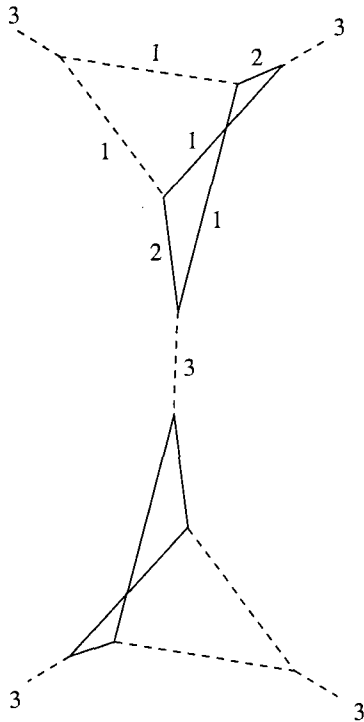
$$\mathcal{S}_{B_3 B_3}(\theta) : \left[\frac{4}{3} - \frac{1}{\lambda}\right]^2 \left[\frac{1}{3} + \frac{1}{\lambda}\right] \left[\frac{2}{3}\right]^3 \left[\frac{2}{\lambda} - \frac{1}{3}\right] \left[\frac{2}{\lambda} - \frac{2}{3}\right] \left[\frac{1}{\lambda}\right]^3$$



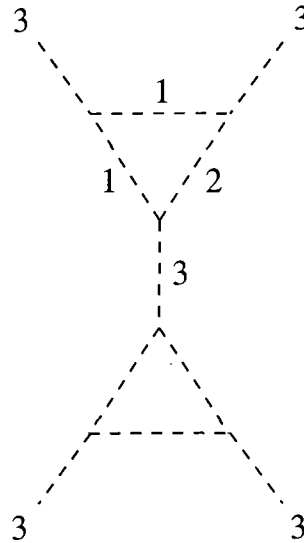
$$\left[\frac{4}{3} - \frac{1}{\lambda}\right]^2 : \frac{3}{2} < \lambda < 3$$



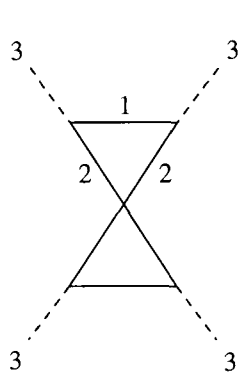
$$\left[\frac{1}{3} + \frac{1}{\lambda}\right] : \frac{3}{2} < \lambda < 3$$



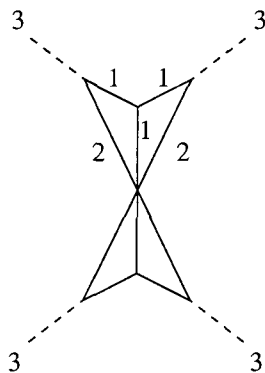
$$\left[\frac{2}{3}\right]^3 : \frac{3}{2} < \lambda < 2$$



$$\left[\frac{2}{3}\right]^3 : \lambda > 2$$



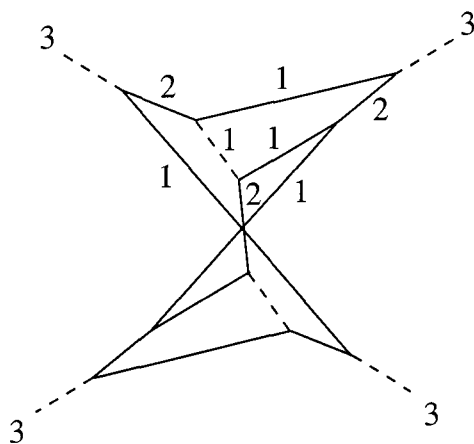
$$\left[\frac{2}{\lambda} - \frac{1}{3}\right] : \frac{3}{2} < \lambda < 3$$



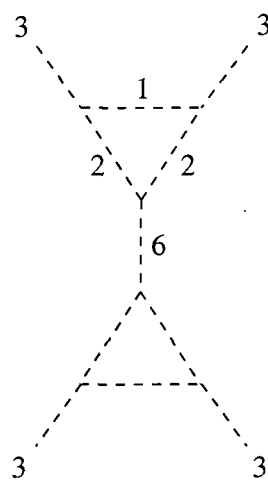
$$\left[\frac{2}{\lambda} - \frac{2}{3}\right] : \frac{3}{2} < \lambda < \frac{9}{4}$$



$$\left[\frac{2}{\lambda} - \frac{2}{3}\right] : \lambda > \frac{9}{4}$$

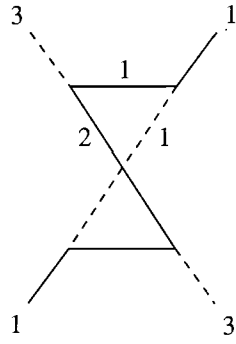


$$\left[\frac{1}{\lambda}\right]^3 : \frac{3}{2} < \lambda < \frac{9}{4}$$

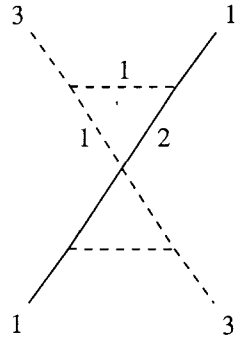


$$\left[\frac{1}{\lambda}\right]^3 : \lambda > \frac{9}{4}$$

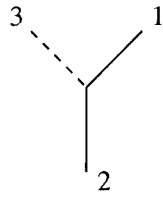
$$\mathcal{S}_{B_3\mathcal{K}_1}(\theta) : \left[\frac{1}{3}\right]^2 \left[\frac{1}{3} + \frac{1}{\lambda}\right] \left[\frac{1}{\lambda}\right]$$



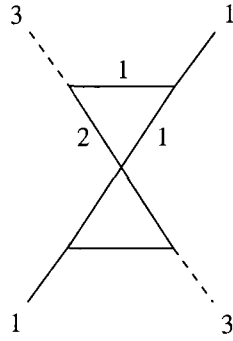
$$\left[\frac{1}{3}\right]^2 : \frac{3}{2} < \lambda < 2$$



$$\left[\frac{1}{3}\right]^2 : \lambda > 2$$

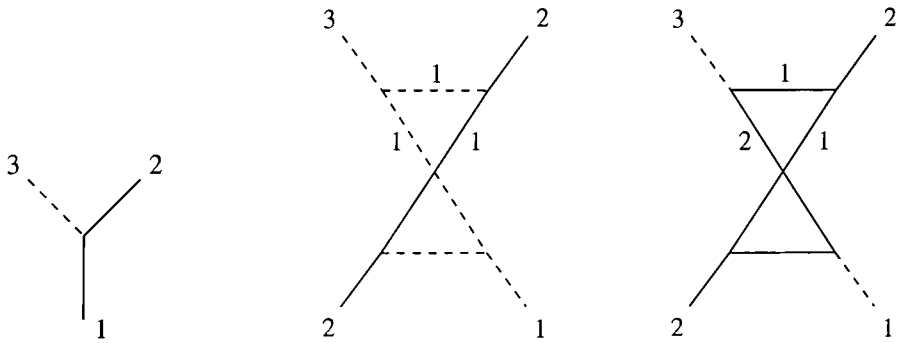


$$\left[\frac{1}{3} + \frac{1}{\lambda}\right] : \lambda > \frac{3}{2}$$



$$\left[\frac{1}{\lambda}\right] : \frac{3}{2} < \lambda < \frac{9}{4}$$

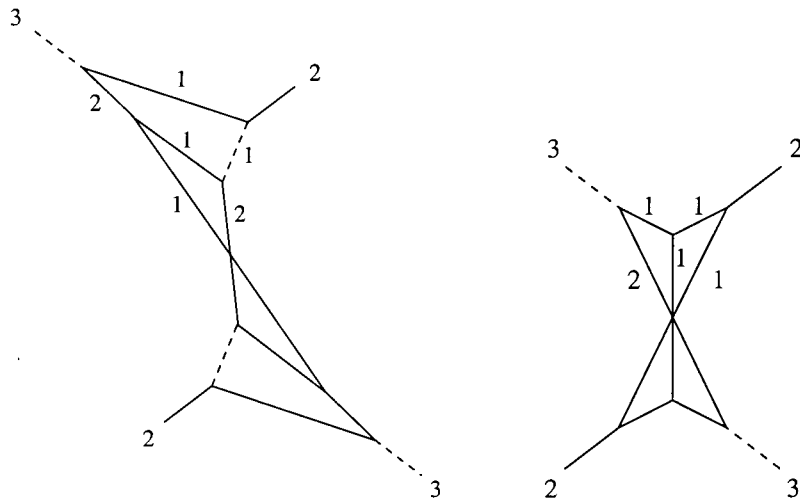
$$\mathcal{S}_{B_3K_2}(\theta) : \left[\frac{2}{3} + \frac{1}{2\lambda}\right] \left[1 - \frac{1}{2\lambda}\right]^2 \left[\frac{3}{2\lambda}\right] \left[\frac{1}{3} + \frac{1}{2\lambda}\right] \left[\frac{3}{2\lambda} - \frac{1}{3}\right]$$



$$\left[\frac{2}{3} + \frac{1}{2\lambda}\right] : \lambda > \frac{3}{2}$$

$$\left[1 - \frac{1}{2\lambda}\right]^2 : \frac{3}{2} < \lambda < 9$$

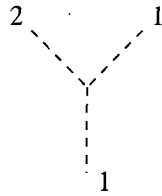
$$\left[\frac{3}{2\lambda}\right] : \frac{3}{2} < \lambda < \frac{15}{4}$$



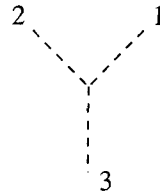
$$\left[\frac{1}{3} + \frac{1}{2\lambda}\right] : \frac{3}{2} < \lambda < \frac{9}{4}$$

$$\left[\frac{3}{2\lambda} - \frac{1}{3}\right] : \frac{3}{2} < \lambda < \frac{9}{4}$$

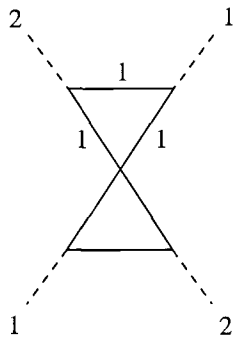
$$\mathcal{S}_{B_2 B_1}(\theta) : [1 - \frac{1}{2\lambda}] [\frac{2}{3} - \frac{1}{2\lambda}] [\frac{3}{2\lambda}] [\frac{3}{2\lambda} - \frac{1}{3}]$$



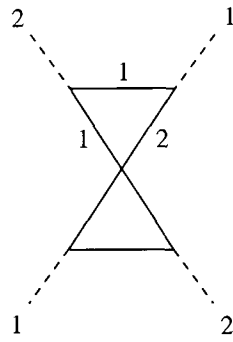
$$[1 - \frac{1}{2\lambda}] : \lambda > 2$$



$$[\frac{2}{3} - \frac{1}{2\lambda}] : \lambda > 2$$

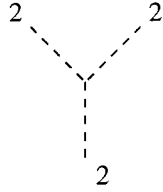


$$[\frac{3}{2\lambda}] : 2 < \lambda < 3$$

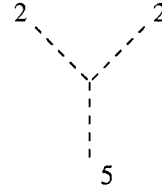


$$[\frac{3}{2\lambda} - \frac{1}{3}] : 2 < \lambda < \frac{5}{2}$$

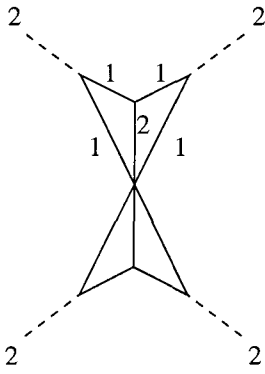
$$\mathcal{S}_{B_2 B_2}(\theta) : \left[\frac{2}{3}\right]\left[\frac{2}{3} - \frac{1}{\lambda}\right]\left[\frac{1}{\lambda} - \frac{1}{3}\right]\left[\frac{2}{\lambda}\right]\left[\frac{2}{\lambda} - \frac{1}{3}\right]\left[1 - \frac{1}{\lambda}\right]^2$$



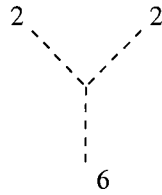
$$\left[\frac{2}{3}\right] : \lambda > 2$$



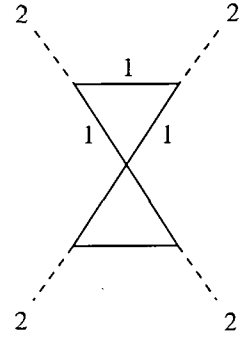
$$\left[\frac{2}{3} - \frac{1}{\lambda}\right] : \lambda > 2$$



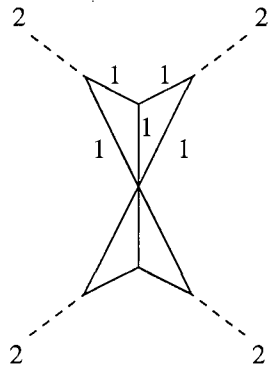
$$\left[\frac{1}{\lambda} - \frac{1}{3}\right] : 2 < \lambda < \frac{9}{4}$$



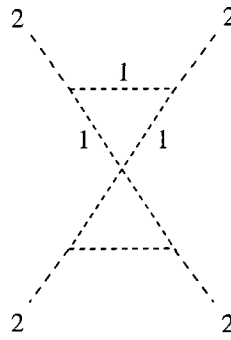
$$\left[\frac{1}{\lambda} - \frac{1}{3}\right] : \lambda > \frac{9}{4}$$



$$\left[\frac{2}{\lambda}\right] : 2 < \lambda < 4$$

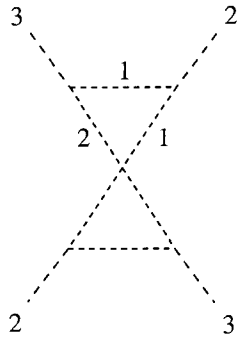


$$\left[\frac{2}{\lambda} - \frac{1}{3}\right] : 2 < \lambda < 3$$

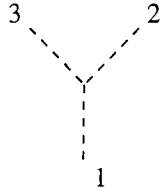


$$\left[1 - \frac{1}{\lambda}\right]^2 : \lambda > 2$$

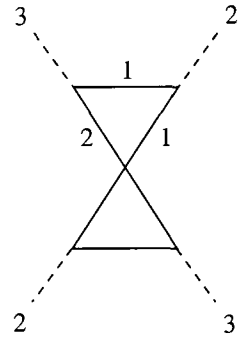
$$\mathcal{S}_{B_3 B_2}(\theta) : \left[\frac{1}{2}\right]\left[\frac{5}{6}\right]\left[\frac{2}{\lambda} - \frac{1}{6}\right]\left[\frac{7}{6} - \frac{1}{\lambda}\right]^2\left[\frac{2}{\lambda} - \frac{1}{2}\right]\left[\frac{5}{6} - \frac{1}{\lambda}\right]^2$$



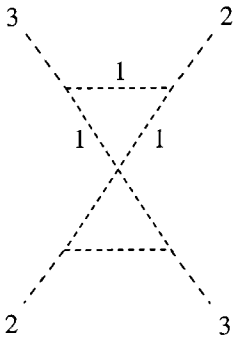
$$\left[\frac{1}{2}\right] : \lambda > 2$$



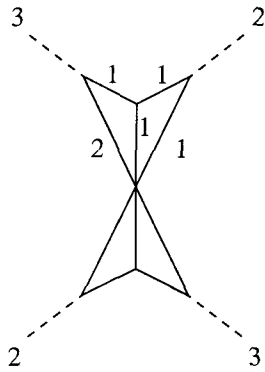
$$\left[\frac{5}{6}\right] : \lambda > 2$$



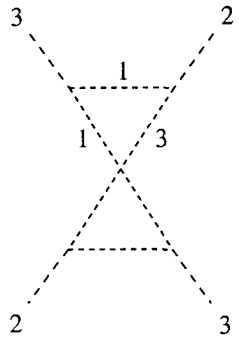
$$\left[\frac{2}{\lambda} - \frac{1}{6}\right] : 2 < \lambda < \frac{7}{2}$$



$$\left[\frac{7}{6} - \frac{1}{\lambda}\right]^2 : 2 < \lambda < 6$$

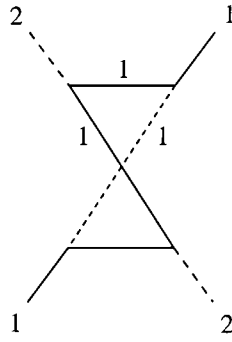


$$\left[\frac{2}{\lambda} - \frac{1}{2}\right] : 2 < \lambda < \frac{9}{4}$$

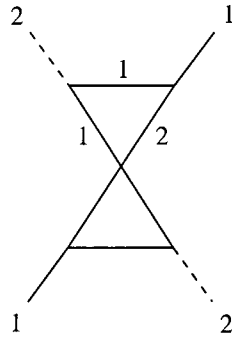


$$\left[\frac{5}{6} - \frac{1}{\lambda}\right]^2 : \lambda > 2$$

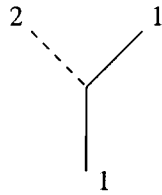
$$\mathcal{S}_{B_2K_1}(\theta) : \left[\frac{1}{2}\right]\left[\frac{1}{6}\right]\left[\frac{1}{2} + \frac{1}{\lambda}\right]\left[\frac{1}{6} + \frac{1}{\lambda}\right]$$



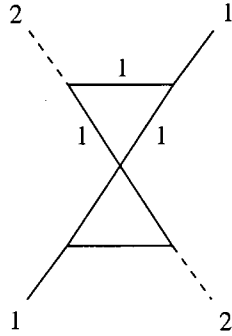
$$\left[\frac{1}{2}\right] : 2 < \lambda < 3$$



$$\left[\frac{1}{6}\right] : 2 < \lambda < \frac{9}{4}$$

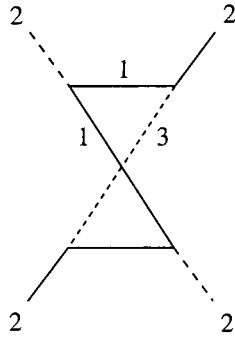


$$\left[\frac{1}{2} + \frac{1}{\lambda}\right] : \lambda > 2$$

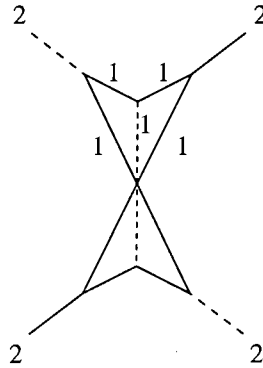


$$\left[\frac{1}{6} + \frac{1}{\lambda}\right] : 2 < \lambda < 3$$

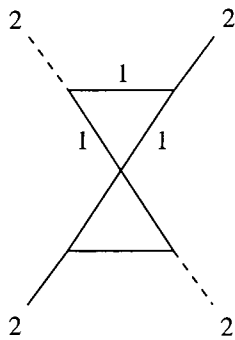
$$\mathcal{S}_{B_2K_2}(\theta) : \left[\frac{1}{2} - \frac{1}{2\lambda}\right]^2 \left[\frac{1}{6} + \frac{1}{2\lambda}\right]^2 \left[\frac{1}{6} + \frac{3}{2\lambda}\right] \left[\frac{3}{2\lambda} - \frac{1}{6}\right]$$



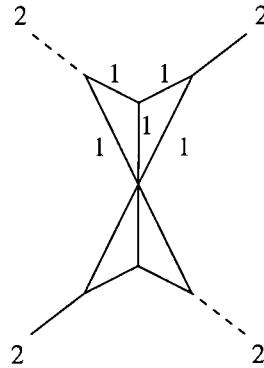
$$\left[\frac{1}{2} - \frac{1}{2\lambda}\right]^2 : 2 < \lambda < 3$$



$$\left[\frac{1}{6} - \frac{1}{2\lambda}\right]^2 : 2 < \lambda < 3$$

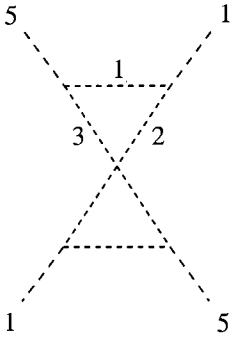


$$\left[\frac{1}{6} + \frac{3}{2\lambda}\right] : 2 < \lambda < \frac{9}{2}$$

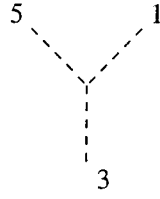


$$\left[\frac{3}{2\lambda} - \frac{1}{6}\right] : 2 < \lambda < 3$$

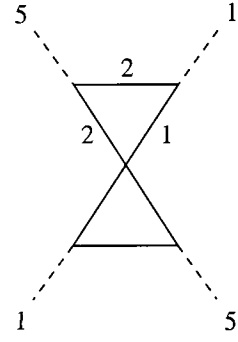
$$\mathcal{S}_{B_5 B_1}(\theta) : \left[\frac{1}{3}\right]^2 \left[\frac{4}{3} - \frac{1}{\lambda}\right] \left[\frac{1}{3} + \frac{1}{\lambda}\right] \left[\frac{2}{\lambda} - \frac{2}{3}\right] \left[\frac{2}{\lambda} - \frac{1}{3}\right] \left[1 - \frac{1}{\lambda}\right]^2$$



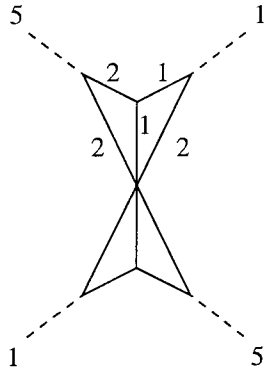
$$\left[\frac{1}{3}\right]^2 : \lambda > 2$$



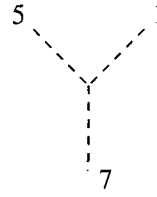
$$\left[\frac{4}{3} - \frac{1}{\lambda}\right] : \lambda > 2$$



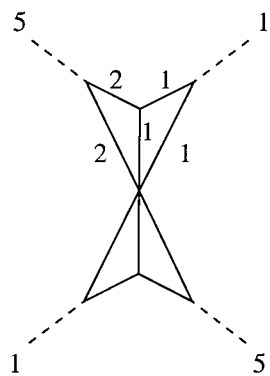
$$\left[\frac{1}{3} + \frac{1}{\lambda}\right] : 2 < \lambda < \frac{5}{2}$$



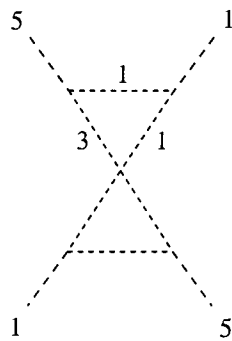
$$\left[\frac{2}{\lambda} - \frac{2}{3}\right] : 2 < \lambda < \frac{9}{4}$$



$$\left[\frac{2}{\lambda} - \frac{2}{3}\right] : \lambda > \frac{9}{4}$$

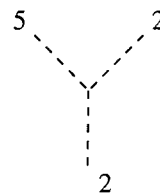
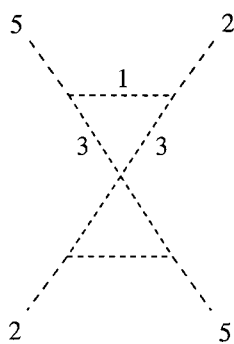
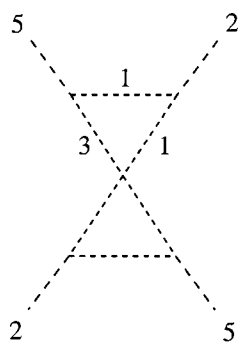


$$\left[\frac{2}{\lambda} - \frac{1}{3}\right] : 2 < \lambda < \frac{9}{4}$$



$$\left[1 - \frac{1}{\lambda}\right]^2 : \lambda > 2$$

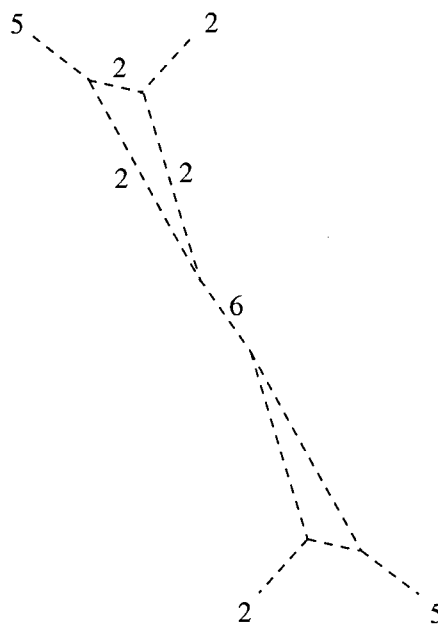
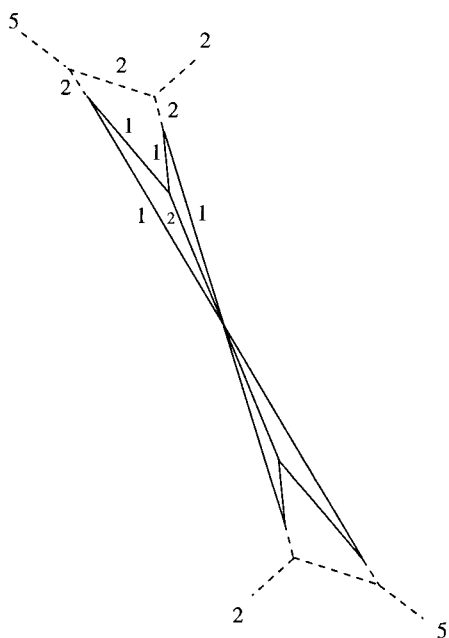
$$\mathcal{S}_{B_5 B_2}(\theta) : \left[\frac{4}{3} - \frac{3}{2\lambda}\right]^2 \left[1 - \frac{3}{2\lambda}\right]^2 \left[\frac{2}{3} + \frac{1}{2\lambda}\right] \left[\frac{1}{3} + \frac{1}{2\lambda}\right]^3 \left[1 - \frac{1}{2\lambda}\right]^2 \left[\frac{5}{2\lambda} - \frac{1}{3}\right] \left[\frac{5}{2\lambda} - \frac{2}{3}\right]$$



$$\left[\frac{4}{3} - \frac{3}{2\lambda}\right]^2 : 2 < \lambda < 5$$

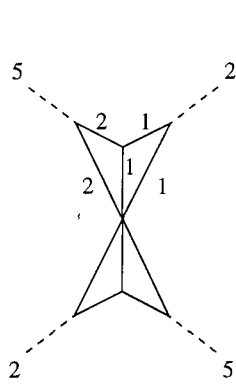
$$\left[1 - \frac{3}{2\lambda}\right]^2 : \lambda > 2$$

$$\left[\frac{2}{3} + \frac{1}{2\lambda}\right] : \lambda > 2$$

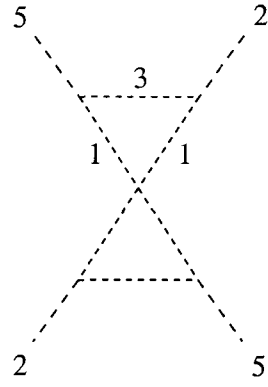


$$\left[\frac{1}{3} + \frac{1}{2\lambda}\right]^3 : 2 < \lambda < \frac{9}{4}$$

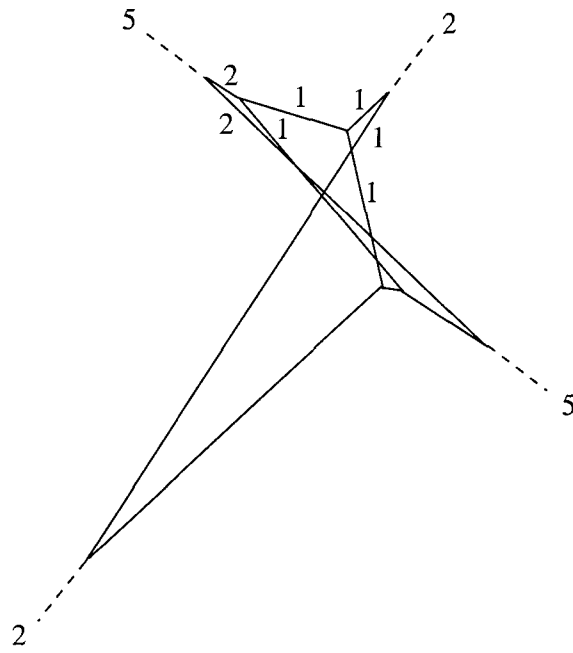
$$\left[\frac{1}{3} + \frac{1}{2\lambda}\right]^3 : \lambda > \frac{9}{4}$$



$$\left[\frac{5}{2\lambda} - \frac{1}{3}\right] : 2 < \lambda < \frac{9}{4}$$

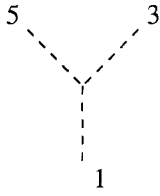


$$\left[1 - \frac{1}{2\lambda}\right]^2 : \lambda > 2$$

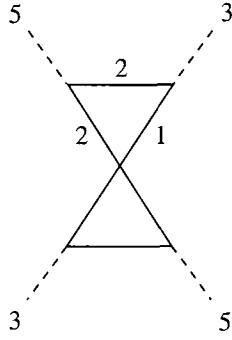


$$\left[\frac{5}{2\lambda} - \frac{2}{3}\right] : 2 < \lambda < \frac{9}{4}$$

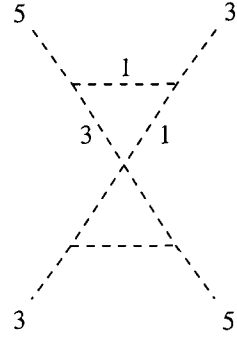
$$\mathcal{S}_{B_5 B_3}(\theta) : \left[\frac{7}{6} - \frac{1}{2\lambda}\right] \left[\frac{1}{6} + \frac{3}{2\lambda}\right] \left[\frac{3}{2} - \frac{3}{2\lambda}\right]^2 \left[\frac{5}{2\lambda} - \frac{5}{6}\right] \left[\frac{1}{2} + \frac{1}{2\lambda}\right]^3 \left[\frac{3}{2\lambda} - \frac{1}{6}\right]^3 \left[\frac{5}{2\lambda} - \frac{1}{2}\right] \left[\frac{5}{6} - \frac{1}{2\lambda}\right]^4$$



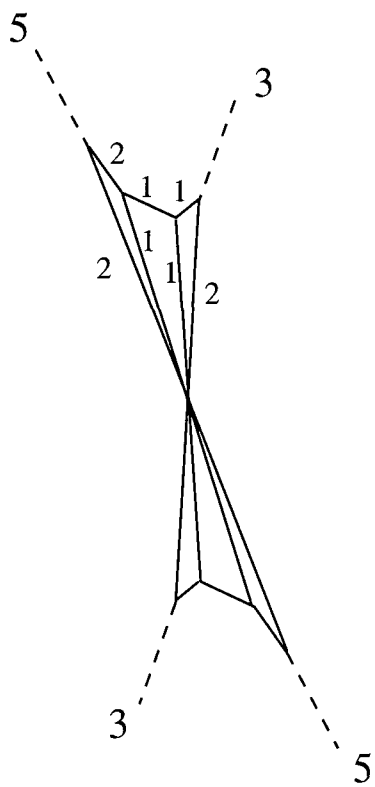
$$\left[\frac{7}{6} - \frac{1}{2\lambda}\right] : \lambda > 2$$



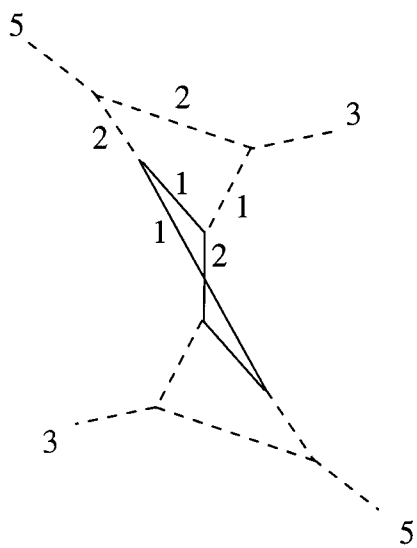
$$\left[\frac{1}{6} + \frac{3}{2\lambda}\right] : 2 < \lambda < \frac{7}{2}$$



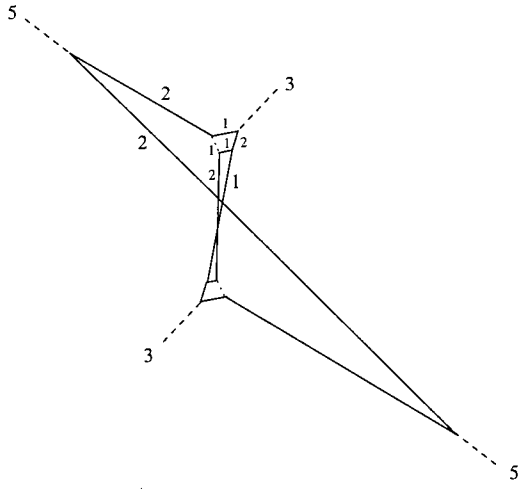
$$\left[\frac{3}{2} - \frac{3}{2\lambda}\right]^2 : 2 < \lambda < 3$$



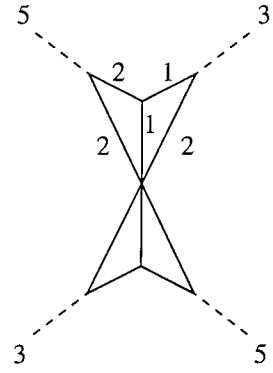
$$\left[\frac{5}{2\lambda} - \frac{5}{6}\right] : 2 < \lambda < \frac{9}{4}$$



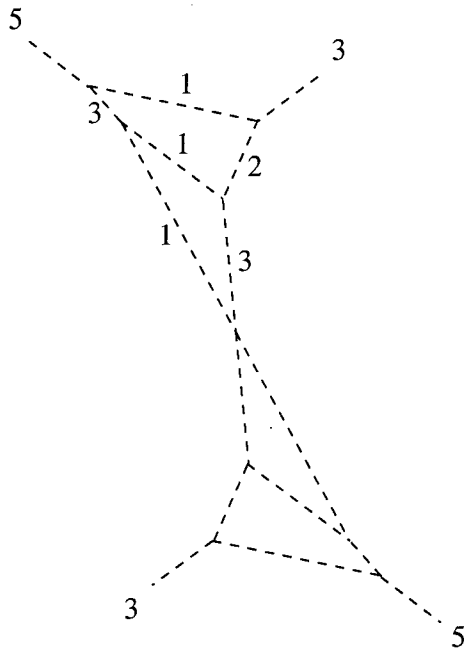
$$\left[\frac{1}{2} + \frac{1}{2\lambda}\right]^3 : 2 < \lambda < \frac{5}{2}$$



$$\left[\frac{3}{2\lambda} - \frac{1}{6}\right]^3 : 2 < \lambda < \frac{9}{4}$$

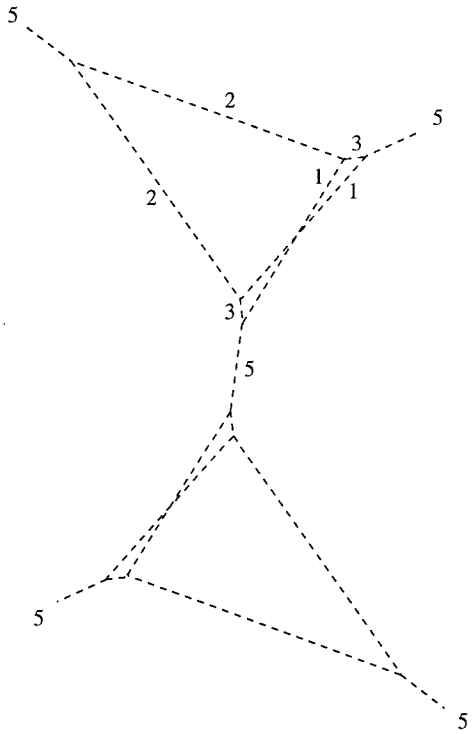


$$\left[\frac{5}{2\lambda} - \frac{1}{2}\right] : 2 < \lambda < \frac{9}{4}$$

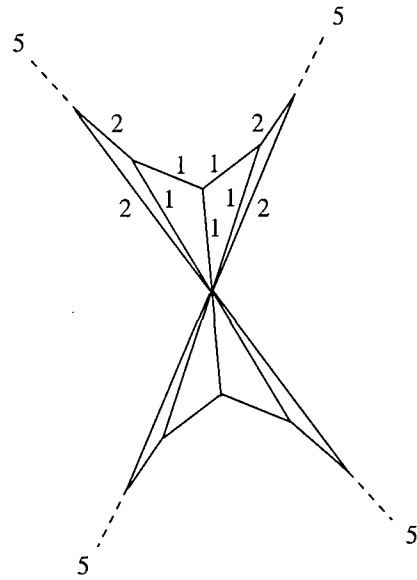


$$\left[\frac{5}{6} - \frac{1}{2\lambda}\right]^4 : \lambda > 2$$

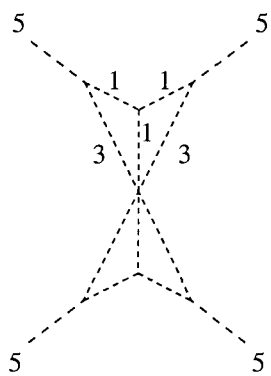
$$\mathcal{S}_{B_5 B_5}(\theta) : \left[\frac{5}{3} - \frac{2}{\lambda}\right]^2 \left[\frac{2}{3}\right]^5 \left[\frac{3}{\lambda} - 1\right] \left[\frac{3}{\lambda} - \frac{2}{3}\right] \left[\frac{1}{\lambda}\right]^5 \left[\frac{1}{3} + \frac{1}{\lambda}\right]^3 \left[\frac{4}{3} - \frac{2}{\lambda}\right]^3 \left[\frac{2}{\lambda}\right] \left[\frac{4}{3} - \frac{1}{\lambda}\right]^2$$



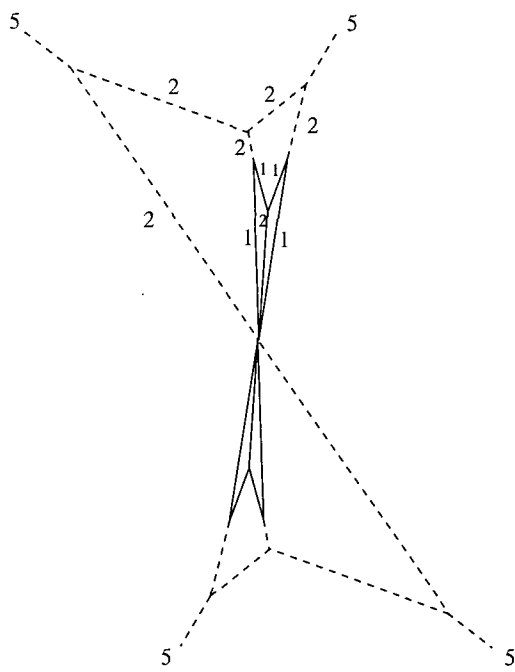
$$\left[\frac{2}{3}\right]^5 : \lambda > 2$$



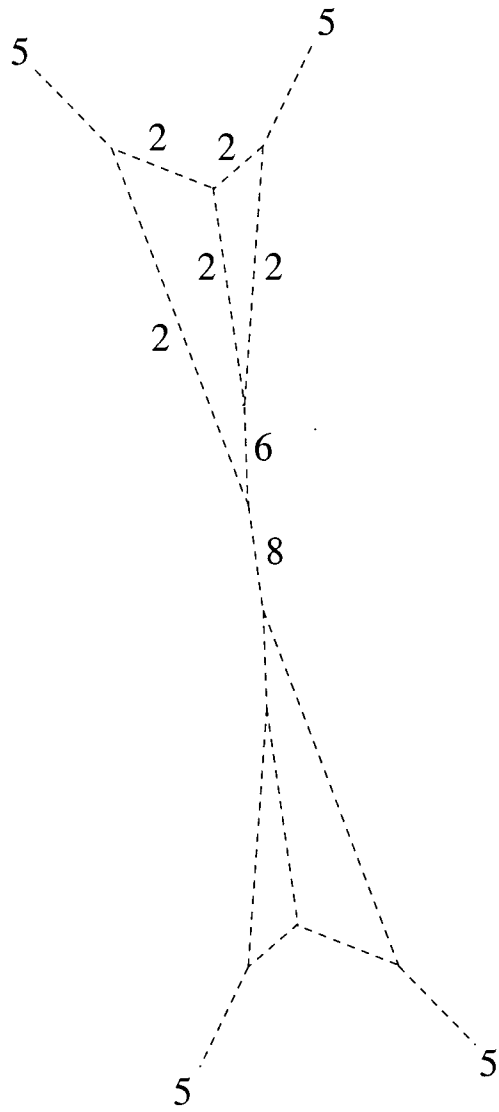
$$\left[\frac{3}{\lambda} - 1\right] : 2 < \lambda < \frac{9}{4}$$



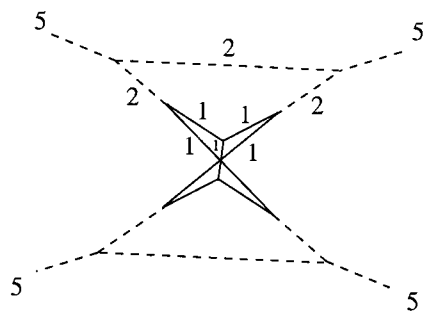
$$\left[\frac{4}{3} - \frac{2}{\lambda}\right]^3 : 2 < \lambda < \frac{9}{2}$$



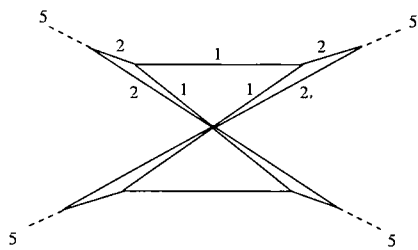
$$\left[\frac{1}{\lambda}\right]^5 : 2 < \lambda < \frac{9}{4}$$



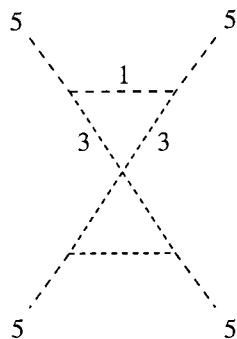
$$\left[\frac{1}{\lambda}\right]^5 : \lambda > \frac{9}{4}$$



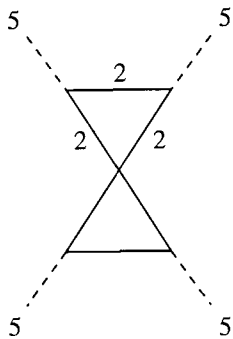
$$\left[\frac{1}{3} + \frac{1}{\lambda}\right]^3 : 2 < \lambda < 3$$



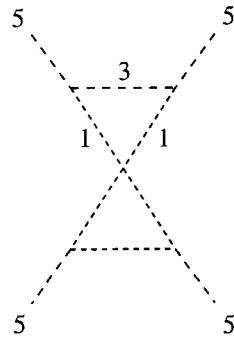
$$\left[\frac{3}{\lambda} - \frac{2}{3}\right] : 2 < \lambda < \frac{9}{4}$$



$$\left[\frac{5}{3} - \frac{2}{\lambda}\right]^2 : 2 < \lambda < 3$$

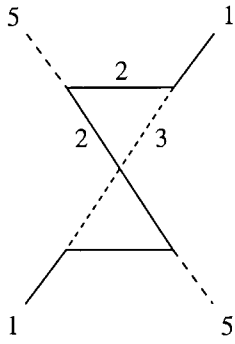


$$\left[\frac{2}{\lambda}\right] : 2 < \lambda < 4$$

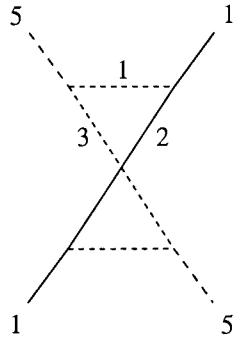


$$\left[\frac{4}{3} - \frac{1}{\lambda}\right]^2 : 2 < \lambda < 3$$

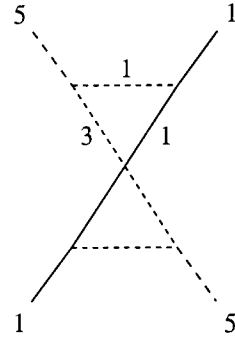
$$\mathcal{S}_{B_3 K_1}(\theta) : \left[\frac{1}{2} - \frac{1}{2\lambda}\right]^2 \left[\frac{5}{6} - \frac{1}{2\lambda}\right]^2 \left[\frac{1}{6} + \frac{3}{2\lambda}\right] \left[\frac{3}{2\lambda} - \frac{1}{6}\right]$$



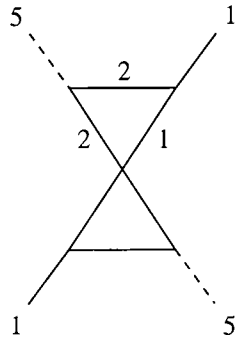
$$\left[\frac{1}{2} - \frac{1}{2\lambda}\right]^2 : 2 < \lambda < \frac{9}{4}$$



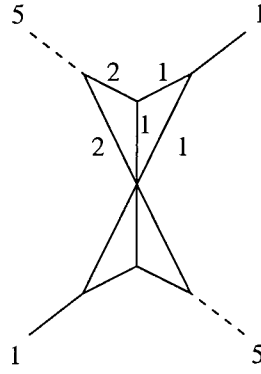
$$\left[\frac{1}{2} - \frac{1}{2\lambda}\right]^2 : \lambda > \frac{9}{4}$$



$$\left[\frac{5}{6} - \frac{1}{2\lambda}\right]^2 : \lambda > 2$$

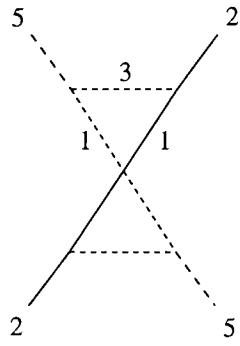


$$\left[\frac{1}{6} + \frac{3}{2\lambda}\right] : 2 < \lambda < \frac{9}{4}$$

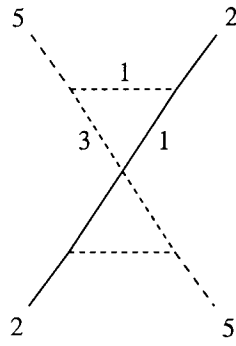


$$\left[\frac{3}{2\lambda} - \frac{1}{6}\right] : 2 < \lambda < \frac{9}{4}$$

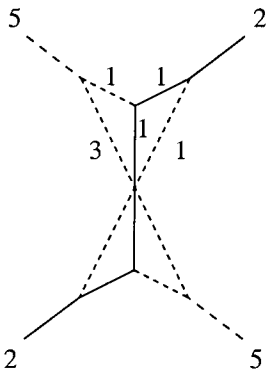
$$\mathcal{S}_{B_5K_2}(\theta) : \left[\frac{5}{6}\right]^2 \left[\frac{1}{2}\right]^2 \left[\frac{7}{6} - \frac{1}{\lambda}\right]^2 \left[\frac{5}{6} - \frac{1}{\lambda}\right]^3 \left[\frac{1}{2} + \frac{1}{\lambda}\right] \left[\frac{2}{\lambda} - \frac{1}{6}\right] \left[\frac{2}{\lambda} - \frac{1}{2}\right]$$



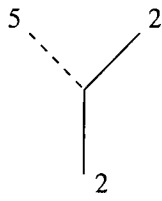
$$\left[\frac{5}{6}\right]^2 : \frac{15}{7} < \lambda < 15$$



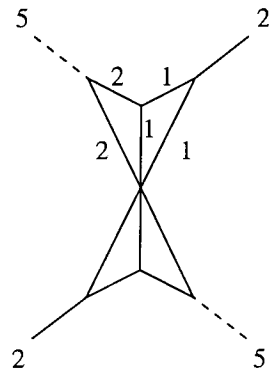
$$\left[\frac{7}{6} - \frac{1}{\lambda}\right]^2 : 2 < \lambda < 6$$



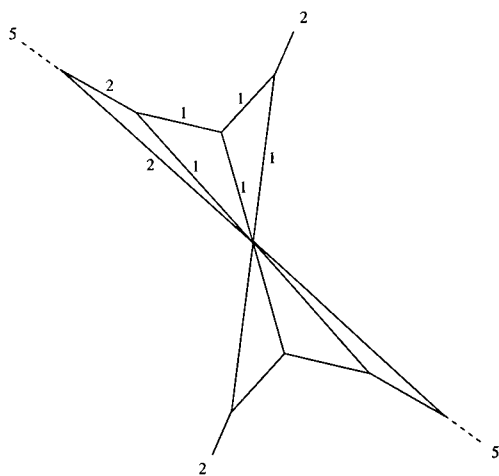
$$\left[\frac{5}{6} - \frac{1}{\lambda}\right]^3 : 2 < \lambda < 3$$



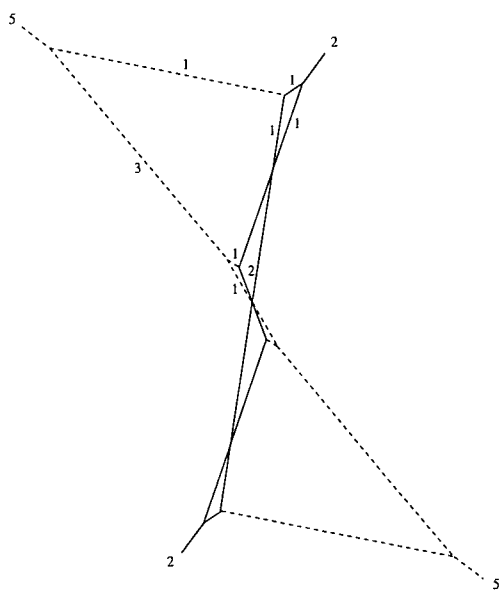
$$\left[\frac{1}{2} + \frac{1}{\lambda}\right] : \lambda > 2$$



$$\left[\frac{2}{\lambda} - \frac{1}{6}\right] : 2 < \lambda < \frac{9}{4}$$



$$\left[\frac{2}{\lambda} - \frac{1}{2}\right] : 2 < \lambda < \frac{9}{4}$$



$$\left[\frac{1}{2}\right]^2 : 2 < \lambda < 3$$

Appendix C

Yang-Baxter equations for 'excluded' boundary condition

These are the full Yang-Baxter equations, whose reductions at $\theta_2 = \frac{i\pi}{2}$ are considered in section (5.4.3) of chapter 5. The shorthand $R_i S_j R_k S_l$ for $R_i(\theta_1) S_j(\theta_1 + \theta_2) R_k(\theta_2) S_l(\theta_2 - \theta_1)$ is used throughout.

1.

$$\begin{aligned} & R_1 S_3 R_2 S_1 + (q-4) R_1 S_2 R_2 S_0 + R_1 S_2 R_2^A S_0 + R_2 S_1 R_1 S_1 \\ & + (q-4) R_2 S_0 R_1 S_0 + R_2 S_0 R_1^A S_0 + (q-4) R_2 S_1 R_2 S_1 + (q-4)(q-5) R_2 S_0 R_2 S_0 \\ & + (q-4) R_2 S_0 R_2^A S_0 = R_2 S_3 R_1 S_3 + (q-3) R_2 S_2 R_1 S_2 + R_2 S_2 R_1^A S_2 \\ & + R_1 S_1 R_2 S_3 + (q-4) R_1 S_0 R_2 S_2 + R_1 S_0 R_2^A S_2 + (q-4) R_2 S_1 R_2 S_3 \\ & + (q-4) R_2 S_0 R_2^A S_2 + (q-4)^2 R_2 S_0 R_2 S_2 \end{aligned}$$

2.

$$\begin{aligned} & R_1 S_1 R_2 S_2 + (q-4) R_1 S_0 R_2 S_2 + R_1 S_0 R_2^A S_2 + R_2 S_2 R_1 S_3 \\ & + R_2 S_3 R_1 S_2 + (q-4) R_2 S_2 R_1 S_2 + R_2 S_2 R_1^A S_2 + (q-4) R_2 S_0 R_2 S_3 \end{aligned}$$

$$\begin{aligned}
& +(q-4)R_2S_1R_2S_2 + (q-4)R_2S_0R_2^AS_2 + (q-4)(q-5)R_2S_0R_2S_2 \\
& = (q-4)^2R_2S_0R_2S_0 + (q-3)R_2S_0R_2^AS_0 + R_1S_2R_2S_1 \\
& \quad + (q-4)R_1S_2R_2S_0 + R_1S_2R_2^AS_0 + (q-4)R_2S_0R_2S_1
\end{aligned}$$

3.

$$\begin{aligned}
& R_1S_1R_2S_2 + R_1S_0R_2S_3 + (q-5)R_1S_0R_2S_2 + R_1S_0R_2^AS_2 + (q-4)R_2S_2R_1S_2 \\
& \quad + R_2S_3R_1S_2 + R_2S_2R_1S_3 + R_2S_2R_1^AS_2 + (q-5)R_2S_0R_2S_3 \\
& +(q-4)R_2S_1R_2S_2 + (q-4)R_2S_0R_2^AS_2 + [(q-4) + (q-5)^2]R_2S_0R_2S_2 \\
& = R_2S_0R_1S_1 + R_2S_1R_1S_0 + (q-5)R_2S_0R_1S_0 + R_2S_0R_1^AS_0 \\
& +(q-4)R_2S_1R_2S_0 + (q-5)^2R_2S_0R_2S_0 + (q-4)R_2S_0R_2^AS_0 + R_1S_2R_2S_1 \\
& \quad + R_1S_3R_2S_0 + (q-5)R_1S_2R_2S_0 + R_1S_2R_2^AS_0 + (q-5)R_2S_0R_2S_1
\end{aligned}$$

4.

$$\begin{aligned}
& R_1S_1R_2S_0 + R_2S_3R_2S_0 + R_2S_0R_1S_1 + R_2S_1R_1S_0 \\
& +(q-5)R_2S_0R_1S_0 + R_2S_0R_1^AS_0 + (q-5)R_2S_1R_2S_0 \\
& = (2q-9)R_2S_0R_2S_0 + R_2S_0R_2^AS_0 + R_2S_2R_2S_0 + R_1S_0R_2S_1
\end{aligned}$$

5.

$$\begin{aligned}
& R_1^AS_2R_1S_3 + (q-3)R_1^AS_2R_1S_2 + R_1^AS_3R_1^AS_2 \\
& +(q-3)^2R_2^AS_0R_2S_2 + (q-2)R_2^AS_1R_2^AS_2 + (q-3)R_2^AS_0R_2S_3 \\
& = R_1S_3R_1S_2 + (q-3)R_1S_2R_1S_2 + R_1S_2R_1^AS_3 \\
& +(q-3)R_2S_1R_2S_2 + (q-3)(q-4)R_2S_0R_2S_2 + (q-3)R_2S_0R_2^AS_3
\end{aligned}$$

6.

$$\begin{aligned}
& R_1^A S_2 R_2 S_1 + (q-4)R_1^A S_2 R_2 S_0 + R_1^A S_3 R_2^A S_0 + (q-4)^2 R_2^A S_0 R_2 S_0 \\
& + (q-3)R_2^A S_1 R_2^A S_0 + R_2^A S_0 R_1 S_1 + (q-4)R_2^A S_0 R_1 S_0 + R_2^A S_1 R_1^A S_0 \\
& + (q-4)R_2^A S_0 R_2 S_1 = R_2 S_3 R_1 S_2 + (q-3)R_2 S_2 R_1 S_2 + R_2 S_2 R_1^A S_3 \\
& + R_1 S_1 R_2 S_2 + (q-4)R_1 S_0 R_2 S_2 + R_1 S_0 R_2^A S_3 + (q-4)R_2 S_1 R_2 S_2 \\
& + (q-4)^2 R_2 S_0 R_2 S_2 + (q-4)R_2 S_0 R_2^A S_3
\end{aligned}$$

7.

$$\begin{aligned}
& (q-3)R_1^A S_0 R_2 S_2 + R_1^A S_1 R_2^A S_2 + R_2^A S_2 R_1 S_3 + (q-3)R_2^A S_2 R_1 S_2 \\
& + R_2^A S_3 R_1^A S_2 + (q-3)R_2^A S_0 R_2 S_3 + (q-3)(q-4)R_2^A S_0 R_2 S_2 \\
& + (q-3)R_2^A S_1 R_2^A S_2 = (q-3)R_1 S_2 R_2 S_0 + R_1 S_2 R_2^A S_1 \\
& + (q-3)(q-4)R_2 S_0 R_2 S_0 + (q-3)R_2 S_0 R_2^A S_1
\end{aligned}$$

8.

$$\begin{aligned}
& (q-4)R_1^A S_0 R_2 S_0 + R_1^A S_1 R_2^A S_0 + R_2^A S_2 R_2 S_1 + (q-4)R_2^A S_2 R_2 S_0 \\
& + R_2^A S_3 R_2^A S_0 + R_2^A S_0 R_1 S_1 + (q-4)R_2^A S_0 R_1 S_0 + R_2^A S_1 R_1^A S_0 \\
& + (q-4)R_2^A S_0 R_2 S_1 + (q-4)(q-5)R_2^A S_0 R_2 S_0 + (q-4)R_2^A S_1 R_2^A S_0 \\
& = (q-3)R_2 S_2 R_2 S_0 + R_2 S_2 R_2^A S_1 + (q-4)R_1 S_0 R_2 S_0 \\
& + R_1 S_0 R_2^A S_1 + (q-4)^2 R_2 S_0 R_2 S_0 + (q-4)R_2 S_0 R_2^A S_1
\end{aligned}$$

9.

$$\begin{aligned}
& R_1^A S_0 R_1 S_1 + (q-4)R_1^A S_0 R_1 S_0 + R_1^A S_1 R_1^A S_0 + R_2^A S_2 R_2 S_1 \\
& + (q-4)R_2^A S_2 R_2 S_0 + R_2^A S_3 R_2^A S_0 + (q-4)^2 R_2^A S_0 R_2 S_0 + (q-3)R_2^A S_1 R_2^A S_0
\end{aligned}$$

$$\begin{aligned}
&+(q-4)R_2^A S_0 R_2 S_1 = R_1 S_1 R_1 S_0 + (q-4)R_1 S_0 R_1 S_0 + R_1 S_0 R_1^A S_1 \\
&\quad + R_2 S_3 R_2 S_0 + (q-4)R_2 S_2 R_2 S_0 + R_2 S_2 R_2^A S_1 \\
&+(q-4)R_2 S_1 R_2 S_0 + (q-4)(q-5)R_2 S_0 R_2 S_0 + (q-4)R_2 S_0 R_2^A S_1
\end{aligned}$$

10.

$$\begin{aligned}
&R_1^A S_0 R_2 S_3 + (q-4)R_1^A S_0 R_2 S_2 + R_1^A S_1 R_2^A S_2 + (q-3)R_2^A S_2 R_1 S_2 \\
&\quad + R_2^A S_2 R_1 S_3 + R_2^A S_3 R_1^A S_2 + [(q-3) + (q-4)^2]R_2^A S_0 R_2 S_2 \\
&\quad + (q-3)R_2^A S_1 R_2^A S_2 + (q-4)R_2^A S_0 R_2 S_3 \\
&= R_2 S_1 R_1 S_0 + (q-4)R_2 S_0 R_1 S_0 + R_2 S_0 R_1^A S_1 + R_1 S_3 R_2 S_0 \\
&\quad + (q-4)R_1 S_2 R_2 S_0 + R_1 S_2 R_2^A S_1 + (q-4)R_2 S_1 R_2 S_0 \\
&\quad + (q-4)(q-5)R_2 S_0 R_2 S_0 + (q-4)R_2 S_0 R_2^A S_1
\end{aligned}$$

11.

$$\begin{aligned}
&R_1^A S_0 R_2 S_1 + (q-5)R_1^A S_0 R_2 S_0 + R_1^A S_1 R_2^A S_0 + (q-4)R_2^A S_2 R_2 S_0 \\
&+ R_2^A S_2 R_2 S_1 + R_2^A S_3 R_2^A S_0 + [(q-4) + (q-5)^2]R_2^A S_0 R_2 S_0 + (q-4)R_2^A S_1 R_2^A S_0 \\
&\quad + (q-4)R_2^A S_0 R_1 S_0 + R_2^A S_0 R_1 S_1 + R_2^A S_1 R_1^A S_0 + (q-5)R_2^A S_0 R_2 S_1 \\
&\quad = R_2 S_1 R_1 S_0 + (q-4)R_2 S_0 R_1 S_0 + R_2 S_0 R_1^A S_1 + R_2 S_3 R_2 S_0 \\
&\quad + (q-4)R_2 S_2 R_2 S_0 + R_2 S_2 R_2^A S_1 + R_1 S_1 R_2 S_0 + (q-5)R_1 S_0 R_2 S_0 \\
&+ R_1 S_0 R_2^A S_1 + (q-5)R_2 S_1 R_2 S_0 + (q-5)^2 R_2 S_0 R_2 S_0 + (q-5)R_2 S_0 R_2^A S_1
\end{aligned}$$

12.

$$\begin{aligned}
&R_1 S_0 R_2 S_1 + (2q-7)R_2 S_0 R_2 S_0 = R_2 S_0 R_1 S_1 \\
&+ R_2 S_1 R_1 S_0 + (q-4)R_2 S_0 R_1 S_0 + R_1 S_1 R_2 S_0 + (q-4)R_2 S_1 R_2 S_0
\end{aligned}$$

13.

$$\begin{aligned} & (q-3)R_1^A S_0 R_2 S_2 + R_1^A S_1 R_2^A S_3 + (q-2)R_2^A S_2 R_1 S_2 \\ & + R_2^A S_3 R_1^A S_3 + (q-3)^2 R_2^A S_0 R_2 S_2 + (q-3)R_2^A S_1 R_2^A S_3 \\ & = (q-3)R_2^A S_0 R_1 S_0 + R_2^A S_1 R_1^A S_1 + (q-3)R_1^A S_2 R_2 S_0 \\ & + R_1^A S_3 R_2^A S_1 + (q-3)(q-4)R_2^A S_0 R_2 S_0 + (q-3)R_2^A S_1 R_2^A S_1 \end{aligned}$$

Appendix D

Calculation of normalization factor for ‘excluded’ boundary condition

Let $p(\theta)$ be such that

$$p(\theta)p(-\theta) = 1 \quad \text{and} \quad h(2\theta)p\left(\frac{i\pi}{2} + \theta\right) = p\left(\frac{i\pi}{2} - \theta\right).$$

This we may rewrite as

$$p\left(\theta - \frac{i\pi}{2}\right)p\left(\theta + \frac{i\pi}{2}\right) = \frac{1}{h(2\theta)}. \quad (\text{D.1})$$

Defining $f(\theta)$ and $g(\theta)$ by

$$f(\theta) = \partial_\theta \ln[p(\theta)] ; \quad g(2\theta) = \partial_\theta \ln[h(2\theta)]$$

equation (D.1) becomes

$$f\left(\theta - \frac{i\pi}{2}\right) + f\left(\theta + \frac{i\pi}{2}\right) = -g(2\theta)$$

$$\Rightarrow 2 \cosh\left(\frac{\pi k}{2}\right) \tilde{f}(k) = -\tilde{g}(k) \quad (\text{D.2})$$

where

$$\tilde{f}(k) = \frac{1}{2\pi} \int_{-\infty}^{\infty} f(\theta) e^{ik\theta} d\theta ; \quad \tilde{g}(k) = \frac{1}{2\pi} \int_{-\infty}^{\infty} g(2\theta) e^{ik\theta} d\theta.$$

From this we see that, for $\tilde{g}(k) = \tilde{g}(-k)$,

$$\begin{aligned} f(\theta) &= -\frac{1}{2} \int_{-\infty}^{\infty} \frac{\tilde{g}(k) e^{-ik\theta} dk}{\cosh\left(\frac{\pi k}{2}\right)} \\ \Rightarrow \ln[p(\theta)] &= -\int_0^{\infty} \frac{\tilde{g}(k) \sin(k\theta) dk}{\cosh\left(\frac{\pi k}{2}\right) k} \end{aligned}$$

For the case in point,

$$h(2\theta) = \frac{\cosh\left[\lambda\left(\theta - \frac{i\pi}{3}\right)\right] \sinh\left[\lambda\left(\theta + \frac{i\pi}{3}\right)\right] \sinh\left[\lambda\left(\frac{2\pi i}{3} + \theta\right)\right]}{\cosh\left[\lambda\left(\theta + \frac{i\pi}{3}\right)\right] \sinh\left[\lambda\left(\theta - \frac{i\pi}{3}\right)\right] \sinh\left[\lambda\left(\frac{2\pi i}{3} - \theta\right)\right]}$$

which leads to

$$\begin{aligned} \tilde{g}(k) &= \frac{\lambda}{\pi} \int_{-\infty}^{\infty} \left(\frac{1}{\sinh\left[\lambda\left(\frac{2\pi i}{3} + 2\theta\right)\right]} + \frac{1}{\sinh\left[\lambda\left(\frac{2\pi i}{3} - 2\theta\right)\right]} \right) e^{ik\theta} d\theta \\ &\quad + \frac{i\lambda}{\pi} \int_{-\infty}^{\infty} \frac{\sin\left(\frac{4\pi\lambda}{3}\right) e^{ik\theta} d\theta}{\cos\left(\frac{4\pi\lambda}{3}\right) - \cosh(\lambda 2\theta)}. \end{aligned}$$

The first two terms may be integrated using the identity

$$\frac{1}{4} \int_{-\infty}^{\infty} \frac{e^{-imx} dm}{\cosh\left(\frac{\pi m}{2}\right)} = \frac{\sinh(x)}{\sinh(2x)}$$

from which we find that

$$\begin{aligned} &\frac{\lambda}{\pi} \int_{-\infty}^{\infty} \left(\frac{1}{\sinh[\lambda(i\pi\alpha + 2\theta)]} + \frac{1}{\sinh[\lambda(i\pi\alpha - 2\theta)]} \right) e^{ik\theta} d\theta \\ &= 2i \frac{\cosh\left[\pi k\left(\frac{\alpha}{2} - \frac{1}{4\lambda}\right)\right] \sinh\left(\frac{\pi k}{4\lambda}\right)}{\sinh\left(\frac{\pi k}{2\lambda}\right)} \end{aligned}$$

for $-\frac{1}{2} < \frac{a}{2} - \frac{1}{4\lambda} < \frac{1}{2}$. The integration of the remaining term makes use of the identity

$$\frac{1}{2} \int_{-\infty}^{\infty} \frac{\sin(\frac{\pi a}{b}) e^{-imx} dm}{b [\cosh(\frac{\pi m}{b}) + \cos(\frac{\pi a}{b})]} = \frac{\sinh(ax)}{\sinh(bx)} \quad 0 < a < b$$

which may be recast in the form

$$\frac{\lambda}{\pi} \int_{-\infty}^{\infty} \frac{\sin(\lambda 2\pi\alpha) e^{ik\theta} d\theta}{\cos(\lambda 2\pi\alpha) - \cosh(\lambda 2\theta)} = \frac{\sinh[\pi k(\alpha - \frac{1}{2\lambda})]}{\sinh(\frac{\pi k}{2\lambda})} \quad 0 < 2\alpha - \frac{1}{\lambda} < \frac{1}{\lambda}.$$

Substituting for $\tilde{g}(k)$, equation (D.2) becomes

$$\ln[p(\theta)] = -i \int_0^{\infty} \left(\frac{2 \cosh[\pi k(\frac{1}{3} - \frac{1}{4\lambda})] \sinh(\frac{\pi k}{4\lambda}) + \sinh[\pi k(\frac{2}{3} - \frac{1}{2\lambda})]}{\sinh(\frac{\pi k}{2\lambda}) \cosh(\frac{\pi k}{2})} \right) \frac{\sin(k\theta) dk}{k} \quad (\text{D.3})$$

It is now possible to express $p(\theta)$ in terms of an infinite product of gamma functions. As an example, consider the expression

$$\begin{aligned} & -i \int_0^{\infty} \frac{\sinh(\pi k\alpha) \sin(k\theta) dk}{\sinh(\frac{\pi k}{2\lambda}) \cosh(\frac{\pi k}{2}) k} \\ &= - \int_0^{\infty} \frac{\left(e^{\pi k(\alpha + \frac{i\theta}{\pi})} + e^{-\pi k(\alpha + \frac{i\theta}{\pi})} - e^{\pi k(\alpha - \frac{i\theta}{\pi})} - e^{-\pi k(\alpha - \frac{i\theta}{\pi})} \right) e^{-\pi k(\frac{1}{2\lambda} + \frac{1}{2})}}{(1 - e^{-\frac{\pi k}{\lambda}})(1 + e^{-\pi k})} \frac{dk}{k} \\ &= - \int_0^{\infty} \sum_{n=1}^{\infty} (-1)^n \frac{\left(e^{-\pi k(-\alpha + \frac{\theta}{i\pi})} + e^{-\pi k(\alpha - \frac{\theta}{i\pi})} - e^{-\pi k(-\alpha - \frac{\theta}{i\pi})} - e^{-\pi k(\alpha + \frac{\theta}{i\pi})} \right)}{1 - e^{-\frac{\pi k}{\lambda}}} \\ & \quad \times \frac{e^{-\pi k(\frac{2n+1}{2} + \frac{1}{2\lambda})} dk}{k} \\ &= - \int_0^{\infty} \sum_{n=1}^{\infty} \frac{\left(e^{-t(-\alpha\lambda + X)} + e^{-t(\alpha\lambda - X)} - e^{-t(-\alpha\lambda - X)} - e^{-t(\alpha\lambda + X)} \right)}{1 - e^{-t}} \end{aligned}$$

$$\times \frac{\left(e^{-t((4n-3)\frac{\lambda}{2} + \frac{1}{2})} - e^{-t((4n-1)\frac{\lambda}{2} + \frac{1}{2})} \right) dt}{t}$$

where $X = \frac{\lambda\theta}{i\pi}$. From the integral representation of $\ln(\Gamma(z))$,

$$\ln(\Gamma(z)) = \int_0^\infty \left[(z-1)e^{-t} + \frac{e^{-tz} - e^{-t}}{1 - e^{-t}} \right] \frac{dt}{t} \quad \text{Re}(z) > 0,$$

we obtain the identity

$$\ln \left(\frac{\Gamma(a)\Gamma(b)}{\Gamma(c)\Gamma(d)} \right) = \int_0^\infty \frac{e^{-ta} + e^{-tb} - e^{-tc} - e^{-td}}{1 - e^{-t}} \frac{dt}{t} \quad a + b - c - d = 0.$$

This gives us

$$-i \int_0^\infty \frac{\sinh(\pi k\alpha) \sin(k\theta) dk}{\sinh(\frac{\pi k}{2\lambda}) \cosh(\frac{\pi k}{2}) k} = \sum_{n=1}^\infty \ln \left(\frac{\Omega_n(X)}{\Omega_n(-X)} \right).$$

where

$$\Omega_n(X) = \frac{\Gamma[(4n-3)\frac{\lambda}{2} + \frac{1}{2} - \alpha\lambda - X] \Gamma[(4n-1) + \frac{1}{2} + \alpha\lambda - X]}{\Gamma[(4n-1)\frac{\lambda}{2} + \frac{1}{2} - \alpha\lambda - X] \Gamma[(4n-3) + \frac{1}{2} + \alpha\lambda - X]}.$$

For $\alpha = \frac{2}{3} - \frac{1}{2\lambda}$, this gives us an expression for the second term on the righthand side of equation (D.3). The first term may be treated in a similar fashion, resulting in the solution

$$p(\theta) = \prod_{k=1}^\infty \frac{\Phi_k(X)}{\Phi_k(-X)}$$

where

$$\begin{aligned} \Phi_k(X) &= \frac{\Gamma[(4k-1)\frac{\lambda}{2} + \frac{1}{2} - \frac{\lambda}{3} - X] \Gamma[(4k-1)\frac{\lambda}{2} + \frac{\lambda}{3} - X] \Gamma[(4k-1)\frac{\lambda}{2} + \frac{2\lambda}{3} - X]}{\Gamma[(4k-3)\frac{\lambda}{2} + \frac{1}{2} - \frac{\lambda}{3} - X] \Gamma[(4k-3)\frac{\lambda}{2} + \frac{\lambda}{3} - X] \Gamma[(4k-3)\frac{\lambda}{2} + \frac{2\lambda}{3} - X]} \\ &\times \frac{\Gamma[(4k-3)\frac{\lambda}{2} + 1 - \frac{\lambda}{3} - X] \Gamma[(4k-3)\frac{\lambda}{2} + \frac{1}{2} + \frac{\lambda}{3} - X] \Gamma[(4k-3)\frac{\lambda}{2} - \frac{2\lambda}{3} + 1 - X]}{\Gamma[(4k-1)\frac{\lambda}{2} + 1 - \frac{\lambda}{3} - X] \Gamma[(4k-1)\frac{\lambda}{2} + \frac{1}{2} + \frac{\lambda}{3} - X] \Gamma[(4k-1)\frac{\lambda}{2} - \frac{2\lambda}{3} + 1 - X]} \end{aligned}$$

Bibliography

- [1] Leung Chim and Alexander Zamolodchikov. Integrable field theory of the q -state Potts model with $0 < q < 4$. *International Journal of Modern Physics*, A7(21):5317–5335, 1992.
- [2] Leung Chim. Boundary S-matrix for the integrable q -Potts model. *Journal of Physics*, A28:7039, 1994.
- [3] J. L. Cardy and G. Delfino. Universal amplitude ratios in the two-dimensional q -state Potts model and percolation from quantum field theory. *Nuclear Physics*, B519:551–578, 1998.
- [4] R. J. Baxter. *Exactly Solved Models in Statistical Mechanics*. Academic Press, 1982.
- [5] G. E. Andrews, R. J. Baxter, and P. J. Forrester. Eight-vertex SOS model and generalized Rogers-Ramanujan-type identities. *Journal of Statistical Physics*, 35:193, 1984.
- [6] J. Zinn-Justin. *Quantum Field Theory and Critical Phenomena*. Oxford University Press, 1989.
- [7] Giorgio Parisi. *Statistical Field Theory*. Addison Wesley, 1988.

- [8] R. B. Potts. *Proc. Cambridge Phil. Soc.*, 48:106, 1952.
- [9] E. M. Fortuin and P. Kasteleyn. *Physica*, 57:536, 1972.
- [10] R. J. Baxter. Potts model at critical temperature. *Journal of Physics*, C6:L445, 1973.
- [11] A. M. Polyakov. *J.E.T.P. Letters*, 12:381, 1970.
- [12] A. A. Belavin, A. M. Polyakov, and A. B. Zamolodchikov. Infinite conformal symmetry in two-dimensional quantum field theory. *Nuclear Physics*, B241:333–380, 1984.
- [13] P. Ginsparg. Applied conformal field theory. In *Les Houches XLIX - Champs, Cordes et Phénomènes Critiques*. Elsevier, 1989.
- [14] John L. Cardy. Conformal invariance and statistical mechanics. In *Les Houches XLIX - Champs, Cordes et Phénomènes Critiques*. Elsevier, 1989.
- [15] John L. Cardy. Conformal invariance. In *Phase Transitions*, volume 11. Academic Press, 1987.
- [16] A. B. Zamolodchikov. Integrable field theory from conformal field theory. *Advanced Studies in Pure Mathematics*, 19:641–674, 1989.
- [17] Alexander B. Zamolodchikov and Alexey B. Zamolodchikov. Factorized S-matrices in two dimensions as the exact solutions of certain relativistic quantum field theory models. *Annals of Physics*, 120:253–291, 1979.
- [18] A. B. Zamolodchikov. Factorised S-matrices and lattice statistical systems. *Sov. Sci. Rev., Physics*, 2:1–40, 1980.

- [19] V. A. Fateev and A. B. Zamolodchikov. Conformal field theory and purely elastic S-matrices. *International Journal of Modern Physics*, A5(6):1025–1048, 1990.
- [20] G. Mussardo. Off-critical statistical models: Factorized scattering theories and bootstrap program. *Phys. Rep.*, 218:215–379, 1992.
- [21] R. Shankar and E. Witten. S-matrix of the supersymmetric nonlinear σ model. *Physical Review D*, 17(8):2134–2143, 1978.
- [22] Stephen Parke. Absence of particle production and factorization of the S-matrix in 1+1 dimensional models. *Nuclear Physics*, B174:166–182, 1980.
- [23] M. Karowski. On the bound state problem in 1 + 1 dimensional field theories. *Nuclear Physics*, B153:244–252, 1979.
- [24] V. S. Dotsenko. Critical behaviour and associated conformal algebra of the Z_3 Potts model. *Nuclear Physics*, B235:54–74, 1984.
- [25] V. S. Dotsenko and V. A. Fateev. Conformal algebra and multipoint correlation functions in 2d statistical models. *Nuclear Physics*, B240:312–348, 1984.
- [26] Sidney Coleman and H. J. Thun. On the prosaic origin of the double poles in the Sine-Gordon S-matrix. *Communications in Mathematical Physics*, 61:31–39, 1978.
- [27] R. J. Eden, P. V. Landshoff, D. I. Olive, and J. C. Polkinghorne. *The Analytic S-Matrix*. Cambridge University Press, 1966.

- [28] E. Corrigan, P. E. Dorey, and R. Sasaki. On a generalised bootstrap principle. *Nuclear Physics*, B408:579–599, 1993.
- [29] H. W. Braden, E. Corrigan, P. E. Dorey, and R. Sasaki. Affine Toda field theory and exact S-matrices. *Nuclear Physics*, B338:689–746, 1990.
- [30] G. Sotkov and C. J. Zhu. Bootstrap fusions and tricritical Potts model away from criticality. *Physics Letters*, B229:391–397, 1989.
- [31] P. Christe and G. Mussardo. Integrable systems away from criticality: the Toda field theory and S-matrix of the tricritical Ising model. *Nuclear Physics*, B330:465–487, 1990.
- [32] Alexander Berkovich, Barry M. McCoy, and Paul A. Pearce. The perturbations $\phi_{2,1}$ and $\phi_{1,5}$ of the minimal models $m(p, p')$ and the trinomial analogue of Bailey’s lemma. Preprint ITPSB 97-50, hep-th/9712220.
- [33] Vladimir Fateev, Sergei Lukyanov, Alexander Zamolodchikov, and Alexei Zamolodchikov. Expectation values of local fields in Bullough-Dodd model and integrable perturbed conformal field theories. Preprint CLNS 97/1510, RU-97-74, hep-th/9709034.
- [34] John L. Cardy. Conformal invariance and surface critical behaviour. *Nuclear Physics*, B240:514–532, 1984.
- [35] John L. Cardy. Operator content of two-dimensional conformally invariant theories. *Nuclear Physics*, B270:186–204, 1986.
- [36] John L. Cardy. Effect of boundary conditions on the operator content of two-dimensional conformally invariant theories. *Nuclear Physics*, B275:200–218, 1986.

- [37] John L. Cardy. Boundary conditions, fusion rules and the Verlinde formula. *Nuclear Physics*, B324:581–596, 1989.
- [38] H. Saleur and M. Bauer. On some relations between local height probabilities and conformal invariance. *Nuclear Physics*, B320:591–624, 1989.
- [39] Subir Ghoshal and Alexander Zamolodchikov. Boundary S-matrix and boundary state in two-dimensional integrable quantum field theory. *International Journal of Modern Physics*, A9(21):3841–3885, 1994.
- [40] Andreas Fring and Roland Koberle. Factorized scattering in the presence of reflecting boundaries. *Nuclear Physics*, B421:159–172, 1994.
- [41] Akira Fujii and Ryu Sasaki. Boundary effects in integrable field theory on a half line. *Prog. Theor. Phys.*, 93:1123–1134, 1995.
- [42] Carlo Acerbi, Giuseppe Mussardo, and Gabor Takacs. private communication.
- [43] F. A. Smirnov. Exact S-matrices for $\phi_{1,2}$ -perturbated minimal models of conformal field theory. *International Journal of Modern Physics*, A6(8):1407–1428, 1991.

